REGULATION OF GLUTAMATE DEHYDROGENASE AND LACTATE DEHYDROGENASE IN THE FREEZE TOLERANT WOOD FROG, *RANA SYLVATICA*

by

TRONG D. NGUYEN

B.Sc. Hons. Biochemistry
Carleton University, 2014

A thesis submitted to the Faculty of Graduate and Postdoctoral Affairs in partial fulfillment of the requirements for the degree of

MASTER OF SCIENCE

in

BIOLOGY

CARLETON UNIVERSITY
OTTAWA, ONTARIO, CANADA

The undersigned hereby recommend to the Faculty of Graduate Studies and Postdoctoral Affairs acceptance of this thesis

REGULATION OF GLUTAMATE DEHYDROGENASE AND LACTATE DEHYDROGENASE IN THE FREEZE TOLERANT WOOD FROG, *RANA SYLVATICA*

submitted by

Trong D. Nguyen

In partial fulfillment of the requirements for the degree of Master of Science

_____

Chair, Department of Biology

_____

Thesis Supervisor

Carleton University

TABLE OF CONTENTS

ABSTRACT

Freeze tolerance is a survival strategy used by the wood frog, *Rana sylvatica*, for winter survival. Drastic changes to physiology and biochemistry are required to enter a state of metabolic rate depression in order to reestablish homeostasis during whole-body freezing. Enzymes are biocatalysts that mediate these metabolic functions and regulate survival of this environmental stress. This thesis explores the properties and regulation of two key enzymes of carbohydrate metabolism (lactate dehydrogenase, LDH) from liver and amino acid metabolism (glutamate dehydrogenase, GDH) from skeletal muscle. The studies showed that allosteric effectors play a role in differentially regulating these enzymes between freezing and control conditions. Furthermore, reversible protein phosphorylation appears to be a common regulatory mechanism reducing activity of both LDH and GDH in the frozen state. Altogether, these studies support theories that multiple mechanisms of enzyme regulation, particularly protein phosphorylation, contribute to the reorganization of metabolism during freeze tolerance.

ACKNOWLEDGMENTS

First and foremost, Dr. Kenneth B. Storey and Jan Storey: Thank you for your astonishing support throughout the years. For showing and explaining science, not only in aspects related to enzymology but the little valuable lessons that will be carry on for a lifetime. I cannot begin to express the gratitude for accepting me into the lab and nurturing my curiosity to become the scientist that I consider myself to be now. I want to thank Ken for the opportunity to conduct amazing research at the bench and challenging me to personify enzymes. Your passion and rigor for scientific excellence is something inspires me to find in wherever I end up. Next Jan: The mastermind behind every word that comes out of the lab, thank you for your unwavering patience in my writing and presentations. Without your edits and insights, I would be just a rambling word salad artist. Thank you both very much for everything!

To the Storey Lab members: It has been a wild ride for sure. It is difficult to not interact with the bunch of you lots being in a small, confined space. Thanks to everybody during my time in the lab, for the lab group is a dynamic entity that changes with time: old people leave and new people join, and I am glad to be a part of it. Each of you made a difference and positive impact during my studies. Thanks for the comradery and lasting memories.

Lastly, my family and friends: I am not sure where I will be without their loving support. Family who probably still do not know want I do but encourage me to pursue my interests. Friends who pretend to understand what I studying and take the time to listen to my corybantic explanations. I enjoyed my time in the Storey lab; I would like to think I have learned, grown, and changed for the better during the process. Nevertheless, this is not the end, yet, another milestone towards greatness.

LIST OF ABBREVIATIONS

ADP	adenosine diphosphate
ALT	alanine aminotransferase
AMP	adenosine monophosphate
AMPK	AMP-activated protein kinase
APS	ammonium persulfate
AST	aspartate aminotransferase
ATP	adenosine triphosphate
CAMK	Ca^{2+}/calmodulin-dependent protein kinase
CDK	cyclin-dependent kinase
CM	carboxymethyl
dH_2O	deionized water
EC	enzyme commission number
ECL	enhanced chemiluminescence
EDTA	ethylenediaminetetraacetic acid
EGTA	ethylene glycol-bis(2-aminoethylether)-N,N,N',N'-tetraacetic acid
ETC	electron transport chain
F6P	fructose-6-phosphate
FAD/$FADH_2$	flavin adenine dinucleotide oxidized/reduced form
G1P	glucose-1-phosphate
G6P	glucose-6-phosphate
GDH	glutamate dehydrogenase
GTP	guanosine triphosphate
I_{50}	inhibitor concentration at half-maximal enzyme inhibition
INP	ice nucleating protein
K_a	activator concentration at half-maximal enzyme activation
KCl	potassium chloride
kDa	kilodalton
K_{50}	inhibition concentration at mid-point of the inhibition curve
K_m	substrate concentration at half-maximal enzyme velocity
LDH	lactate dehydrogenase
Me-lys	methylated lysine
MES	2-(N-morpholino)ethanesulfonic acid
MPA	microplate analysis
MRD	metabolic rate depression
NaCl	sodium chloride
NAD(P)$^+$/NAD(P)H	nicotinamide adenine dinucleotide (phosphate) oxidized/reduced form
NH_4Cl	ammonium chloride
P-ser	phosphorylated serine
P-thr	phosphorylated threonine
P-tyr	phosphorylated tyrosine
PAGE	polyacrylamide gel electrophoresis
pCO_2	partial pressure of carbon dioxide
Pi	phosphate
PKA	protein kinase A
PMSF	phenylmethylsulfonyl fluoride
PTM	posttranslational modification
PVDF	polyvinylidene difluoride

RPP	reversible protein phosphorylation
SDS	sodium dodecyl sulfate
SEM	standard error of the mean
TBS	tris-buffered saline
TBST	tris-buffered saline with Tween® 20
TEMED	tetramethylethylenediamine
TRIS	tris(hydroxymethyl)aminomethane
$\mathbf{V_{max}}$	maximum enzyme rate or velocity

LIST OF TABLES

LIST OF FIGURES

Chapter 1 – General Introduction

Physiological Adaptations

To survive unforgiving environments, organisms must undergo changes at the biochemical and physiological level to cope with a decrease in resources available (i.e. food sources, access to water, and sufficient amounts of oxygen). In addition to the depletion of resources, environmental parameters (such as temperature, humidity, salinity) will also shift conditions away from optimal ranges. Having both limited resources and environmental stressors has led to the use of metabolic rate depression (MRD) as a principal strategy for survival by many animals (Storey and Storey, 1990; Storey and Storey, 2004). MRD is essential for prolonging endogenous fuel reserves in order to extend the survival period when resource availability is scarce. The ability to regulate reversible transitions to and from hypometabolic states under conditions of environmental stress is conserved across taxonomic groups and broadly applicable to various functions of the cell (Storey and Storey, 2004). In some cases, small mammals and reptiles may experience a decrease in metabolic rate to as low as just 1-20% of their baseline resting rate under winter conditions (Storey & Storey, 1990; Storey & Storey 1992). Likewise, hibernating amphibians are capable of up to 75% metabolic depression in order to minimize ATP demands under hypoxic conditions (Donohoe and Boutilier, 1998). The ability to transition into a hypometabolic state while maintaining homeostasis is quintessential for stress survival.

MRD orchestrates radical changes on the behavioral, physiological, and biochemical level. Typical behavioral and physiological responses during cold survival include cessation of movement, limited ventilation, and slowing of cardiac activity. Furthermore, other vital organs such as the kidney show reduced filtration and brain the

can undergo substantial alteration in neurological organization (Storey and Storey, 2004). These physiological responses will consequentially impair the fitness of the animal and, hence, animals must often fortify their defenses or seek shelter, not only to brace against temporal changes of the seasons but also threats of predation. It is important to note that a myriad of factors act in concert to govern the regulatory process by which animals transition into a state of hypometabolism. Factors such as the accumulation of urea (Costanzo et al., 2014; Muir et al., 2008) and increase in pCO_2 levels (Sinclair et al., 2013) occur as a result of decreased kidney filtration and respiration function, respectively.

Survival Strategies & Freezing Stress

A need to survive cold climates has led to the adaptation of many coping strategies. For instance, animals can elude exposure to ambient subzero temperatures by various methods such as seasonal migration to warmer climates which is an effective method for animals capable of traversing great distances (e.g. Canada geese). Animals without migratory capability, may escape to thermally buffered environments (e.g. fishes) or alter their environment to make it more habitable (e.g. humans). In these cases, animals are not placed in situations where they are at risk of freezing, unless they are very unfortunate. However, other animals must endure subzero temperatures and employ one of two main strategies to survive below 0°C: (1) freeze avoidance and (2) freeze tolerance. Freeze avoidance is a survival strategy that prevents body fluids from freezing at subzero temperatures by supercooling (i.e. body fluids remain liquid to low subzero temperatures). Supercooling of body fluids with the aid of antifreeze agents is a strategy adopted by many insects (Hakim et al., 2013) and reptiles (Lowe et al., 1971) to survive the cold. Antifreeze

agents lower the freezing point of intra- and extracellular fluids to prevent ice crystal formation. Freeze avoidance strategies are widely used by many cold-hardy animals living at high latitudes or altitudes. However, some animals use the opposite strategy and instead of employing methods to prevent body fluids from freezing, they adopt strategies that actively promote freezing and then deal with the repercussions through adaptation.

Freeze tolerance as a strategy for cold survival has been discovered independently through many evolutionary events across several taxonomic linages, spanning from insects (Ring, 1982; Lee et al., 1995) and other invertebrates (Aarset, 1982; Block, 1991) to reptiles (Storey and Storey, 1992; Storey, 2006) and amphibians (Storey, 1990; Costanzo et al., 2015). These different organisms all share common adaptive mechanisms in order to tolerate freezing. These include promoting the freezing of bodily fluids through a controlled process of ice nucleation. The facilitation of ice nucleation is guided by ice nucleators such as bacteria found on the skin or gut or ice nucleating proteins (INPs) prompted through skin contact with existing ice crystals from the environment (Lee and Costanzo, 1998; Zachariassen and Kristiansen, 2000). Organisms avail one or more of these methods to trigger ice nucleation at subzero temperatures. INPs work to induce slow freezing at temperatures just below the freezing point of body fluids and thereby avoid extensive supercooling. By doing so, they can allow the organism time to elicit other freeze tolerance adaptations. Without INPs, freezing triggered from a deeply supercooled state will cause an instantaneous rapid production of unorganized ice crystals that can result in tissue injuries or death. The distribution and size of ice crystals is chaperoned by INPs establishing ice crystal formation extracellularly in order to avoid intracellular damage by ice. As ice crystals increase in size in extracellular spaces, moderated by INPs, cell

dehydration is occurring concurrently through the loss of water into extracellular ice masses (Fuller, 2004). Some organisms produce cryoprotectants (e.g. glucose or glycerol) during freezing. The colligative properties of these cryoprotectants act to limit water loss from cells by counteracting the osmotic imbalance and maintaining cell volume. Cryoprotectants create a higher solute concentration inside the cells and thereby retain more water inside the cell, which keeps cells from shrinking too much. This also alleviates a potential danger from high intracellular ion (e.g. Na^+, K^+, Ca^{2+}) concentrations (i.e. ionic strength) that could rise to lethal levels if these were the only solutes opposing the loss of water from cells (Williams and Lee, 2011). The interplay between dehydration and osmotic stress is emphasized through the loss of water to form ice crystals during the events of freezing. The stresses that would typically cause damage are minimized due to the effects of both INPs and cryoprotectants.

Long periods of exposure to freezing temperatures can lead to potentially dire consequences for animals that lack adequate adaptation for cold survival by supercooling. Ice crystallization occurs as temperature drops below 0°C. The formation of ice crystals within an animal's body imparts stresses on the intracellular and extracellular milieu through ischemic, dehydration, and osmotic strain. Gas exchange and nutrient accessibility impaired by the physical boundaries of the ice ultimately leads to ischemic insult to the surrounding tissue. By virtue of dehydration, ice formation in extracellular spaces raises the osmolality of the remaining extracellular fluids. This creates an osmotic imbalance with respect to intracellular fluid that is corrected by water flowing out of the cells to dilute extracellular fluids (Lee et al., 1992). As more extracellular fluid freezes, this process perpetuates. If cell volume shrinks too much, then membrane lipids can be forced out of

their bilayer structure (into a non-reversible gel state) thereby causing a loss of membrane physiological functions and potentially rupturing membranes in conjunction with the ice-induced mechanical tension. Similar damage can also be observed at the tissue and organ level though sheering and puncturing wounds during ice crystal growth (Storey, 1990). Hence, freeze tolerant animals synthesize cryoprotective metabolites that are retained in the cell, thereby raising the osmolality intracellularly until a balance is achieved between intra- and extracellular fluids during subzero temperature. At the physiological level, motility is physically restricted due to ice formation, especially freezing of the blood plasma that brings the heartbeat to a stop, and ice formed within the abdominal cavity limits lung capacity to halt respiration. Eventually, heartbeat and respiration come to a complete halt. At the risk of instantaneous lethality due to supercooling strategies, the damage for non-adapted organisms is irreversible and could mean certain death (Mazur, 1984; Storey and Storey, 1988). To this end, evolution has garnered various fascinating means for cold hardiness survival strategies.

Metabolic Rate Depression

Despite the reduction of cellular damage through usage of INPs for controlling ice formation in the extracellular cavities and cryoprotectants to help regulate cell volume reduction and stabilize macromolecules, animals must also contend with the physiological aspects of freezing bodily fluids. Freezing is taxing because it imposes anoxic, dehydration, and osmotic stresses on cells. Furthermore, other factors such as mechanical disruption due to ice formation and extended periods of inactivity contribute to physical stress on the body. Although freeze tolerant animals have evolved mechanisms for survival, they are not

completely exempt from these stress factors. Freezing of body fluids leads to the cessation of blood flow and halts cardiac and brain function leading to fatal consequences for animals without the necessary adaptation. During the onset of freezing, cellular metabolism shifts towards hypoxic and then anoxic conditions, where (1) organisms must alter the means of ATP production from aerobic to anaerobic synthesis of ATP and (2) they must extend their use of stored anaerobic fuel reserves in the form of glycogen for an indeterminate amount of time until conditions allow for thawing. Transitioning between aerobic and anaerobic states has been documented pertaining to various animal models (Churchill and Storey, 1992a; Churchill and Storey, 1992b; Packard et al., 2004). Aerobic conditions allow oxygen to be the terminal electron acceptor in the electron transport chain (ETC) required for ATP production by oxidative phosphorylation. However, oxygen-driven ATP production is not a viable option when blood plasma freezes such that cellular access to oxygen cannot be replenished. Hence, glycolysis is shunted towards lactate fermentation in many animals when oxygen supplies are depleted (Jackson and Ultsch, 2010; Storey, 2007). This allows for the regeneration of reductive molecules such as NADH to maintain anaerobic glycolytic ATP output. By virtue of lactate fermentation, metabolic rate is depressed in regards to the ETC since oxygen is unavailable and the Krebs cycle is suppressed since pyruvate undergoes fermentation during anaerobic glycolysis. However, this not the main basis for MRD in animals, since MRD is also centrally controlled and coordinated by mechanisms (e.g. post-translational modifications) that suppress and/or inhibit facets of metabolism to balance suppression of all aspects of metabolism. As animals enter a frozen state facing the cessation of most vital functions, they are not in a

true state of suspended animation, as select tissue-specific metabolic activity is maintained to continuously produce energy, albeit at lower levels.

The halt in respiration leading to oxygen deprivation is not the only hurdle when it comes to freezing. Motility is restricted/halted during freezing, hence, nutrient resources are primarily dependent on fuels stored prior to freezing in the form of glycogen. Survival would not be possible if active baseline ATP usage rates were maintained during freezing, since glycogen storages would be quickly depleted before the winter was over. Through reducing metabolic rate, the expenditure of energy is vastly reduced to provide the animal an extended duration for glycogen reserves to be exhausted. Freeze tolerant animals evolved mechanisms to prolong glycogen rations by entering a state of hypometabolism for the duration of the freezing period which is globally coordinated by MRD (Storey, 1990; Storey and Storey, 1988). Some of the most energy intensive pathways, for example gene expression or protein synthesis, are metabolically demanding cellular processes requiring great amounts of ATP to power DNA replication, protein synthesis or the cell cycle (Salazar-Roa and Malumbres, 2016; Zhang and Storey, 2012). As a result, transcription and subsequently translation are suppressed during hypometabolism (Al-Fageeh and Smales, 2006; Gualerzi et al., 2003; Storey and Storey, 2004). On the other hand, survival pathways have been determined to be upregulated during freezing such as genes implicated in fibrinogen synthesis that are linked to tissue injury (Cai and Storey, 1997a) and tissue-specific freeze response proteins *fr47* (Sullivan et al., 2015) and *fr10* (Cai and Storey, 1997b). The ability to suppress metabolism is an adaptive response that is not solely unique in freeze tolerant animals since it is also found mammalian hibernators (Stieler et al., 2011; Wu et al., 2013a), anoxia tolerant turtles (Brooks and Storey, 1988;

Krivoruchko and Storey, 2010; Storey, 2007), and estivating frogs and invertebrates (Storey and Storey, 1990; Thomas and Agard, 1992). The commonality amongst these organisms is the ability to selectively downregulate various metabolic pathways, while maintaining certain pathways that are vital for survival. Rather that undergoing global suppression of total metabolic function by entering a state of suspended animation, these animals opt to regulate quintessential pathways necessary for survival.

Integrally regulated at the transcriptional level, MRD is partially mediated by transcription factors that play an essential role in selective gene expression. Stress-induced signals elicit a torrent of signal transduction systems activating selected transcription factors and the genes under their control (O'Hara et al., 1999; Storey and Storey, 2004). During hypometabolic states, the downregulation of certain transcription factors alters gene expression, thus invoking a paradigm shift cascaded through the transcriptional to the physiological scale. Control of MRD also occurs post-transcriptionally by microRNA (Bansal et al., 2016; Biggar and Storey, 2012; Morin et al., 2008; Wu et al., 2013b). MicroRNAs are able to quickly silence or mark mature mRNA transcripts for degradation (Bartel, 2004; Filipowicz et al., 2008) or by sequestration in processing bodies for storage (Bley et al., 2015; Eulalio et al., 2007). Hence, they are an efficient and energetically affordable means of modulating protein translation. In other words, microRNA regulation provides an inexpensive method of shutting down costly protein synthesis and provides the possibility of mRNA storage in stress granules to be used when conditions become more suitable. Albeit protein synthesis is downregulated, the existing pool of proteins undergo shifts in regulation as well. Enzymes and signaling proteins will deplete ATP and other cellular resources, if they are not kept in check. At the post-translational level, proteins are

regulated via segregation, degradation or modification to alleviate biochemical energy constraints. Regulation of proteins or enzymes using the latter strategy, known as post-translation modifications (PTMs), is the key to unlocking the complexity of the proteome.

Post-Translational Modifications

Biochemical conservation of energetics during states of hypometabolism is often accomplished by PTMs (Knorre et al., 2009). Covalent modification can alter the activity state and/or the conformation of its target. This allows the chemical repertoire of roughly 20 common amino acids to be vastly expanded through the modification of specific functional groups allowing for an even greater degree of protein interaction. The importance of PTMs as a regulatory mechanism lies in the fact that they can be added or removed to change protein functionality without the necessity for protein biosynthesis or gene transcription. In terms of energetics, PTMs are considered much less costly compared to the demands of *de novo* synthesis of proteins. Many PTMs have specific responsibilities when invoked (e.g. ubiquitination typically signals for protein degradation). The plethora of both known and unknown PTMs and their abilities to alter the properties of proteins is deemed to be of significant interest for they serve as a language for the regulation of proteins with respect to the study of hypometabolic states and environmental stress.

Phosphorylation by protein kinases is a common PTM that is frequently used for regulating enzymatic activity (Khoury et al., 2011) and when paired with specific protein phosphatases, serves a multifunctional regulatory role known as reversible protein phosphorylation (RPP). Protein kinases add covalently bound phosphate groups of other proteins, whereas phosphate groups are removed by the action of protein phosphatases

(Hunter, 1995). Two major types of protein kinases are: (1) serine/threonine-specific protein kinases that phosphorylate the hydroxyl group of serine or threonine residues, and (2) tyrosine-specific protein kinases that phosphorylate the hydroxyl group of tyrosine. These protein kinases play an active role in chemical signaling during stress; some examples are protein kinase A (PKA), AMP-activated protein kinase (AMPK), and Ca^{2+}/calmodulin-dependent protein kinase (CAMK) that each play large roles in metabolic regulation (Dawson and Storey, 2012). Phosphorylation is involved in nearly all aspects of regulation of cellular processes such as the action of cyclin-dependent kinases (CDK) in the cell cycle (Suryadinata et al., 2010), cyclic AMP second messengers for intercellular communication (Cheng et al., 1998), actin-activated ATPase activity of myosin for cellular motility (Scholey, 1986) and many more. The interest in phosphorylation in particular is that this form of PTM has also been implicated in demonstrating a potential role in the stress-responsive control of metabolic enzymes (Abboud and Storey, 2013). Studies have shown that RPP is crucial in various types of hypometabolic states, for instance mammalian hibernation (Storey, 1987a), aestivation (Childers and Storey, 2016), and anoxia tolerance (Brooks and Storey, 1993). Although, the direct effect of phosphorylation upon protein function has not been confirmed for all modifications, the data suggest that PTMs act as a fundamental method whereby the cell dynamically regulates metabolic pathways.

The reversible nature of phosphorylation allows cells to alter the conditions of the system in an energetically feasible manner. By selectively modifying the phosphorylation states of specific enzymes during stress conditions, metabolism can be suppressed or activated. Hence, it is not surprising that RPP has an integral role in wood frog freeze tolerance. During freezing events, phosphorylation modulates enzymes of glycolysis

enabling the production of cryoprotective agents such as glucose for freezing survival (Dieni and Storey, 2008; Dieni and Storey, 2011). Antioxidant defense enzymes in wood frogs such as catalase (Dawson and Storey, 2016) and superoxide dismutase (Dawson et al., 2015) are also modulated by RPP regulation. Therefore, changes in phosphorylation states are indicative of regulatory changes contributing to global MRD.

Freeze Tolerance Animal Model

Freeze tolerance is the ability to withstand the formation of extracellular ice crystals within the body and thereby endure prolonged exposures to subzero temperatures (Storey and Storey, 1992). The wood frog (*Rana sylvatica*) has garnered interest for its natural freeze tolerance and it is the major model for studies of freezing survival by a vertebrate animal. These amphibians are capable of surviving days or weeks with as much as 65% of their total body water trapped in extracellular ice masses (Storey, 1990). Wood frogs range over a vast area of North America from the Appalachian mountains of the southern USA, across the deciduous forests of the eastern USA and Canada, the northern boreal forests, and into most of Alaska (Lee et al., 1992). They exhibit geographic differences in freeze tolerance with Alaskan frogs able to survive down to temperatures approximately 10 degrees Celsius lower than the lethal limits for more temperate locales (Costanzo et al., 2015). The wood frog utilizes multiple adaptive mechanisms triggered by the onset of ice nucleation such as localization of extracellular ice formation (Knight and Duman, 1986), osmoregulation of cell volume (Neufeld and Leader, 1998), stabilization of subcellular composition (Crowe et al., 1987), and ischemia tolerance (Storey and Storey, 2017). The wood frog spends its winter seasons frozen amongst leaf litter on the boreal forest floor.

Ambient temperatures above the snowpack may drop as low as -20ºC but temperatures of the hibernacula generally fluctuate around 0°C to -5ºC and provide protection from dramatic changes in air temperature above the snowpack (Larson et al., 2014). Wood frogs assume a water-holding position by crouching into a ball; this helps to minimize desiccation while frozen. Internal ice nucleation begins at a gradual controlled pace mediated by skin contact with environmental ice or the action of non-specific nucleators such as gut bacteria in the intestinal lumen or INPs in the blood to trigger and regulate the distribution and size of ice crystal formation (Storey and Storey, 1985). The freeze tolerance capacity of the wood frog is aided by the activation of pro-survival pathways that increase the accumulation of cryoprotectants. Ice nucleation signals the liver to mobilize large quantities of glycogen in the form of glucose that is exported via the blood to other organs (Costanzo et al., 1993). The colligative properties of cryoprotectants protect intracellular fluids from freezing by increasing the solute concentration in the cell. During freezing, the wood frog may accumulate 250-300 mM glucose intracellularly as opposed to control levels at approximately 5 mM (Storey and Storey, 1984; Storey and Storey, 1986). Glucose serves as a cryoprotectant through its function in retaining enough water inside the cell to prevent damage to the subcellular architecture. Hence, not only does carbohydrate metabolism provide the means for ATP generation but also cryoprotection during freezing survival. The enzymes that maintain these biochemical pathways undergo their own regulation.

Life in the frozen state strips away the most basic of vital signs that sustain life. The heart stops beating, ventilation is halted and the blood ceases to pump, hence oxygen as a substrate for cellular biochemistry is not long a viable option. The wood frog copes

with limited oxygen by transiting from oxidative phosphorylation as the source of ATP production to anaerobic glycolysis during freezing. Lactate and alanine accumulate over time from pyruvate that is the terminal product of glycolysis with ATP produced from two substrate-level phosphorylation reactions (Storey and Storey, 1984). Without the ability to forage for food, glycogen and glucose become finite for the duration of the freeze. Hence, a shift to a lower metabolic rate can help to sustain life until environmental conditions are better suited for thawing. This is accomplished through downregulation of nonessential pathways and the maintenance and/or upregulation of pro-survival pathways towards a hypometabolic equilibrium. Characterization of MRD and hypometabolic states in the wood frog have been well studied. For example, the role of epigenetic mechanisms (Storey, 2015) and microRNA regulation of gene transcripts (Bansal et al., 2016) in governing MRD and freeze tolerance has recently been demonstrated. Another example would be the RPP involved in energetically demanding processes during wood frog freezing (Abboud and Storey, 2013). Although many animals provide fascinating strategies for winter survival, adaptations in preserving life at subzero temperature for this anuran illustrate the principles needed for a deeper understanding of organ cryopreservation and ischemic injuries.

Metabolic Enzymes

The mechanisms that dictate metabolic rate appear to involve a coordinated system of a specific subset of regulatory enzymes or proteins that modulate cellular processes (Storey and Storey, 1990). Most enzymes are specialized proteins (with the exceptions of ribozymes) that are responsible for lowering the activation energy required for a

biochemical reaction and thereby increase the rate of the reaction. These macromolecular biological catalysts alter the environment by stabilizing the transition state, providing an alternate reaction route, and/or by destabilizing the ground state of the substrate (Benkovic and Hammes-Schiffer, 2003; Warshel et al., 2006). Almost all metabolic processes require enzymatic catalysis to guide the reaction at a sufficient turnover rate in order sustain life. Hence, it is not surprising that key metabolic enzymes regulate MRD strategies during states of hypometabolism. Enzymes have specific functions that fall broadly into six classifications: (1) oxidoreductases; (2) transferases; (3) hydrolases; (4) lyases; (5) isomerases; and (6) ligases. This top-level organization features the ability of the enzymes to perform oxidation/reduction reactions, transfer functional groups, catalyze hydrolysis reactions, and cleave, isomerize, or join molecules, respectively, with amazing accuracy. For relevancy, the focus of the current thesis will be upon oxidoreductases or more specifically a subclass that known as dehydrogenases which oxidize a substrate by reducing an electron acceptor (such as NAD^+ or FAD). For this reason, dehydrogenases have a pivotal role in many aspects of metabolism ranging from carbohydrate breakdown to amino acid synthesis, for instance, lactate dehydrogenase (LDH) and glutamate dehydrogenase (GDH), respectively. Both enzymes are found ubiquitously within eukaryotes and use the reducing potential of oxidizing agents as cofactors to overcome the activation barriers of their biochemical reactions. GDH is an enzyme localized to the mitochondria where it plays a crucial role in the interconversion of glutamate and α-ketoglutarate (Schmidt and Schmidt, 1988), thereby playing key roles in both carbon and nitrogen metabolism (Stillman et al., 1993). LDH is localized to the cytoplasm and is responsible for the interconversion between lactate and pyruvate (Markert, 1984). By replenishing the NAD^+

that is needed by the glyceraldehyde-3-phosphate dehydrogenase reaction of glycolysis, LDH allows glycolysis to keep running to produce ATP when mitochondrial metabolism is compromised by lack of oxygen. Hence, both enzymes contribute their functions to their own pathways but overall play a larger role in the cell. During a state of freezing, the changes in metabolism can be studied through the shifts in the proteome.

Objective

Some animals possess the capacity to suppress their metabolic rate in order to survive environmental stresses. This requires the coordination of biochemical changes that are often mediated by PTMs. Many enzymes are regulated by this mechanism including many species that are capable of entering hypometabolic states, such as the freeze tolerant wood frog (*Rana sylvatica*). These animals survive cold temperatures by depressing their metabolic rate and entering hypometabolism that allows for prolonged catabolism of endogenous fuel reserves. In this state, fuel usage mainly depends upon glycogen reserves while ultimately preserving protein catabolism. However, sustaining long-term viability will inevitably drain carbohydrate resources such that protein may eventually also becomes a valuable source of fuel. To this end, fuels sources from carbohydrate versus nitrogenous sources undergo rigorous regulation by enzymes. The present research seeks to determine whether PTMs may provide differential regulation of the enzymatic activities of LDH and GDH in control versus frozen states. Studying the freeze tolerance induced by hypometabolism in the wood frog will provide insight for this phenomenon.

Hypotheses and Predictions

It is hypothesized that during hypometabolism, the enzymes LDH and GDH will both experience suppression of kinetic activity contributing a role in freeze tolerance survival as part of MRD strategy in the wood frog (*Rana sylvatica*) animal model. The following predications were experimentally tested:

1. The activity of muscle GDH in the glutamate-oxidizing direction will exhibit suppression during the frozen state, since the generation of α-ketoglutarate is not in demand for further oxidation in the Krebs cycle during anaerobiosis. In the glutamate-synthesizing direction, GDH will also be suppressed since major biosynthesis processes are downregulated during freezing, this would include glutamate synthesis.
2. The activity of liver LDH in the lactate-oxidizing direction will be suppressed since there will probably be an accumulation of pyruvate from anaerobic glycolysis. In the lactate-synthesizing direction, LDH will also be suppressed since lactate accumulation may be harmful; in addition, there are various other routes of removing pyruvate from the system whilst still regenerating NADH reducing potential.

Chapter 2 – Regulation of skeletal muscle glutamate dehydrogenase from a freeze tolerant wood frog

Introduction

The wood frog is one of just a few amphibians that is known to tolerate freezing of its body fluids as an adaptive strategy for winter survival (Costanzo and Lee, 2013; Storey and Storey, 2017). Situated in the subnivean space between the insulating layers of leaf litter and snow, the wood frog endures prolonged freezing exposures interspersed with intermittent thawing (Storey and Storey, 1988). Dramatic changes to its physiological and biochemical profiles are mandatory for winter survival involving adjustments such as depressed metabolic rate, coordination of ice growth through its body, and accumulation of glucose as a cryoprotectant during the onset of freezing (Storey and Storey, 2017). In addition, freeze-induced cessation of respiration and circulation impairs the ability for gas exchange and its distribution. This restricts access of both oxygen and nutrients to corporal tissues resulting in an anoxic state and ischemia that can lead to oxidative stress (Storey, 1990). Encased in ice for the majority of the winter months, the wood frog must rely solely on endogenous finite fuel sources for survival. On that account, a limited fuel reserve and extended period of inactivity are two major problems that affect tissues during freezing conditions. Fuel reserves are stored as glycogen in the liver in high amounts prior to freezing (Costanzo et al., 2015). At the onset of freezing, wood frogs trigger a massive hepatic glycogenolysis to produce glucose that is rapidly delivered to its corporal tissues prior to the cessation of circulation (Storey and Storey, 2017). Glucose is used as a cryoprotectant that permeates the cells of tissues and organs and by colligative action reduces the dehydration of cells that, in turn, limits the amount of extracellular ice that can form (Costanzo and Lee, 2013). Extracellular ice formation excludes solutes from the ice lattice and, hence, the concentration of solutes in the remaining extracellular fluid rises.

This draws water out of cells by osmosis since solute concentrations are greater extracellularly compared to inside the cell. By sequestering compatible solutes within the cell that are not freely permeable (i.e. glucose and urea), the cell is still able to retain some water that would otherwise be lost to extracellular ice. This can keep cell volumes from shrinking below a critical minimum where irreparable structural damage is done due to excessive compression. For example, accumulation of approximately 30 μmol/g dry weight of urea in skeletal muscle during wood frog freezing serves as both a means of cryoprotection and osmoprotection (Costanzo and Lee, 2005). Amphibians accumulate urea during a state of low water potential, which is an adaptive response to maintaining hydration in desiccating environments. The potential for freeze tolerance is highly dependent on the cryoprotectant levels that can be mobilized to the peripheral tissues prior to freezing (Costanzo et al., 1993). Therefore, both energy conservation and cryoprotective strategies are coordinated to sustain long-term survival in the freeze tolerant wood frog.

Despite the ability to tolerate freezing, the wood frog is not exempt from the detriments of ischemia stress and a risk of injury upon reperfusion during thawing recovery. Thus, maintenance of long-term viability of frozen muscle tissue under the ischemic conditions requires adjustments to cellular energetics (Dieni and Storey, 2011). During winter conditions, skeletal muscles exhibit >30% reduction in mass compared to summer frogs (Costanzo et al., 2015) although it is likely that muscular atrophy is also due to a proteolytic response that is induced by altered physiological state prior to freezing (Sridhara, 1979). It has also been shown that tissue-specific regulation of the anti-apoptotic pathway in the muscle tissue resulted in an overall decrease in apoptosis and an increase in cell survival during anoxic conditions (Gerber et al., 2016). Analogous studies during

hypometabolic conditions such as hibernation (West et al., 2006) and estivation (Hudson and Franklin, 2002) have shown reduced rates of protein synthesis and oxidative damage of muscle tissues. The energetic demands of the muscle due it its oxygen conformance and typical hypoxia-tolerance capacity suggest that hypoperfusion is possibly a key mechanism for MRD (West et al., 2006). Hence, skeletal muscle during freeze tolerance serves as a model for anoxia as well.

In the wood frog, freezing of the body is followed by extensive but reversible dehydration of the organs. Organ dehydration and the glycemic response often incur as a consequence of freezing, yet amphibians are well known for their prowess as regards dehydration tolerance (Churchill and Storey, 1995). It is understood that wood frogs exhibit marked geographical variation in freeze tolerance. The skeletal muscle was determined to be influenced by the magnitude of freezing, frozen frogs elicit around 23-29% dehydration for Ohioan phenotype (Costanzo et al., 2013) whereas about 50% dehydration was recorded for Alaskan wood frogs (Costanzo et al., 2015). Limited dehydration of the organs is not only confined to reducing mechanical damage to tissue structural architecture but it also reduced solvent volume by concentrating osmolytes (Lee and Costanzo, 1998). It was determined that concentrations of glucose levels increased considerably during the frozen state and the muscle itself has a storage of glycogen that can be used as fermentable fuel during the initial stages of freezing (Storey and Storey, 1984). Given the glucose and glycogen patterns already present, the muscle is capable of making a significant amount of its own glucose cryoprotectant from muscle glycogen storages.

Glutamate dehydrogenase (GDH; E.C. 1.4.1.3) is a regulatory enzyme that is a major link between amino acid and carbohydrate metabolism within eukaryotic cells,

hence, contributes a critical role in maintaining carbon and nitrogen balance. This enzyme is localized to the mitochondrial matrix and facilitates the reversible interconversion between L-glutamate to α-ketoglutarate and ammonium ion using $NAD(P)^+$-linked oxidative deamination. This two-step catalysis is initiated with the formation of α-iminoglutarate, a Schiff base intermediate formed between ammonium ion and α-ketoglutarate condensation releasing a water molecule (Fisher et al., 1982; Srinivasan et al., 1988). The Schiff base establishes the proper stereochemistry of the α-carbon atom of the hemiaminal to be protonated by NAD(P)H via hydride transfer forming the L-isomer of glutamate. This reaction is reversible, through the deprotonation of the α-amino group of L-glutamate. The hydride transfer to $NAD(P)^+$, forms the Schiff base intermediate (Stillman et al., 1993). The second-step follows the attack of a water molecule on the α-carbon atom of the Schiff base intermediate releasing ammonia and α-ketoglutarate. The extensive production of free ammonia in tissue is highly toxic for cells. In amphibians, excess ammonia is commonly converted to urea for excretion.

Under conditions of amino acid catabolism, α-ketoglutarate is shuttled toward to the Krebs cycle to generate NADH and $FADH_2$ reducing potential for ATP production via oxidative phosphorylation. Under aerobic conditions where GDH undergoes amino acid anabolism, the Krebs cycle contributes the bulk of the reducing potential (i.e. NADH and $FADH_2$) that perpetuates the electron transport chain (ETC). Hence, not only does GDH contribute a substantial link towards the Krebs through its catalytic product α-ketoglutarate but the ammonia byproduct also serves a major role in nitrogen metabolism via ureagenesis. Ammonia is toxic to cells and causes tissue damage, thus the cell has various ways of restricting the levels of free ammonia (Martinelle and Häggström, 1993). The

ammonia released during the reaction may be protonated by free-floating bicarbonate ions in the system producing ammonium ion and carbon dioxide. Often organisms release the ammonia via ammonium directly into the surrounding environment (i.e. aquatic animals) or as nitrogenous waste bound to carbohydrate in the form of urea (i.e. mammals) or uric acid (i.e. reptiles and birds) which is released through excretion. In mammals or amphibians, synthesis of urea from ammonia occurs in the urea cycle, which occurs primarily in the liver and to a lesser extent in the kidney. It is important to note that urea also plays an important role during freeze tolerance within the wood frog as a cryoprotectant.

Reversible transamination reactions involving glutamate are a primary process by which amino groups are introduced onto carbon skeletons to synthesize amino acids, and, oppositely, a primary route to deaminate amino acids. GDH can also catalyze the reverse reaction by combining ammonium to α-ketoglutarate forming L-glutamate, whereby oxidizing NADH to NAD^+. L-glutamate is an amino acid used by almost all living things during the biosynthesis of proteins. This catalysis mediated by GDH is an important gate entry to the biosynthesis of numerous amino acids (glutamate, glutamine, arginine, and proline). Amino acid synthesis and consequentially the synthesis of proteins are both energetically costly ventures. Hence, regulation is important when organisms are confronted with extreme environmental stress such as subzero temperatures and lack of food associated with the winter season. The role of GDH links amino acid and carbohydrate metabolism in the cell, both of which are valuable commodities when resources are scarce. Elucidation of the properties of GDH from skeletal muscle of frozen frogs was accomplished in this study. The function of enzymes are implicated by their regulation of

kinetic properties. These modulations are suspected to arise from RPP invoking a structural change in enzyme conformation between control and frozen forms of GDH. The changes observed will provide insight into the regulation of GDH and its functions in amino acid metabolism, urea production, and global MRD during the freeze tolerance of the wood frog.

Materials and Methods

Animals

Male wood frogs (*R. sylvatica*) were captured from the Ottawa, Ontario region during the spring season. Animals were washed in a tetracycline bath prior to being placed in plastic containers with damp sphagnum moss at 5ºC for one week. Control conditioned frogs were sampled from this treatment. For freezing exposure, frogs were placed in closed plastic boxes with damp paper toweling layered basally and placed in an incubator set at -4ºC. A cooling period of 45 minutes was allowed for body temperature of frogs to adjust to below -0.5ºC and trigger nucleation due to skin contact with ice crystals formed on moist toweling. Control and frozen frogs were euthanized by pithing. Striated hind-leg skeletal muscle was immediately excised and flash-frozen in liquid nitrogen. All tissue samples were stored at -80ºC until use. The Carleton University Animal Care Committee, in accordance with the Canadian Council on Animal Care guidelines, approved all animal handling protocols used in this study.

Preparation of muscle tissue lysates for protein purification

Flash-frozen muscle tissue samples were crushed under liquid nitrogen and homogenized 1:5 w:v in ice-cold homogenization buffer A (25 mM MES buffer at pH 6.2,

25 mM β-glycerophosphate, 2.5 mM EDTA, 2.5 mM EGTA, 15 mM 2-mercaptoethanol and 10% v:v glycerol) with the addition of a couple of crystals of phenylmethylsulfonyl fluoride (PMSF). Samples were homogenized on ice with a Polytron PT1000 homogenizer, and then centrifuged at 13,500 × *g* at 4ºC for 30 minutes. Supernatant was decanted and stored at 4ºC until used in the following protein purification.

Purification of glutamate dehydrogenase (GDH)

A 4.0 mL aliquot of crude supernatant was applied to a carboxymethyl-Sepharose® (CM) anionic-exchange chromatography column (1.5 cm × 4 cm), previously equilibrated with 50 mL of homogenization buffer A. The CM column was then washed with 50 mL homogenization buffer A to elute unbound proteins. GDH activity was then eluted from the CM column utilizing a pH gradient, pH 6.2–8.0 (adapted from Scopes, 1977) from homogenization buffer A to homogenization buffer B (consisting of 25 mM TRIS buffer at pH 8.0, 25 mM β-glycerophosphate, 2.5 mM EDTA, 2.5 mM EGTA, 15 mM 2-mercaptoethanol and 10% v:v glycerol) across a 30 mL volume. A final additional 10 mL of homogenization buffer B was used to elute the remaining column volume. Fractions of 40 drops per tube (approximately 1.4 mL) were collected using an automated fraction collector (Gilson Medical Electronics Inc., Middleton, WI, USA) and 15 µL from each fraction was assayed to detect GDH activity (cf. enzyme kinetic assay for methodology). Peak fractions of GDH activity were pooled and used for subsequent analysis.

Determination of relative protein concentrations

Soluble protein concentrations of extracts were determined by the Bio-Rad protein assay adapted from Bradford (1976) using Bio-Rad Protein Assay Dye Reagent Concentrate (Bio-Rad; Cat. No. 500-0006). Briefly, dye reagent concentrate was diluted 1:4 v:v with dH_2O. Aliquots of 10 µL protein samples were added to 190 µL of diluted dye reagent in a 96-well microplate and incubated for 5 minutes to maximize dye binding. Relative absorbance was recorded using Thermo Labsystem Multiskan spectrophotometer (Thermo Scientific, Waltham, MA, USA) at 595 nm. Protein concentrations were then interpolated using a bovine serum albumin (BSA) standard curve.

Enzyme kinetic assay

GDH activity was measured spectrophotmetrically at 340 nm using a Multiskan plate reader with high shaking. Optimized reactions for maximal activity in the glutamate-synthesizing direction were carried out in a total volume of 200 µL containing of 15 µL of enzyme sample, 0.2 mM NADH, 200 mM NH_4Cl, and 1 mM α-ketoglutarate. Optimal conditions for the glutamate-oxidizing direction were determined to consist of 15 µL of enzyme preparation, 1 mM NAD^+, and 50 mM L-glutamate in a total volume of 200 µL. Assays were initiated with the final addition of GDH enzyme. K_m and I_{50} values were determined from modifications of the above optimal conditions where one parameter (substrate or inhibitor) was varied while all other reaction conditions were those stated above. Note that I_{50} GTP and K_a ADP parameters were also assessed at optimal substrate concentrations values.

SDS-Polyacrylamide Gel Electrophoresis (SDS-PAGE)

Purification of GDH was assessed using SDS-PAGE analysis. Samples containing GDH were mixed in 5:1 v:v with a modified Laemmli loading buffer (consisting of 100 mM TRIS at pH 6.8, 4% w:v SDS, 20% v:v glycerol, 0.2% w:v bromophenol blue, and 10% v:v 2-mercaptoethanol) and boiled for 5 minutes prior to storage at -20ºC until use. Samples were loaded on a 5% stacking gel (125 mM TRIS at pH 8.8, 5% v:v acrylamide/bis-acrylamide, 0.1% w:v SDS, 0.15% w:v ammonium persulfate (APS), and 0.1% v:v TEMED) and resolved on a 10% SDS-polyacrylamide gel (400 mM TRIS at pH 6.8, 10% v:v acrylamide/bis-acrylamide, 0.1% w:v SDS, 0.2% w:v APS, and 0.1% v:v TEMED). Proteins were electrophoretically separated using the Mini-PROTEAN Tetra Cell system (Bio-Rad, Hercules, CA, USA) at room temperature under constant voltage at 180 V for 55 minutes in SDS-PAGE running buffer (25 mM TRIS-base at pH 8.5, 190 mM glycine, and 0.1% w:v SDS). A molecular standard PiNK Plus Prestained Protein Ladder (GeneDireX, Inc., Cat. No. PM005-0500) and a commercially purified sample of GDH from bovine liver (Sigma Life Science, Cat. No. G2626) were also run on every gel. Following completion of gel electrophoresis, the gels were either (1) stained directly in Coomassie blue solution or (2) transferred onto polyvinylidene difluoride (PVDF) membrane for Western blotting.

For direct staining using Coomassie blue, the gels were submerged in Coomassie blue staining solution (0.25 % w:v Coomassie brilliant blue, 7.5% v:v acetic acid, and 50% v:v methanol) with gentle rocking motion for approximately 2 hours. Gel were then transferred to destaining solution (10% v:v acetic acid and 25% v:v methanol) overnight with gentle rocking. The gels were rehydrated in dH_2O until protein bands become

apparent. Images were recorded using ChemiGenus Bio Imaging System (Syngene, Frederick, MD, USA).

Western blotting

Protein immunoblotting was used for identification of GDH and to assess changes in posttranslational modifications (PTMs) between partially purified GDH from control and 24-hour frozen frogs. Following completion of SDS-PAGE separation, the proteins were transferred onto methanol-activated PVDF membrane using a wet transfer procedure. Electroblotting was carried out in the Mini Trans-Blot® Cell (Bio-Rad, Hercules, CA, USA) at 4ºC under constant amperage at 160 mA for 110 minutes in transfer buffer (25 mM TRIS-base at pH 8.5, 190 mM glycine, and 20% v:v methanol). Following completion of wet transfer, the membrane was washed 3 × 5 minutes in Tris-buffered saline with Tween 20 (TBST; 20 mM TRIS-base at pH 7.6, 140 mM NaCl, and 0.05% v/v Tween-20) at room temperature with gentle rocking. Full membranes were incubated separately in the following primary antibodies overnight at 4ºC with gentle rocking:

(1) Anti-glutamate dehydrogenase rabbit polyclonal (Applied Biological Materials Inc., Cat. No. Y052277) diluted 1:2000 in TBST;

(2) Anti-phosphoserine rabbit polyclonal (Invitrogen, Cat. No. 61-8100) diluted 1:1000 in TBST;

(3) Anti-phosphothreonine rabbit polyclonal (Invitrogen, Cat. No. 71-8200) diluted 1:1000 in TBST;

(4) Anti-phosphotyrosine mouse monoclonal (Invitrogen, Cat. No. 13-6600) diluted 1:1000 in TBST;

(5) Anti-methylated lysine rabbit polyclonal (StressMarq Biosciences Inc., Cat. No. SPC-158) diluted 1:1000 in TBST.

Primary antibody solutions were removed the following day. The membranes were washed 3 × 5 minutes in TBST prior to incubation with peroxidase-conjugated secondary antibody towards the respective host epitope for 20 minutes at room temperature with gentle rocking:

(1) Goat anti-rabbit IgG [H&L] (BioShop Canada Inc., Cat. No. APA007P) diluted 1:8000 in TBST;

(2) Rabbit anti-mouse IgG [H&L] (BioShop Canada Inc., Cat. No. APA005P) diluted 1:8000 in TBST.

Secondary antibodies were removed prior to 3 × 5 minute washes in TBST. Membranes were visualized by enhanced chemiluminescence (ECL) with a mixture of hydrogen peroxide and luminol for detection using ChemiGenius Bio Imaging System (Syngene, Frederick, MD, USA). After a satisfactory exposure was captured, the membranes were stained with Coomassie blue to visualize protein loaded into each lane for use in standardizing ECL signals to protein amount. Immunoblot quantification and densitometry analysis was performed using GeneTools Image Analysis Software (Syngene, Frederick, MD, USA, v. 4.02).

Data and Statistical Analysis

All enzyme kinetics data were analyzed using Microplate Analysis program (MPA; Brooks, 1994) and kinetic parameters were calculated using nonlinear least-squares regression program (Kinetics v. 3.51; Brooks, 1992) modelled to the Hill equation ($h > 0$) in order to determined K_m and I_{50} values.

All statistical analysis was performed using SigmaPlot (Systat Software Inc., San Jose, CA, USA, v. 12.5). Data between control and 24-hour frozen samples were analyzed using two-tailed Student's *t*-test with accounting for multiple variance; a statistical difference was accepted where $p < 0.05$.

Results

Purification of GDH from the skeletal muscle of R. sylvatica

GDH was functionally purified from skeletal muscle tissue of control and 24-hour frozen *R. sylvatica* with the use of CM column chromatography and elution with a pH 6.2 – 8.0 gradient (Figure 2.1). Collection and pooling of the peak tubes of eluate from the CM column yielded a 5.12- and 5.49-fold purification of the control and frozen forms of GDH, respectively (Table 2.1). The overall purification resulted in a final specific activity of 17.8 mU/mg for control GDH with a final yield of 19.5% while the frozen form of GDH had a specific activity of 18.3 mU/mg with a final yield of 18.2% (Table 2.1). In parallel, the purification of both control and frozen forms of GDH resulted in similar values for specific activity, fold purification, and activity yield when starting from a similar initial tissue mass.

As a result of this single-step purification scheme, GDH was functionally purified, with some contaminating proteins remaining, as determined by gel electrophoresis and visualized by Coomassie blue staining (Figure 2.2). The identity of GDH was determined by Western blot analysis using a protein-specific anti-GDH antibody (see Supplementary Figure 1). GDH had an apparent subunit molecular weight of ~60 kDa as determined by SDS-PAGE relative migration distance (Figure 2.2).

Basic kinetic properties of GDH

Analysis of GDH from skeletal muscle of control and frozen wood frogs revealed that the enzyme displayed hyperbolic substrate saturation in both the glutamate-oxidizing direction (Figure 2.3a) and glutamate-synthesizing direction (Figure 2.3b). Let it be noted that all statistically significant values were accepted with $p < 0.05$ via Student's *t*-test unless otherwise stated. In the glutamate-oxidizing direction, K_m value for glutamate was 7.8-fold higher in the frozen condition (2.51 ± 0.18 mM) compared to the control value (0.32 ± 0.03 mM). In same catalytic direction, the K_m NAD^+ showed a 25% decrease from control conditions (967 ± 61.6 μM) to the frozen (725 ± 74.6 μM) forms of GDH.

In the opposite glutamate-synthesizing direction, the analysis of K_m α-ketoglutarate showed no significant changes between control and frozen conditions (Table 2.2). However, the analysis of I_{50} α-ketoglutarate found a significant 1.1-fold increase between control (1.26 ± 0.05 mM) and frozen (1.41 ± 0.01 mM) conditions. Moreover, there was a 2.0-fold increase in the K_m NH_4^+ between control (30.5 ± 0.68 mM) and frozen (60.3 ± 0.18 mM) conditions.

Kinetic activity of GDH with ADP activation

Kinetic parameters under the influence of ADP activation were found to be significantly different in some instances between the control and frozen conditions. In the glutamate-oxidizing direction with ADP present, no significant differences were found for either K_m glutamate (6.39 ± 0.01 mM) or K_m NAD^+ (84.4 ± 1.44 μM) between control and frozen (6.03 ± 0.17 mM and 55.1 ± 10.8 μM, respectively) forms of GDH (Table 2.2). In the glutamate-synthesizing direction during ADP activation, the analysis of K_m α-

ketoglutarate also revealed no significant changes between control and frozen conditions. However, a 2.1-fold increase was noted for I_{50} α-ketoglutarate values between GDH from control (14.7 ± 1.96 mM) and frozen (30.3 ± 1.17 mM) states. The analysis of K_m NH_4^+ in the presence of ADP showed a significant 17% decrease between control (31.4 ± 0.89 mM) and frozen (26.1 ± 0.54 mM) forms of GDH.

ADP activation dramatically increased GDH maximal activity, as seen by the ADP-dependent fold increase in glutamate relative V_{max} of 1.92 ± 0.13 in the glutamate-oxidizing direction for control GDH, and a 2.55 ± 0.11 fold increase for frozen GDH (Table 2.2). In the glutamate-synthesizing direction, there was also an increase in relative V_{max} with α-ketoglutarate as the substrate by 5.97 ± 0.40 fold in the presence of ADP in the control condition and by 2.36 ± 0.05 fold for the frozen form of GDH.

Table 2.3 tabulates the activator concentration producing half-maximal enzyme activation (K_a) of ADP. Analysis of K_a ADP in the glutamate-oxidizing direction showed no statistical changes in this parameter between the control conditions (2.77 ± 1.20 μM with a fold activation of 3.46) compared to frozen GDH (2.77 ± 0.27 μM with fold activation of 3.37). In the opposite glutamate-synthesizing direction, however, the K_a ADP decreased by 75% between control GDH (15.3 ± 1.09 μM with fold activation of 4.31) and enzyme from frozen frogs (3.87 ± 0.59 μM with fold activation of 2.64).

Kinetic activity of GDH with GTP regulation

GTP is a potent inhibitor of GDH and its influence on GDH is shown in Table 2.3. In the glutamate-oxidizing direction, the analysis of I_{50} GTP showed no statistical difference between the enzyme from control (12.7 ± 4.60 nM) and frozen (15.1 ± 1.11 nM)

conditions. The same was also true in the glutamate-synthesizing condition, where there was no significant change between control (5.53 ± 0.39 nM) and frozen (4.49 ± 0.72 nM) I_{50} GTP values in the absence or presence of ADP (Table 2.3). However, when 0.5 mM ADP was added the I_{50} GTP of control GDH increased dramatically (1300 ± 86.7 nM) by 102-fold compared to the I_{50} GTP without ADP. Likewise, in the frozen condition I_{50} GTP in the presence of ADP (1140 ± 86.1 nM) increased by 76.1-fold compared to just GTP without ADP. Distinct statistically significant changes ($p < 0.05$) were also observed for the glutamate-synthesizing direction, where the control form of GDH showed an I_{50} GTP in the presence of ADP of 423 ± 9.77 nM, a dramatic 76.6-fold increase compared to the I_{50} without ADP. Similarly, an increase of 98.9-fold was observed for GDH from frozen frogs with I_{50} GTP in the presence of 0.5 mM ADP being 444 ± 8.61 nM compared to in the presence of just GTP alone.

Post-translational modifications of GDH

Western blot analysis was used to identify GDH among other proteins during electrophoretic separation (Supplementary Figure 1). Western blot was also used to assess potential PTMs between control and frozen forms of partially purified skeletal muscle GDH. Phosphorylation on serine residues of the frozen form of GDH was determined to be 2.5-fold greater ($p < 0.05$) than on the control form of GDH (Figure 2.4). However, there were no significant changes between phosphorylation of threonine or tyrosine residues, and no observed difference in methylated lysine residues between control and frozen conditions.

Table 2.1. Partial purification and yield of muscle GDH from ~1.0 g tissue of (a) control and (b) 24-hour frozen *R. sylvatica*.

(a) Steps	Total Protein (mg)	Total Activity (mU)	Specific Activity (mU/mg)	Fold Purification	Activity Yield (%)
Crude	13.4	46.7	3.47	--	--
Carboxymethyl[1]	0.83	14.8	17.8	5.12	19.5

(b) Steps	Total Protein (mg)	Total Activity (mU)	Specific Activity (mU/mg)	Fold Purification	Activity Yield (%)
Crude	15.2	50.8	3.34	--	--
Carboxymethyl[1]	1.14	21.0	18.3	5.49	18.2

1. Carboxymethyl GDH activity was eluted with pH 6.2–8.0 gradient

Table 2.2. Kinetic parameters of partially purified muscle GDH from control and 24-hour frozen *R. sylvatica*.

Parameter	Control ± SEM	Frozen ± SEM
Glutamate-oxidizing direction (glutamate → α-ketoglutarate, pH 8.0)		
K_m L-glutamate (mM)	0.32 ± 0.03	2.51 ± 0.18[a]
K_m NAD^+ (μM)	967 ± 61.6	725 ± 74.6[a]
K_m L-glutamate (mM) + 0.5 mM ADP	6.39 ± 0.01[b]	6.03 ± 0.17[b]
K_m NAD^+ (μM) + 0.5 mM ADP	84.4 ± 1.44[b]	55.1 ± 10.8[b]
Relative V_{max} (0.5 mM ADP/no ADP)	1.92 ± 0.13	2.55 ± 0.11[a]
Glutamate-synthesizing direction (α-ketoglutarate → glutamate, pH 7.2)		
K_m α-ketoglutarate (mM)	0.25 ± 0.02	0.21 ± 0.01
I_{50} α-ketoglutarate (mM)	1.26 ± 0.05	1.41 ± 0.01[a]
K_m NH_4^+ (mM)	30.5 ± 0.68	60.3 ± 0.18[a]
K_m α-ketoglutarate (mM) + 0.5 mM ADP	0.60 ± 0.04[b]	0.52 ± 0.01[b]
I_{50} α-ketoglutarate (mM) + 0.5 mM ADP	14.7 ± 1.96[b]	30.3 ± 1.17[ab]
K_m NH_4^+ (mM) + 0.5 mM ADP	31.4 ± 0.89	26.1 ± 0.54[ab]
Relative V_{max} (0.5 mM ADP/no ADP)	5.97 ± 0.40	2.36 ± 0.05[a]

a. – indicates a significant statistical difference between control and 24-hour frozen conditions via Student's *t*-test, two-tailed, $p < 0.05$

b. – indicates a significant statistical difference between no ADP and addition of 0.5 mM ADP via Student's *t*-test, two-tailed, $p < 0.05$

Table 2.3. Effects of activator and inhibitor on kinetic parameters of GDH from muscle of control and 24-hour frozen *R. sylvatica*.

Parameter	**Control ± SEM**	**Frozen ± SEM**
Glutamate-oxidizing direction (glutamate → α-ketoglutarate, pH 8.0)		
I_{50} Mg-GTP (nM)	12.8 ± 4.60	15.1 ± 1.11
I_{50} Mg-GTP (nM) + 0.5 mM ADP	1300 ± 86.7[b]	1140 ± 86.1[b]
K_a ADP (μM) [Fold Activation]	2.77 ± 1.20 [3.46]	2.77 ± 0.27 [3.37]
Glutamate-synthesizing direction (α-ketoglutarate → glutamate, pH 7.2)		
I_{50} Mg-GTP (nM)	5.53 ± 0.39	4.49 ± 0.72
I_{50} Mg-GTP (nM) + 0.5 mM ADP	424 ± 9.77[b]	444 ± 8.61[b]
K_a ADP (μM) [Fold Activation]	15.3 ± 1.09 [4.31]	3.87 ± 0.59[a] [2.64]

a. – indicates a significant statistical difference between control and 24-hour frozen conditions via Student's *t*-test, two-tailed, $p < 0.05$

b. – indicates a significant statistical difference between no ADP and addition of 0.5 mM ADP via Student's *t*-test, two-tailed, $p < 0.05$

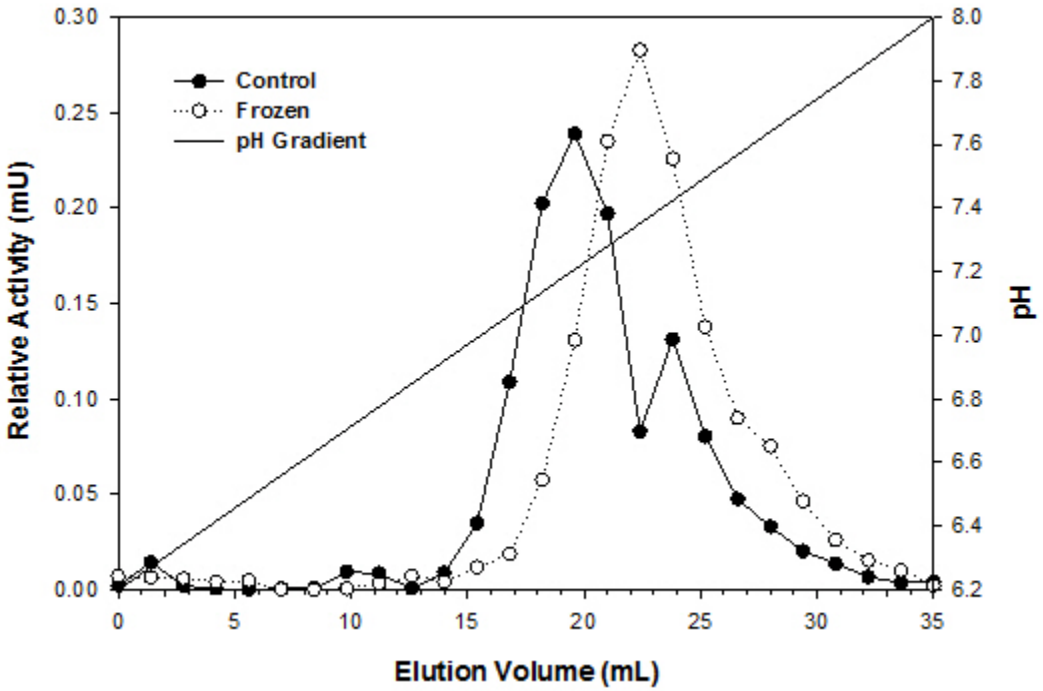

Figure 2.1. Typical carboxymethyl-Sepharose elution profile for relative GDH activity from muscle tissue of control and 24-hour frozen *R. sylvatica* using pH 6.2–8.0 gradient. Elution profiles for control and 24-hour frozen samples are from different purification trials but superimposed for viewing convenience. Elution profiles also exclude prior wash steps with homogenization buffer after addition of sample.

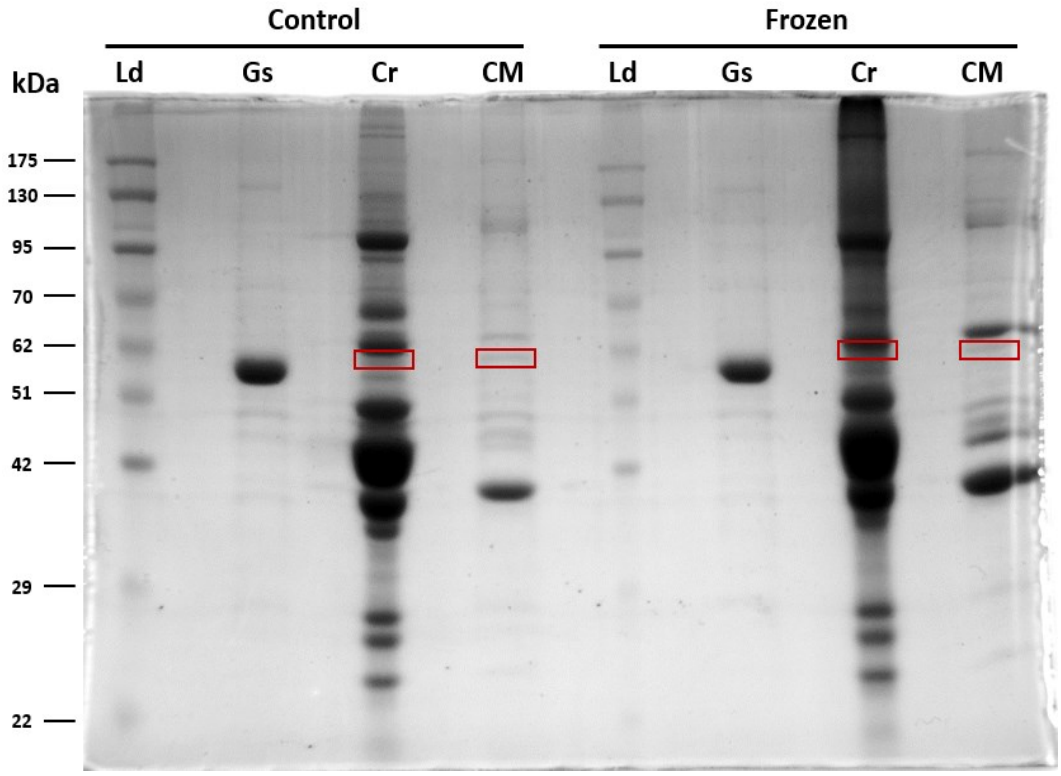

Figure 2.2. A 10% resolving SDS-PAGE run at 180 V for 55 minutes for the sequential partial-purification of muscle GDH from control and 24-hour frozen *R. sylvatica*. The band for GDH boxed at approximately 60 kDa. Ld, Molecular weight ladder (FroggaBio); Gs, GDH standard (Sigma Life Science); Cr, crude homogenate; CM, pooled peak fractions from carboxymethyl-Sepharose eluate.

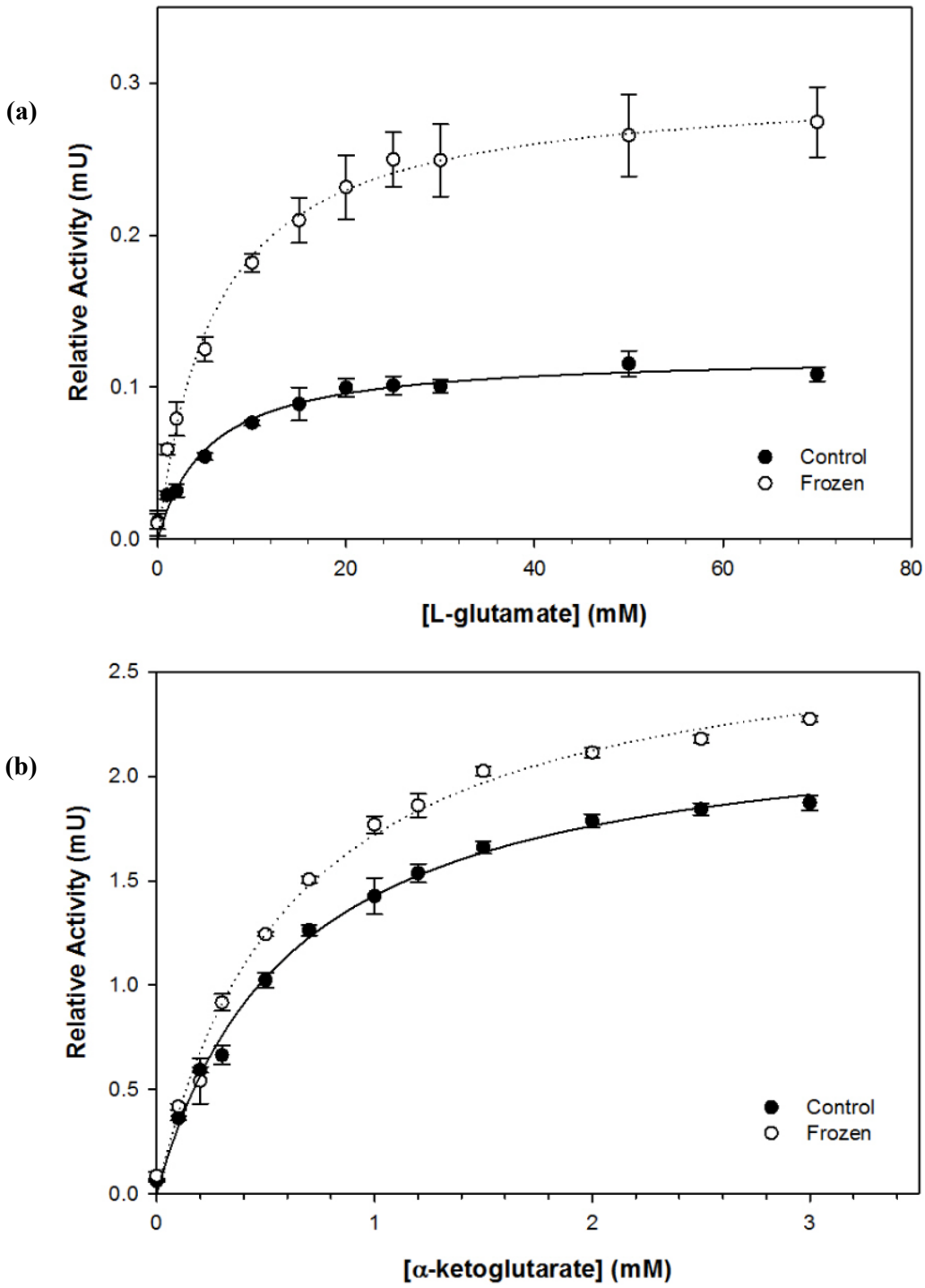

Figure 2.3. Michaelis-Menten plots used to extract the substrate concentration producing half-maximal enzyme velocity (K_m) catalyzed by functionally purified GDH from muscle of control and 24-hour frozen *R. sylvatica* in the (a) glutamate-oxidizing direction and (b) glutamate-synthesizing direction both with ADP activation. Data expressed as mean ± SEM (n = 3-4), independent replicates on enzyme samples.

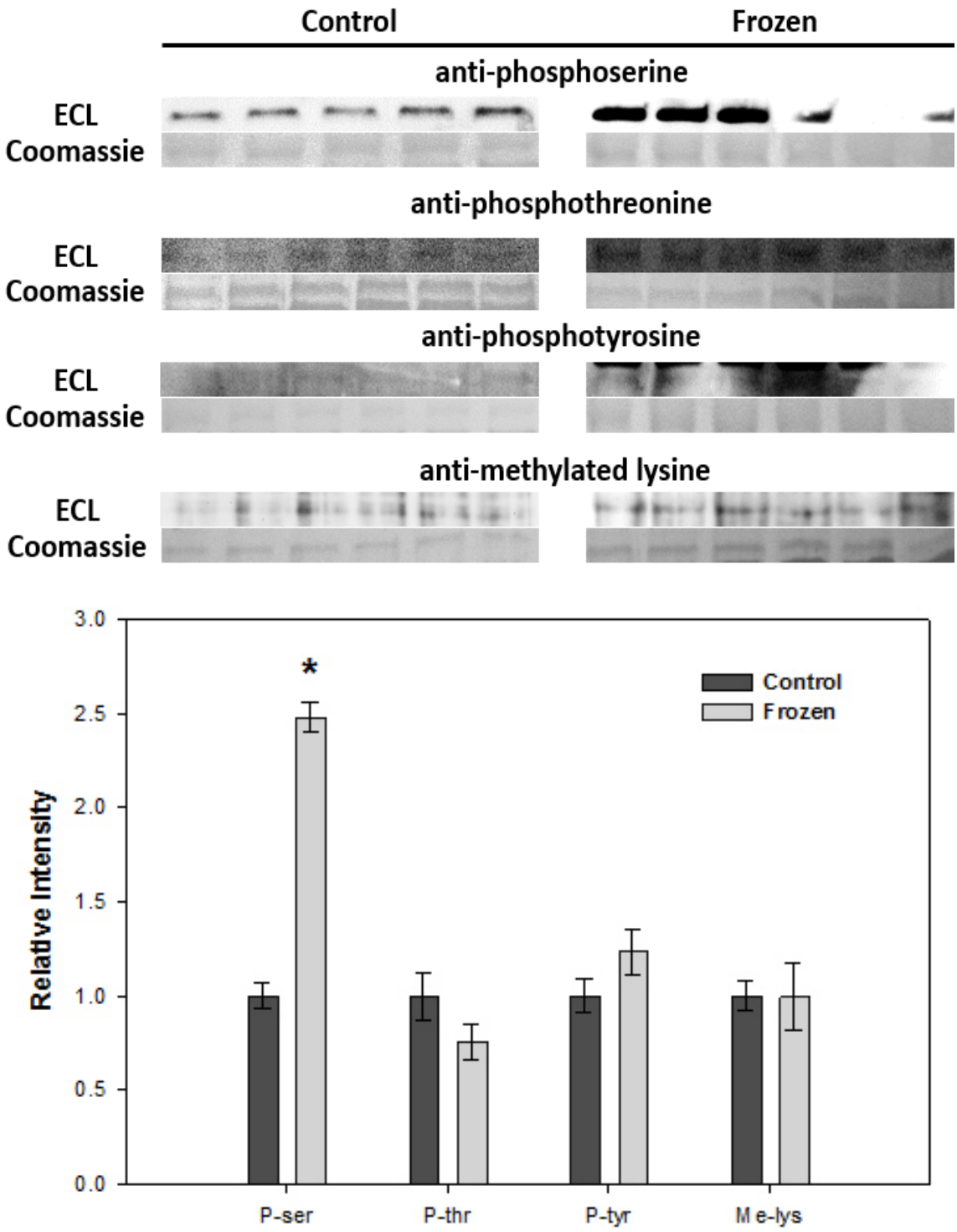

Figure 2.4. Quantification of post-translational modifications of GDH from muscle tissue of control and 24-hour frozen *R. sylvatica*. Chemiluminescence signal intensities were standardized to the protein loaded amount (as determined by secondary Coomassie staining). Data for GDH from frozen muscle expressed are relative to control values set to 1. Data expressed as mean ± SEM (n = 5-6). * – indicates a significant statistical difference between control and 24-hour frozen conditions via Student's t-test, two-tailed, $p < 0.05$.

Discussion

Certain species of amphibians exhibit an extraordinary ability to sustain life at subzero temperatures. The wood frog possesses a novel ability to tolerate freezing by entering a state of hypometabolism that largely depends on MRD to decrease energetic demand when fuel resources and oxygen becomes a limiting factor. Regulation of MRD that occur at the enzyme-level serves as a valuable area for investigating mechanisms that govern biochemical pathways. Enzymes such as GDH plays an important role in unifying both carbon and nitrogen metabolism (Stillman et al., 1993). Localized in the mitochondria of eukaryotes, GDH is responsible for the reversible $NAD(P)^+$-linked oxidative deamination of L-glutamate to α-ketoglutarate and ammonia. This makes GDH a fascinating target for analysis, since the substrates and products of GDH are linked to the Krebs cycle, urea cycle, and biosynthesis of various other amino acids (e.g. glutamine, proline, and arginine). The role of skeletal muscle GDH in freeze tolerance was investigated in this study. It is postulated that GDH kinetic properties are regulated through PTMs, which alters the functionality of the enzyme leading to a shift in metabolism towards a poise that is beneficial for freezing survival. Many types of PTMs of proteins and enzymes have been identified but their presence and purpose remains unknown. Work on animal adaptation to environmental stress has demonstrated a widespread influence on RPP in terms of individual enzyme modulation and global MRD (Storey and Storey, 2007). Studies to date have identified a variety of metabolic enzymes found within the skeletal muscle of the wood frog but have yet to be further studied in greater detail (Storey and Storey, 1984). The comparative regulation of GDH has also been studied in a multitude of organisms that experience states of hypometabolism. For instance, the anoxia-tolerant

freshwater turtle (Bell and Storey, 2012), hypoxia-tolerant crayfish (Dawson and Storey, 2012), hibernating ground squirrel (Bell and Storey, 2010), aestivating snails (Ramnanan et al., 2009), and albeit to a lesser degree even the freeze tolerant wood frog (Costanzo et al., 2013). This lack of knowledge of the molecular regulation of wood frog GDH provided the motivation to analyze the properties, regulation, and PTMs of the wood frog muscle enzyme to provide insight into features that facilitate GDH function during freezing. This present study demonstrates that GDH isolated from skeletal muscle of control versus frozen wood frogs displays significantly different properties that strengthen the link between phosphorylation states to kinetic activity.

Skeletal muscle GDH from the tissues of control and 24-hour frozen wood frogs was functionally purified via carboxymethyl-Sepharose column chromatography using a pH-gradient elution (Scopes, 1977). The crude enzyme activity was determined to be 3.47 mU/mg soluble protein for control and 3.34 mU/mg for frozen GDH. This corresponds well with specific enzyme activity ranging between 2.2 to 3.8 mU/mg obtained by Costanzo et al. (2013) detected in crude homogenates in Alaskan wood frogs muscle tissue. Both conditions resulted in a little over 5-fold purification following anionic-exchange chromatography to a final sample with similar activity yield at approximately 18.2-19.5% between control and frozen forms of GDH (Table 2.1). The straightforwardness of column chromatography demonstrates a reproducible means of purifying this enzyme.

Kinetic analysis revealed significant differences in the properties of skeletal muscle GDH between the enzyme from control and frozen conditions. These findings suggest enzymatic regulation that contributes to wood frog endurance of freezing conditions (Table 2.2). The most striking difference is the 7.8-fold decrease of glutamate affinity by the

frozen form of GDH, the K_m glutamate rising from 0.32 ± 0.03 mM for control GDH to 2.51 ± 0.18 mM for frozen GDH. This suggests that GDH-mediated α-ketoglutarate production during freezing is undesirable. During the anoxic state of freezing, the Krebs cycle is metabolically suppressed (Solaini et al., 2010). Hence, Krebs cycle intermediates such as α-ketoglutarate generated from solely glutamate might not serve any purpose during the anoxic conditions of freeze tolerance. Other enzymes such as alanine aminotransferase (ALT) or aspartate aminotransferase (AST) have dual functions linking glutamate to pyruvate or oxaloacetate, respectively, to provide more accessible fuel sources. It is quite possible that the function of ALT and AST supersedes that of GDH during freezing as alanine levels do rise dramatically within leg muscle tissue and aspartate levels decrease substantially during freezing (Storey and Storey, 1986). This coincides with other studies that have shown decreased glutamate affinity during hypoxia indicative of reduced Krebs cycle activity (Bell and Storey, 2010; Bell and Storey, 2012; Dawson and Storey, 2012). It is well known that anaerobic glycolysis is activated during freezing and that oxidative phosphorylation ceases to become a means of ATP production once freezing shuts down breathing and blood circulation (Storey and Storey, 2017). Hence, the glutamate-oxidizing direction of GDH during the frozen state seems to be unfavorable. The central role of glutamate in amino acid synthesis means it is not an amino acid to be catabolized frivolously although it is one of the few that can be used anaerobically. Moreover, the overall pool size of glutamate in the cells is a lot lower than compared to the pools of lipids or glycogen, which can generate a huge amount of acetyl-CoA when they are used as aerobic fuel source. To this end, solely converting glutamate to α-ketoglutarate

does not serve as net contribution to metabolic fuels in terms of downstream energy potential.

In addition to changes in the K_m glutamate, several other kinetic parameters shifted between control and frozen states, supplying further differences between the two forms of GDH. The K_m ammonium was 2-fold higher for the frozen enzyme compared with the control value meaning that the affinity towards ammonium was decreased during freezing. This decrease in affinity may indicate that a rise in systemic ammonium ion concentration is not a trigger for GDH activity during the frozen state. The urea is accumulated for cryoprotection and it is also apparent that ammonia production slowed down (Storey and Storey, 1986). The result is consistent with the decreased GDH activity of the glutamate-synthesizing reaction using ammonia as seen in this study (Table 2.2). Moreover, the reduction in glutamate production seems intuitive since it is well established that protein synthesis is almost inactive during freezing (Storey and Storey, 2017), and the foregoing amino acid synthesis would also be negligible (Costanzo et al., 2015). Another supporting aspect is that GDH activity would be reduced in the frozen state as indicated by the influence by effector molecules. For instance, Table 2.3 shows that frozen GDH was more sensitive to GTP inhibition than control GDH in the presence of ADP activation (i.e. lower I_{50} GTP). Furthermore, frozen GDH was significantly less sensitive to activation by ADP when compared to the control GDH form (i.e. higher K_a ADP). The decrease sensitivity to the adenosine moiety suggests that GDH activity is less likely to be enhanced by the effects of ADP during freezing (Prough et al., 1973). These findings correlate well with the response to anoxia exposure by GDH in the anoxia-tolerant freshwater turtle (Bell and Storey, 2012), since freeze tolerance does engender anoxia-like responses.

The majority of the kinetic properties assessed were consistent with a less active form of GDH in the frozen state, but there are some deviations from this trend. In the glutamate-synthesizing direction, the K_m α-ketoglutarate did not differ between control (0.25 ± 0.02 mM) and frozen (0.21 ± 0.01 mM) forms of GDH. This implies that binding affinity for α-ketoglutarate by GDH was roughly similar suggesting that behavior of enzyme towards α-ketoglutarate remains probably the same in the control and frozen conditions. The apparent notion behind this unchanged K_m α-ketoglutarate between control and freeze states could be inconsequential *in vivo* based on two conjectures. Firstly, despite the suppression of Krebs during freezing, there are metabolic and biosynthetic reactions that depend on one or more reactions of the Krebs cycle or associated reactions. There are other enzymes whose products generate α-ketoglutarate for the anaplerotic reactions, for instance, ALT. Alanine accumulates in mostly all organs in the wood frog during freezing which means that ALT is active and it also uses glutamate (Storey and Storey, 1986). Hence, it is possible that the changes in glutamate and α-ketoglutarate levels can bypassed GDH through ALT under the reversible catalysis of glutamate + pyruvate ⇌ α-ketoglutarate + alanine. Secondly, the concomitant byproduct of ammonium appears to be remain the same concentration compared to increases in the liver during freezing (Storey and Storey, 1986), whereas the K_m ammonium is high (Table 2.2) such that the affinity of GDH for ammonium ion is lowered. Taken altogether it is unlikely that the similarity between K_m α-ketoglutarate of both forms of GDH has a large impact on the pools of α-ketoglutarate during freeze tolerance in the wood frog. Interestingly, high amounts of α-ketoglutarate exhibit a slight inhibitory effect upon GDH (Engel and Dalziel, 1970). The small increase in I_{50} α-ketoglutarate for the frozen condition suggests decreased inhibition

by α-ketoglutarate during the frozen state, however, it may not be physiological relevant. Cellular levels of α-ketoglutarate are roughly in the 0.1 mM range (Whillier et al., 2011). Hence, the I_{50} values determined in this study are 10-100 times greater than cellular levels, such that they are not likely to have an importance in physiological terms. However, the changes in I_{50} values do provide some additional support that there are conformational changes in GDH between control and frozen states, suggesting they are linked by the consequences of PTMs. In summary of all the kinetic parameters analyzed, the general depiction is that GDH experiences a downregulation during hypometabolism. The formation of α-ketoglutarate via GDH is may not be a desired pathway during the frozen state since α-ketoglutarate is low in terms of potential metabolic energy. Likewise, the reverse direction synthesizing glutamate is also likely to be suppressed since there is little need for glutamate for both a means of amino acid synthesis and as source of metabolic fuel during freezing. Overall, the catalysis by GDH does not appear to be poised in any particular direction, however, amino acids are still synthesized during freezing as supported by an accumulation of alanine (Storey and Storey, 1986). In lieu, the action of glutaminase and ALT do not directly involve GDH but their usage of glutamate in the frozen state might be a reason to reduce GDH catabolism of glutamate in the muscle since transamination to form alanine is more pressing use for glutamate than its deamination.

Similar to the case with α-ketoglutarate, the K_m NAD^+ was also unchanged between control and frozen forms of GDH (Table 2.2). It is important to note that with the addition of ADP, the K_m NAD^+ significantly decreased for frozen GDH when compared to the control condition. It appears that ADP binding to GDH induced a conformational change in the enzyme leading to increased affinity for NAD^+. Again, the physiological significance

of this increased affinity is limited due to the typical mitochondrial concentrations of approximately 3 mmol/kg wet weight NAD^+ found *in vivo* skeletal muscle (Li et al., 2009). At these NAD^+ concentrations, GDH would be saturated with the cofactor, potentially generate artifactual K_m values. However, the kinetic difference identified here as well as other kinetic changes listed above support a structural difference between control and 24-hour frozen GDH.

Despite overall GDH suppression during the frozen state, it is still a highly regulated enzyme that is influenced by various nucleotides (Male and Storey, 1982). As seen in Table 2.2, the addition of ADP produced significant changes in most kinetic parameters. Relative V_{max} increased in both catalytic directions and for both control and frozen forms of GDH upon the addition of ADP. This increased rate corresponds well to reports that the adenosine moiety acts by resolving abortive complexes facilitating the opening of the catalytic cleft (Bailey et al., 1982; George and Bell, 1980). Abortive complexes are where the substrate binds to the enzyme prior to the reaction before coenzyme is dissociated, hence, preventing the catalysis from carrying forth (Li et al., 2012). For example, the GDH:glutamate:NADH complex in the oxidative deamination reaction and the GDH:α-ketoglutarate:NAD^+ complex in the reductive amination reaction would be considered abortive complexes. ADP binding towards an allosteric site behind the NAD^+ binding domain allows more substrate binding towards the active site by reducing the affinity of the coenzyme and substrate to the active site (Banerjee et al., 2003; Prough et al., 1973). The proximity between the NAD^+-binding domain and the allosteric ADP binding serves as support for the substantial decrease in K_m NAD^+ when activated with ADP due to possible steric interactions (Peterson and Smith, 1999). ADP activation

plays a large part in the role of GDH in energy metabolism, especially during states of great ATP demand. A high amount of ADP resulting from falling ATP levels would boost the rate of GDH-mediated catalysis. ADP regulation of muscle GDH is likely to be strongly tied to muscle contraction and its energy demands when ATP is being rapidly consumed. This feature supports high intensity contraction, for example, the channeling of α-ketoglutarate into the Krebs cycle plays an anaplerotic role in elevating the total pool of C4 metabolite in the cycle. This enables the input of acetyl-CoA units to increase the total throughput of fuel and generation of NADH/$FADH_2$ that then supports an increase rate of ATP synthesis. It is doubted that this would occur during the frozen state where glycolytic flux is consistently consumed by steady-state anaerobic glycolysis. As the ATP:ADP ratios do not seem to change vastly between control and frozen wood frog skeletal muscle tissue (Storey and Storey, 1984). However, it may not be a major factor influencing GDH-specific muscle tissue during the physiologically relevant frozen state.

Another regulatory mechanism of GDH is allosteric binding by the inhibitor, GTP, which directly contrasts to the effects of ADP, by enhancing the affinity of GDH binding for the product thereby decreasing enzymatic turnover (Koberstein and Sund, 1974; Li et al., 2011). The binding of GTP between the junctions of the NAD^+-binding domain and antenna structure of the enzyme (Peterson and Smith, 1999; Smith et al., 2001) acting as a potent inhibitor by stabilizing abortive complex (Li et al., 2012). Inhibition of GTP is antagonized with the addition of ADP (Banerjee et al., 2003), as seen by an overall increase I_{50} GTP of the control form of GDH for both the forward and reverse direction (Table 2.3). However, a synergistic inhibitory effect was observed between the addition of both GTP

and ADP to the frozen form of GDH in the glutamate-oxidizing direction since the I_{50} values decrease (Table 2.3).

Waning GDH activity during freezing corresponds well with the metabolic changes that occur during freeze tolerance and the anoxic state induced by freezing in the wood frog. Restricted access to oxygen induces a cascade that substantially reduces the Krebs cycle and oxidative phosphorylation via the ETC cessation. Deprived of the core metabolic pathways functioning to generate ATP, the catabolism of glutamate to α-ketoglutarate for the metabolic fuel serves as uneconomical and unnecessary. In terms of efficiency, α-ketoglutarate is a C5 molecule so its net contribution to NADH production can be at the α-ketoglutarate dehydrogenase reaction and the overall pool size of glutamate in cells is a lot lower that the pools of lipids or glycogen that can each generate a huge amount of acetyl-CoA when they are used as aerobic fuel sources. Although it is one of the few that can be used anaerobically, glutamate itself plays central role in amino acid synthesis hence it not likely to be catabolized. Synthesis and export of glutamine from glutamate and alanine from pyruvate transamination with glutamate is also a major way that skeletal muscle exports nitrogenous end products from muscle protein catabolism and sends them to the liver where the nitrogen can either be excreted as urea or used to resynthesize various amino acids. However, it is suspected that the ureagenesis is not active within the frozen wood frog muscle tissue as opposed to the liver (Costanzo et al., 2015; Schiller et al., 2008). Since it stands to reason that if metabolic pathways that utilize the product of glutamate deamination are in less demand under frozen conditions then the glutamate oxidizing-direction of GDH is suppressed by mechanisms to conserve futile biochemical reactions. Moreover, the leg muscle does no work during freezing, as the extremities are first to freeze

and last to resume functioning after thaw (Storey and Storey, 1984; Storey and Storey, 1985). It seems that the leg muscle preferentially accumulates the amino acid alanine as a glycolytic end product rather than lactate during the long-term anaerobiosis engendered by freezing (Storey and Storey, 1986). Hence, transamination of only glutamate via GDH can be masked by the generation of alanine via other transaminase reactions involving glutamate such as glutaminase and ALT.

Phosphorylation of GDH is known to be a regulatory mechanism in Richardson's ground squirrels during hibernation (Bell and Storey, 2010) and freshwater crayfish that transition into an anoxic state (Dawson and Storey, 2012). RPP regulation of GDH activity is not surprising for the wood frog and it is likely to play a part in MRD. Examples of RPP regulation of other enzymes in wood frog skeletal muscle include hexokinase (Dieni and Storey, 2011), lactate dehydrogenase (Abboud and Storey, 2013), and catalase (Dawson and Storey, 2016). Western blots were used to quantify relative changes in phosphorylation states between control and 24-hour frozen forms of GDH. Immunoblot results indicated that frozen GDH had significantly more (2.5-fold greater) phosphorylated serine than GDH from control wood frogs (Figure 2.4). These results support the theory that GDH is regulated by phosphorylation when *R. sylvatica* transitions into the frozen state, as the control form of GDH was significantly less phosphorylated that the frozen form. This lends some credence to the observed changes in kinetic properties between control and frozen forms of GDH.

Conclusion

The present study highlights that the wood frog skeletal muscle GDH undergoes increased protein phosphorylation when frogs transition into the frozen state. Significant differences in phosphorylated serine residues between control and frozen GDH correlated with changes in the kinetic properties that dictate enzymatic activity. Partially purified GDH from skeletal muscle of control and 24-hour frozen frogs possessed different kinetic properties, and in general, the frozen form of GDH exhibited properties that would make it less active in both the forward and reverse directions. By means of Western blotting, it appears that the transition to a less active form of GDH during freezing occurs through RPP of the enzyme, with control GDH being the less phosphorylation form of the enzyme. Together with support from phosphorylation, other significant factors may contribute to regulating GDH activity *in vivo*. This includes the endeavors of nucleotide molecules (ADP and GTP). Many of these factors appear to act in unison to reduce GDH activity during the frozen state in efforts to prevent both the unnecessary synthesis of glutamate and the low energy potential of α-ketoglutarate as a fuel substrate. This regulation of GDH by RPP plays an integral role for the adaptive capacity for wood frogs during freeze tolerance. Ultimately, the suppression of GDH activity identified here coincides with the global MRD observed during wood frog freeze tolerance.

Chapter 3 – Regulation of liver lactate dehydrogenase from a freeze tolerant wood frog

Introduction

Many small animals are capable of entering a hypometabolic state in order to survive the bitter cold and lack of food in the winter. Animals such as the wood frog (*Rana sylvatica*) are marked by an active suppression of their metabolic rate to decrease energy expenditure in response to the drop in body temperature. Wood frogs are equipped with a remarkable ability to tolerant freezing of their body fluids and remain alive. There are a multitude of creatures ranging from reptiles (Storey, 2006) and insects (Levis et al., 2012) to aquatic life (Ramløv, 2000), all with varying degrees of freeze tolerance but in vertebrates few are of the caliber of the wood frog. The wood frog uses glucose as a cryoprotectant for its colligative properties in retaining water within the cell. At the initial detection of ice, the triggering of biochemical pathways that cascades to signal the liver to undergo glycogenolysis, the conversion of glycogen to glucose. A great amount of glucose enters the bloodstream and is quickly transported to surrounding corporeal tissues prior to freezing. Liver glucose levels have been shown to increase 70-folds during this event (Storey and Storey, 1984), beyond the feat of any ordinary mammals. Hence, it can be summarized that freezing initiates from the external skin and skeletal muscle permeating inwards to the vital organs and taking into account the distribution of cryoprotectants from the liver toward distal tissue – that the peripheral tissue has the lowest concentration of glucose compared to the internal tissues. The liver functions as major storage organ for glycogen that can be rapidly mobilized to provide glucose to peripheral tissues as an immediate response to ice nucleation at peripheral body sites. The formation of ice removes intercellular water, as it is incorporated into the ice crystal lattice. Cellular shrinkage may occur as water is moved by osmosis into the vascular space to form ice (Rubinsky et al.,

1990), as evident by the collapse of hepatocyte cells during freezing in nontolerant animals. For freeze tolerant animals, cold survival is maintained through the consistent retention of water within the cells by cryoprotectants and various other strategies (Storey et al., 1992). The wood frog utilizes low-molecular weight osmolytes (e.g. glucose, urea), INPs and antifreeze proteins for active ice management (Storey and Storey, 2017). The mobilization of hepatic glycogen reserves to synthesize glucose serves as effective cryopreservation; however, this dramatically increases glucose levels in the blood. The wood frogs deals with mainly two aspects induced by a hyperglycemic responsible in preparation for freezing: (1) increase glucose production and mobilization from the liver, and (2) overriding the homeostatic controls on rising glucose levels. The former best illustrated by the cryoprotectant production machinery of the wood frog liver. The liver is one of the last organs to freeze and the first to thaw, reflective of its massive levels of glucose. Ice forms in the extracellular spaces, which are primarily composed of sinusoids, revealing an inverse relationship between cellular volume and ice crystal size (Storey et al., 1992). The dynamic state of the liver prior to, during the onset, and during freeze plays a major role in freezing survival for both import and export of glucose and as a primary site of glycogen storage.

Lactate dehydrogenase (LDH; E.C. 1.1.1.27) is an enzyme found ubiquitously in nearly all eukaryotic cells. This cytosolic enzyme catalyzes the reversible interconversion of pyruvate and L-lactate with concomitant of NADH and NAD^+ cofactors, respectively. L-lactate specific LDH is a tetramer composed of H and/or M subunits, generating five possible isoenzymes (H_4, H_3M, H_2M_2, HM_3, and M_4) that are enzymatically similar but are distributed in different tissues and may vary in kinetic parameters (Krieg et al., 1967). For instance, the H_4 isoenzyme is found mainly in heart as well as the brain. The M_4 isoenzyme

is distributed predominantly in liver and striated muscle where it is poised for a main function in the pyruvate reducing-direction. By converting pyruvate to lactate, glycolytic flux is sustained via the regeneration of NAD^+ under conditions where oxygen is restricted/lacking and mitochondrial ATP generation is impaired. The structure of LDH isoform contributes to its functionality, as different forms possess varying affinity towards their substrates. In its tetrameric form, LDH has a molecular weight ranging between 115 to 154 kDa depending on species and isoenzyme (Jaenicke and Knof, 1968). It is relevant to note that other distinct isoenzymes of LDH exist and are adapted to fulfil specific functions (Blanco et al., 1976). The dynamic quaternary structure of LDH within specific tissues lends credence to its phylogenetic conservation in enzymatic function across taxa.

All organs, liver included, accumulate lactate during freezing (Storey and Storey, 1984), since freezing restricts blood flow to all organs and creates an anoxic state. This impedes not only replenishment of metabolic fuel for tissues but also the removal of metabolic waste products. Therefore, LDH functions to support lactate accumulation in the liver as an anaerobic end product during freezing as well as lactate clearance during thawing, where lactate is transported from the liver and multiple extrahepatic organs.

The Cori cycle is one facet of lactate metabolism that highlights the principle role of LDH in both liver and muscle when lactate is accumulated. When oxygen supplies are insufficient during strenuous muscle activity, energy generation in the form of ATP shifts from aerobic to anaerobic metabolism. Glycogen is the main storage fuel utilized by muscle. Glycogenolysis releases glucose-1-phosphate (G1P) from glycogen, then phosphoglucomutase converts it to glucose-6-phosphate (G6P). In order to enter glycolysis, the enzyme phosphoglucose isomerase catalyzes G6P to fructose-6-phosphate

(F6P). ATP is replenished by substrate-level phosphorylation during glycolysis using this pathway. The final step of glycolysis yields pyruvate that typically enters into the Krebs cycle under aerobic conditions. However, when subjected to anaerobic stresses, LDH converts pyruvate to lactate, while regenerating the NAD^+ that is needed by the glyceraldehyde-3-phosphate dehydrogenase reaction in order to keep glycolysis going. Insufficient levels of oxygen within the muscle results in an accumulation of lactate. If unalleviated, the excessive buildup of lactate in the system will cause a decrease in pH leading to acidosis (Kraut and Madias, 2014). The other half of the Cori cycle shifts the metabolic burden from the muscle to the liver. Lactate produced in the muscle is transported via the circulatory system for processing in the liver. Liver-specific LDH converts lactate back into pyruvate which can undergo gluconeogenesis to regenerate glucose. The Cori cycle is complete when glucose enters the bloodstream and is returned to the muscle. However, the Cori cycle does not remain active during the frozen state when circulation is halted but is likely reinstated when frogs thaw to help clear the accumulated lactate in muscle.

Not all lactate is necessarily reconverted to glucose in the liver. The pyruvate derived from lactate is a suitable substrate for aerobic metabolism by mitochondria once the wood frog is thawed. This depends mostly on the metabolic needs of liver as compared with the lactate load that it is faced with from deliveries from extrahepatic tissues.

Wood frog adaptation to freezing stress has been linked to the widespread use of RPP as both a mechanism of enzymatic regulation and control of global MRD (Storey and Storey, 2007). This altered the paradigm that used to consider LDH to be a nonregulatory enzyme that responded simplistically to the availability of its substrate. In particular, PTMs

of proteins and/or enzymes play a high degree of control influencing metabolic pathways that cope with environmental stresses. A comparison of properties of LDH in wood frog skeletal muscle revealed significant changes in kinetic parameters in response to cellular dehydration (Abboud and Storey, 2013). This reveals that PTMs are pertinent to the molecular mechanisms that may underlie dehydration responses for LDH in other animals and it has been shown that liver LDH in freshwater turtle undergoes protein phosphorylation during anoxia stress as well (Xiong and Storey, 2012). PTMs are surmised to be linked to changes in kinetic properties and play an influential aspect in the adaptation during long-term freezing conditioning.

Materials and Methods

Animals

Male wood frogs (*R. sylvatica*) were treated as previously described in Chapter 2. Liver was immediately excised and flash-frozen in liquid nitrogen. All tissue samples were stored at -80ºC until use. The Carleton University Animal Care Committee, in accordance with the Canadian Council on Animal Care guidelines, approved all animal handling protocols used during this study.

Preparation of liver tissue lysates for protein purification

Flash-frozen liver samples were crushed under liquid nitrogen and homogenized 1:10 w:v in ice-cold homogenization buffer C (25 mM potassium phosphate buffer at pH 6.0, 25 mM β-glycerophosphate, 2.5 mM EDTA, 2.5 mM EGTA, 15 mM 2-mercaptoethanol and 10% v:v glycerol) with the addition of a couple of PMSF crystals.

Samples were homogenized on ice with a Polytron PT1000 homogenizer, and then centrifuged at 13,500 × *g* at 4ºC for 30 minutes. Supernatant was decanted and stored at 4ºC until used for LDH protein purification.

Purification of lactate dehydrogenase (LDH)

The following purification was performed independently for liver samples from control (5°C acclimated) and 24-hour frozen (at -3°C) frogs. A 2.0 mL aliquot of crude supernatant was applied to a Cibacron Blue 3GA affinity chromatography column (1.5 cm × 4 cm), previously equilibrated with 30 mL of homogenization buffer C. The column was then washed with 30 mL homogenization buffer C to elute unbound proteins. LDH activity was then eluted from the Cibacron Blue 3GA column using a 0–2 M KCl gradient in homogenization buffer C across a 30 mL volume. Fractions of 40 drops per tube (approximately 1.4 mL) were collected using an automated fraction collector and 10 µL from each fraction was assayed to detect LDH activity (cf. enzyme kinetic assay for methodology). Peak fractions of LDH activity were pooled for subsequent analysis and purification steps.

Pooled peak fractions from the Cibacron Blue 3GA step were introduced onto a phenyl-agarose column (1.5 cm × 4 cm) previously equilibrated with 30 mL homogenization buffer C with 1.0 M KCl added. The phenyl-agarose column was then washed with 30 mL homogenization buffer C to elute unbound proteins. LDH activity was then eluted from the phenyl-agarose column using a 0–50% ethylene glycol gradient in homogenization buffer C across a 30 mL volume. Fractions were collected and assayed similar to the previous purification step.

Pooled peak fractions from the phenyl-agarose purification were then introduced onto a hydroxyapatite column (2.5 cm × 1.0 cm) previously equilibrated with 30 mL homogenization buffer C. The hydroxyapatite column was then washed with 30 mL homogenization buffer C to elute unbound proteins. LDH activity was then eluted from the hydroxyapatite column using a 0–0.5 M potassium phosphate gradient in homogenization buffer C across a 30 mL volume. Fractions were collected, assayed as previously and used for kinetic analysis of LDH.

For Western blotting analysis, a portion of this purified enzyme from the hydroxyapatite column was concentrated 10-fold with Amicon® Ultra-4 Centrifugal filters (Merck Millipore Ltd., UFC801024).

Determination of relative protein concentrations

Soluble protein concentrations of extracts were determined by the Bio-Rad protein assay adapted from the Bradford method as previously described in Chapter 2.

Enzyme kinetic assay

LDH activity was measured spectrophotmetrically by monitoring changes in NAD^+/NADH absorbance at 340 nm, as previously described in Chapter 2 for GDH. Lactate-oxidizing direction were carried forth in a total volume of 200 µL consisting of 10 µL of enzyme sample, 2.5 mM L-lactate, and 1 mM NAD^+. Conditions for the lactate-synthesizing direction were 10 µL of enzyme preparation, 0.25 mM pyruvate, and 0.5 mM NADH in a total volume of 200 µL. Assays were initiated with the final addition of LDH enzyme. K_m and I_{50} values were determined from modifications of the above optimal

conditions where one parameter (substrate) was varied while all other reactions conditions were those stated above.

SDS-Polyacrylamide Gel Electrophoresis (SDS-PAGE)

The purification of LDH was assessed using SDS-PAGE analysis as previously described in Chapter 2. Samples containing LDH were resolved on a 15% SDS-polyacrylamide gel. Proteins were electrophoretically separated at 4ºC under constant voltage at 180 V for 110 minutes in SDS-PAGE running buffer. A protein molecular weight ladder and a commercially purified sample of LDH from bovine heart (Sigma Life Science, Cat. No. L2625) were also run on every gel. Following completion of gel electrophoresis, the gels were either (1) stained directly with Coomassie blue or (2) transferred onto PVDF membrane for Western blotting.

For direct staining using Coomassie blue, the gels were submerged in Coomassie blue staining solution as previously described in Chapter 2. Images were recorded using the ChemiGenus Bio Imaging System.

Western blotting

Immunoblotting was used for identification of LDH and to assess changes in PTMs between partially purified LDH from control and 24-hour frozen frogs, as previously described in Chapter 2. Following completion of wet transfer, the membrane was washed 3 × 5 minutes in TBST at room temperature with gentle rocking. Membranes were blocked using 1% skim milk solution for 10 minutes with gentle rocking at room temperature.

Blocking solution was removed and full membranes were incubated separately in the following primary antibodies overnight at 4ºC with gentle rocking:

(1) Anti-lactate dehydrogenase goat polyclonal (Applied Biological Materials Inc., Cat. No. Y104790) diluted 1:1000 in TBST;

(2) Anti-phosphoserine rabbit polyclonal (Invitrogen, Cat. No. 61-8100) diluted 1:1000 in TBST;

(3) Anti-phosphothreonine rabbit polyclonal (Invitrogen, Cat. No. 71-8200) diluted 1:1000 in TBST;

(4) Anti-methylated arginine mouse monoclonal (Covalab, Cat. No. mab0002) diluted 1:1000 in TBST;

(5) Anti-methylated lysine rabbit polyclonal (StressMarq Biosciences Inc., Cat. No. SPC-158) diluted 1:1000 in TBST.

Primary antibodies were removed the following day. The membranes were washed 3 × 5 minutes in TBST prior to incubation with peroxidase-conjugated secondary antibody towards the respective host epitope for 60 minutes at room temperature with gentle rocking. Secondary antibodies were:

(1) Goat anti-rabbit IgG [H&L] (BioShop Canada Inc., Cat. No. APA007P) diluted 1:4000 in TBST;

(2) Rabbit anti-mouse IgG [H&L] (BioShop Canada Inc., Cat. No. APA005P) diluted 1:4000 in TBST;

(3) Rabbit anti-goat IgG [H&L] (BioShop Canada Inc., Cat. No. APA002P) diluted 1:4000 in TBST.

Secondary antibody solutions were removed, and membranes were washed and visualized by ECL as previously described in Chapter 2 using the GeneTools Image Analysis Software.

Data and Statistical Analysis

All enzyme kinetics data were analyzed using MPA and kinetic parameters were calculated using nonlinear least-squares regression program as previously described in Chapter 2.

Results

Purification of LDH from the liver of R. sylvatica

LDH was partially purified from liver tissue of control and 24-hour frozen *R. sylvatica* by a series of chromatographic steps. LDH activity was eluted with a 0–2 M KCl gradient from a Cibacron Blue 3GA column followed by an elution with a 0–50% ethylene glycol gradient off a phenyl-agarose column and finally using a hydroxyapatite column eluted with a 0–0.5 M phosphate gradient (Figure 3.1). Collection and pooling of the peak fractions yielded a specific activity of crude LDH of 30.7 mU/mg and 102 mU/mg for control and frozen forms of LDH, respectively. Then elution using a 0–2 M KCl gradient from Cibracron Blue resulted in a pooled specific activity of 111 mU/mg for control LDH and 149 mU/mg for frozen LDH. At this step, the control sample had a yield of 80.3% activity with a fold purification of 2.28 while frozen had 69.4% yield and 1.47-fold purification (Table 3.1). Pooled LDH activity was next introduced to a phenyl-agarose column and eluted with a 0–50% ethylene glycol gradient providing a pooled LDH specific

activity of 212 mU/mg for control LDH with a fold purification of 4.36 and activity yield of 47.1%. The enzyme from frozen conditions had the specific activity of 247 mU/mg with a fold purification of 2.43 and an activity yield of 28.1% from the phenyl-agarose step (Table 3.1). The final step of the partial purification was a hydroxyapatite column chromatographic separation where the pooled fraction of LDH was eluted using a 0–0.5 M phosphate gradient. The pooled eluate collected had a 5.77- and 5.03-fold purification for control and frozen forms of LDH, respectively. The overall purification scheme resulted in a final specific activity of 281 mU/mg for the control form of LDH with a final yield of 9.33% whereas frozen LDH had a specific activity of 511 mU/mg with a 24.6% yield.

As a result of the purification scheme, LDH remained partially-purified, with some remaining proteins, as determined by gel electrophoresis and visualized by Coomassie blue staining (Figure 3.2). The identity of LDH was determined by Western blot analysis using a protein-specific anti-LDH antibody (see Supplementary Figure 2). LDH had an apparent subunit molecular weight of ~36 kDa as determined by SDS-PAGE relative migration (Figure 3.2).

Basic kinetic properties of LDH

Analysis of LDH from the liver of control and frozen wood frogs showed that the enzyme displayed hyperbolic substrate saturation in both the lactate-oxidizing direction (Figure 3.3a) and lactate-synthesizing direction (Figure 3.3b). Similarly, substrate inhibition at half-maximal enzyme activity (I_{50}) was modelled to a hyperbolic decline function for the lactate-oxidizing direction (Figure 3.4a) and lactate-synthesizing direction (Figure 3.4b). All reported changes in parameters were determined to be statistically

different via the Student's *t*-test with $p < 0.05$ unless otherwise mentioned. In the lactate-oxidizing direction, the K_m lactate was 1.9-fold higher in the frozen (7.98 ± 0.37 mM) condition compared to the control value (4.18 ± 0.06 mM). A similar result was apparent for the I_{50} value for lactate showing a 1.6-fold increase comparing frozen (423 ± 9.34 mM) to control (265 ± 12.2 mM) conditions. There were no significant differences found in the K_m values for pyruvate in the lactate-synthesizing direction (Table 3.2) but the I_{50} for pyruvate showed a 1.5-fold statistically significant increase from control conditions (9.80 ± 0.70 mM) compared to frozen (14.5 ± 0.44 mM). The analysis of the K_m NAD^+ in the lactate-oxidizing direction showed a 3.4-fold increase over control LDH (1.14 ± 0.05 mM) for the frozen form of LDH (3.85 ± 0.25 mM). In regards to the lactate-synthesizing direction, analysis of the K_m NADH also showed an increase from 15.0 ± 0.69 μM for the control form LDH to a value of 72.9 ± 3.17 μM frozen at, which is a 4.9-fold increase.

Kinetic activity of LDH with urea

Kinetic parameters were analyzed with respects to urea. Urea inhibited enzymatic activity in all cases with a significantly greater effect on the frozen enzyme in both directions. The I_{50} urea values for the lactate-oxidizing direction control conditions (3.05 ± 0.004 M) for the control enzyme and 35% less for frozen LDH (2.00 ± 0.03 M) in the lactate-oxidizing direction. Similar values were seen in the lactate-synthesizing direction, with I_{50} urea values changing from 2.64 ± 0.01 M for the control form of LDH to 2.28 ± 0.03 M for the frozen form, a significant 14% decrease.

Kinetic activity of LDH with salts

Distinct differences in K_{50} NaCl and K_{50} KCl values were found between control and frozen forms of LDH. The analysis of K_{50} NaCl values showed in a 4.3-fold increase from control conditions (109 ± 2.47 mM) to frozen values (465 ± 8.24 mM) in the lactate-oxidizing direction. However, in the lactate-synthesizing direction, NaCl addition generated a 55% decrease in K_{50} NaCl values comparing with controls (983 ± 6.34 mM) to frozen (443 ± 12.8 mM). By contrast, the analysis of K_{50} KCl values showed significant decreases for this parameter for frozen LDH for both directions; compared with the control forms of LDH (518 ± 18.6 mM and 636 ± 13.4 mM) values for the frozen forms (455 ± 13.1 mM and 449 ± 32.4 mM) were reduced by 12 and 29% for the lactate-oxidizing and lactate-synthesizing directions, respectively (Table 3.2).

Kinetic activity of LDH in the lactate-oxidizing direction with glucose

When LDH was assayed in the presence of 200 mM glucose, several kinetic parameters changed significantly ($p < 0.05$) between control and frozen conditions. Analysis of the K_m lactate with glucose between control (3.30 ± 0.19 mM) and frozen (2.88 ± 0.06 mM) conditions showed no statistical difference; however, the I_{50} L-lactate value increased 6.0-fold from control (56.0 ± 1.51 mM) to frozen condition (335 ± 9.12 mM). The addition of glucose also resulted in a 1.5-fold increase in the K_m NAD^+ from 0.91 ± 0.07 mM in the control to 1.36 ± 0.10 mM in frozen in the lactate-oxidizing direction. The effects of both glucose and salts on kinetic activity was also examined yielding some statistical difference between control and frozen states. The analysis of both K_{50} NaCl and K_{50} KCl in the presence glucose showed a 1.3- and 1.1-fold statistically significant increase

when comparing controls (415 ± 6.46 mM and 410 ± 4.21 mM) with the frozen state (547 ± 4.40 mM and 465 ± 12.4 mM, respectively) in the lactate-oxidizing direction.

The lactate-oxidizing direction for control conditions also showed statistically significant changes in the K_m and I_{50} of lactate in the absence versus presence of glucose. Table 3.2 shows the decrease in K_m lactate by 21% from the situation without glucose (4.18 ± 0.06 mM) to conditions with glucose added (3.30 ± 0.19 mM). Similarly, I_{50} lactate also showed a significant 79% decrease between conditions without glucose (265 ± 12.2 mM) to conditions with glucose added (56.0 ± 1.51 mM). Likewise, the K_m NAD^+ decreased by 21% upon the addition of glucose as compared with the control form of LDH.

The analysis of LDH from frozen conditions revealed a 64% and 22% decrease in the lactate-oxidizing direction, respectively for lactate K_m (7.98 ± 0.37 mM to 2.88 ± 0.06 mM without or with glucose, respectively) and I_{50} (424± 9.34 mM for control to 335 ± 9.12 mM with glucose). Likewise, the frozen form of LDH showed a 65% decrease in K_m NAD^+, (from 3.85 ± 0.25 mM to 1.36 ± 0.10 mM) in the presence of glucose in the lactate-oxidizing direction.

Kinetic properties for LDH were also assayed in the presence of salts (NaCl and KCl) with the addition of 200 mM glucose (Table 3.2) resulting in several kinetic parameter changes ($p < 0.05$). Analysis of the K_{50} NaCl showed a 3.8-fold increase from 109 ± 2.47 mM to 415 ± 6.46 mM with the addition of glucose to the control form of LDH. However, the K_{50} KCl values showed a decrease of 21% (518 ± 18.6 mM to 410 ± 4.21 mM) upon the addition of glucose in the lactate-oxidizing direction for control LDH. For LDH from frozen frogs, the analysis of the K_{50} NaCl values increased 1.2-fold (465 ± 8.24 mM to 547

± 4.40 mM) with glucose added. However, no significant change occurred for K_{50} KCl when subjected to 200 mM glucose.

Kinetic activity of LDH in the lactate-synthesizing direction with glucose

When LDH was assayed in the lactate-synthesizing direction with the addition of 200 mM glucose (Table 3.2), several kinetic parameters also changed significantly between control and frozen conditions ($p < 0.05$). Analysis of K_m and I_{50} pyruvate values in the presence of glucose in the lactate-synthesizing direction showed no significant changes between control and frozen forms of LDH. However, the control K_m NADH increased by 2.3-fold from control (34.3 ± 3.67 μM) to frozen LDH (68.3 ± 6.25 μM). The effects of glucose and salts used simultaneously were also examined revealing some statistical changes between control and frozen forms of LDH in the lactate-synthesizing direction. Analysis of K_{50} values for KCl showed a 1.7-fold increase from control LDH (453 ± 9.22 mM) to frozen LDH (786 ± 37.8 mM) with the addition of glucose. However, no statistical difference was seen between control (1240 ± 80.9 mM) and frozen conditions (1050 ± 32.8 mM) for K_{50} NaCl in the presence of 200 mM glucose in the lactate-synthesizing direction.

Analysis of K_m pyruvate values showed a change from 129 ± 3.66 μM to 138 ± 6.47 μM in the presence of 200 mM glucose but no change in I_{50} pyruvate. However, the control form of LDH K_m NADH (15.0 ± 0.69 μM) showed a 2.3-fold increase upon the addition of glucose (34.3 ± 3.67 μM). There was no significant change between the K_m NADH in the frozen condition in the absence versus presence of glucose, similarly, with K_m pyruvate. Interestingly, I_{50} pyruvate decreased by 43% from 14.5 ± 0.44 mM without glucose compared to 8.39 ± 0.78 mM in its presence. Table 3.2 also tabulates the changes

observed in kinetic parameters being influenced by both salts and glucose simultaneously in the lactate-synthesizing direction. The control K_{50} NaCl showed no statistically significant change when glucose was added; however, the control K_{50} KCl showed a 1.4-fold decrease from 636 ± 13.4 mM to 453 ± 9.22 mM with the addition of glucose. Alternatively, frozen LDH showed a 2.4- and 1.7-fold increase in K_{50} for both NaCl (443 ± 12.8 mM to 1050 ± 32.8 mM) and KCl (449 ± 32.4 mM to 786 ± 37.8 mM), respectively, when comparing glucose-absent kinetic parameters to glucose-present kinetics.

Post-translational modifications of LDH

Western blotting was used to identify LDH among other proteins during electrophoretic separation (Supplementary Figure 2) and Western blot analysis was also used to determine the relative changes in PTMs between control and frozen forms of LDH. Quantification revealed that phosphorylation on serine residues of frozen LDH was 8.8-fold higher ($p < 0.05$) than to the control form of LDH (Figure 3.5). Similarly, a change methylation states on lysine residues was observed being 1.5-fold greater for frozen compared to control LDH. There were no statistically significant changes in PTMs observed between control and frozen forms of LDH for phosphorylation of threonine residues or for methyl-arginine levels (Figure 3.5).

Table 3.1. Partial purification and yield of liver LDH from ~0.3 g tissue of (a) control and (b) 24-hour frozen *R. sylvatica*.

(a)

Steps	Total Protein (mg)	Total Activity (mU)	Specific Activity (mU/mg)	Fold Purification	Activity Yield (%)
Crude	18.7	909	30.7	--	--
Cibacron Blue[1]	6.57	730	111	2.28	80.3
Phenyl-agarose[2]	2.02	428	212	4.36	47.1
Hydroxyapatite[3]	0.30	84.8	281	5.77	9.33

(b)

Steps	Total Protein (mg)	Total Activity (mU)	Specific Activity (mU/mg)	Fold Purification	Activity Yield (%)
Crude	18.9	1910	102	--	--
Cibacron Blue[1]	8.88	1330	149	1.47	69.4
Phenyl-agarose[2]	2.17	537	247	2.43	28.1
Hydroxyapatite[3]	0.92	470	511	5.03	24.6

1. Cibacron Blue LDH activity was eluted with 0–2 M KCl gradient
2. Phenyl-agarose LDH activity was eluted with 0–50% ethylene glycol gradient
3. Hydroxyapatite LDH activity was eluted with 0–0.5 M phosphate gradient

Table 3.2. Kinetic parameters of partially purified liver LDH of control and 24-hour frozen *R. sylvatica.*

Parameter	Control ± SEM	Frozen ± SEM
Lactate-oxidizing direction (lactate → pyruvate, pH 8.0)		
K_m L-lactate (mM)	4.18 ± 0.06	7.98 ± 0.37[a]
I_{50} L-lactate (mM)	265 ± 12.2	424 ± 9.34[a]
K_m NAD^+ (mM)	1.14 ± 0.05	3.85 ± 0.25[a]
I_{50} Urea (M)	3.05 ± 0.004	2.00 ± 0.03[a]
K_{50} NaCl (mM)	109 ± 2.47	465 ± 8.24[a]
K_{50} KCl (mM)	518 ± 18.6	455 ± 13.1[a]
K_m L-lactate (mM) + 200 mM glucose	3.30 ± 0.19[b]	2.88 ± 0.06[b]
I_{50} L-lactate (mM) + 200 mM glucose	56.0 ± 1.51[b]	335 ± 9.12[ab]
K_m NAD^+ (mM) + 200 mM glucose	0.91 ± 0.07[b]	1.36 ± 0.10[ab]
K_{50} NaCl (mM) + 200 mM glucose	415 ± 6.46[b]	547 ± 4.40[ab]
K_{50} KCl (mM) + 200 mM glucose	410 ± 4.21[b]	465 ± 12.4[a]
Lactate-synthesizing direction (pyruvate → lactate, pH 7.2)		
K_m pyruvate (μM)	129 ± 3.66	144 ± 0.68[a]
I_{50} pyruvate (mM)	9.80 ± 0.70	14.5 ± 0.44[a]
K_m NADH (μM)	15.0 ± 0.69	72.9 ± 3.17[a]
I_{50} Urea (M)	2.64 ± 0.01	2.28 ± 0.03[a]
K_{50} NaCl (mM)	983 ± 6.34	443 ± 12.8[a]
K_{50} KCl (mM)	636 ± 13.4	449 ± 32.4[a]
K_m pyruvate (μM) + 200 mM glucose	138 ± 6.47	116 ± 9.08
I_{50} pyruvate (mM) + 200 mM glucose	8.65 ± 0.24	8.39 ± 0.78[b]
K_m NADH (μM) + 200 mM glucose	34.3 ± 3.67[b]	68.3 ± 6.25[a]
K_{50} NaCl (mM) + 200 mM glucose	1240 ± 80.9	1050 ± 32.8[b]
K_{50} KCl (mM) + 200 mM glucose	453 ± 9.22[b]	786 ± 37.8[ab]

a. – indicates a significant statistical difference between control and 24-hour frozen conditions via Student's t-test, two-tailed, $p < 0.05$

b. – indicates a significant statistical difference between no glucose and addition of 200 mM glucose via Student's t-test, two-tailed, $p < 0.05$

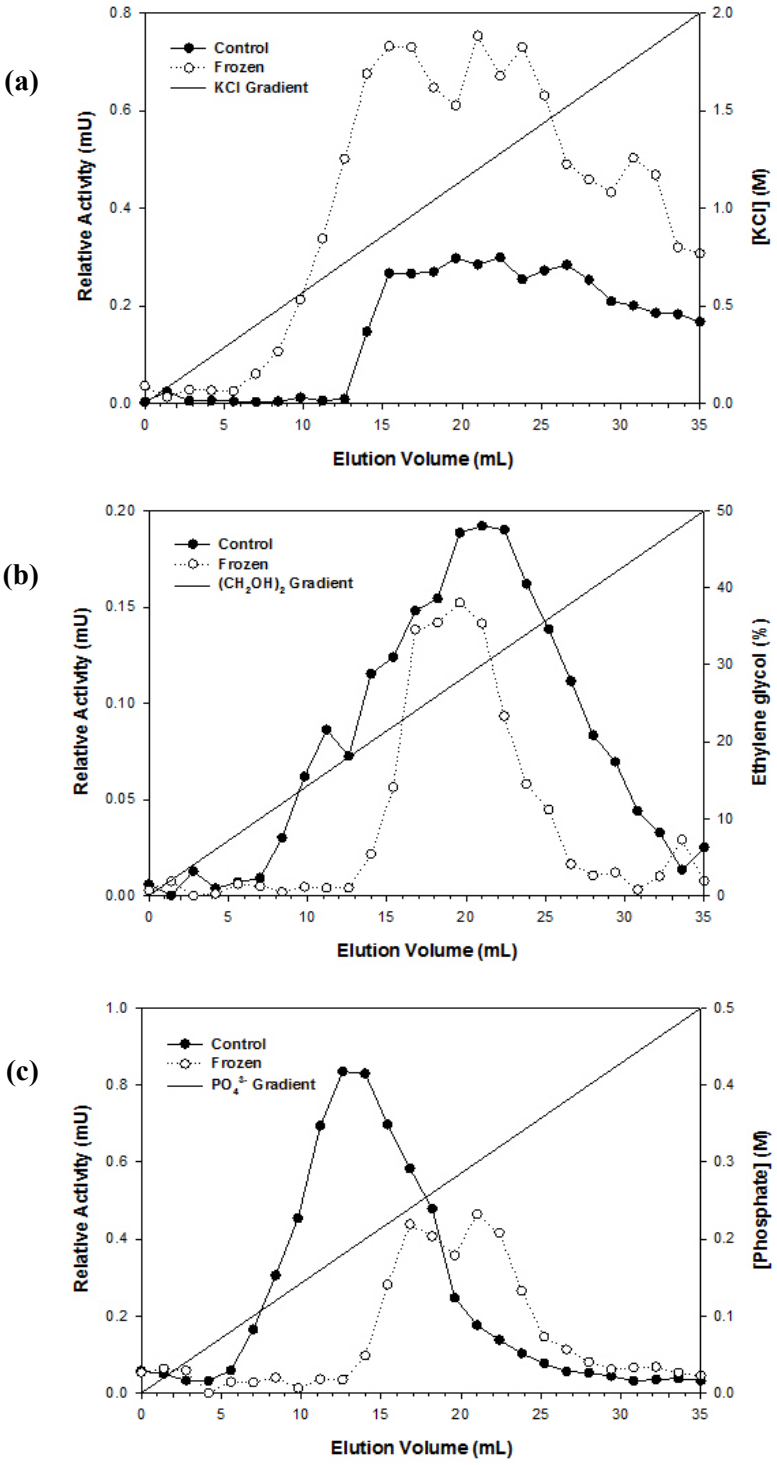

Figure 3.1. Typical elution profile for relative LDH activity from liver tissue of control and 24-hour frozen *R. sylvatica* using an ordered-series of subsequent column chromatography: (a) Cibacron Blue eluted with a 0–2 M KCl gradient; (b) phenyl-agarose eluted a 0–50% ethylene glycol gradient; and (c) hydroxyapatite eluted with a 0–0.5 M phosphate gradient. Elution profiles for control and 24-hour frozen samples are from different purification trials but superimposed for viewing convenience. Elution profiles also exclude prior wash steps with homogenization buffer after addition of sample.

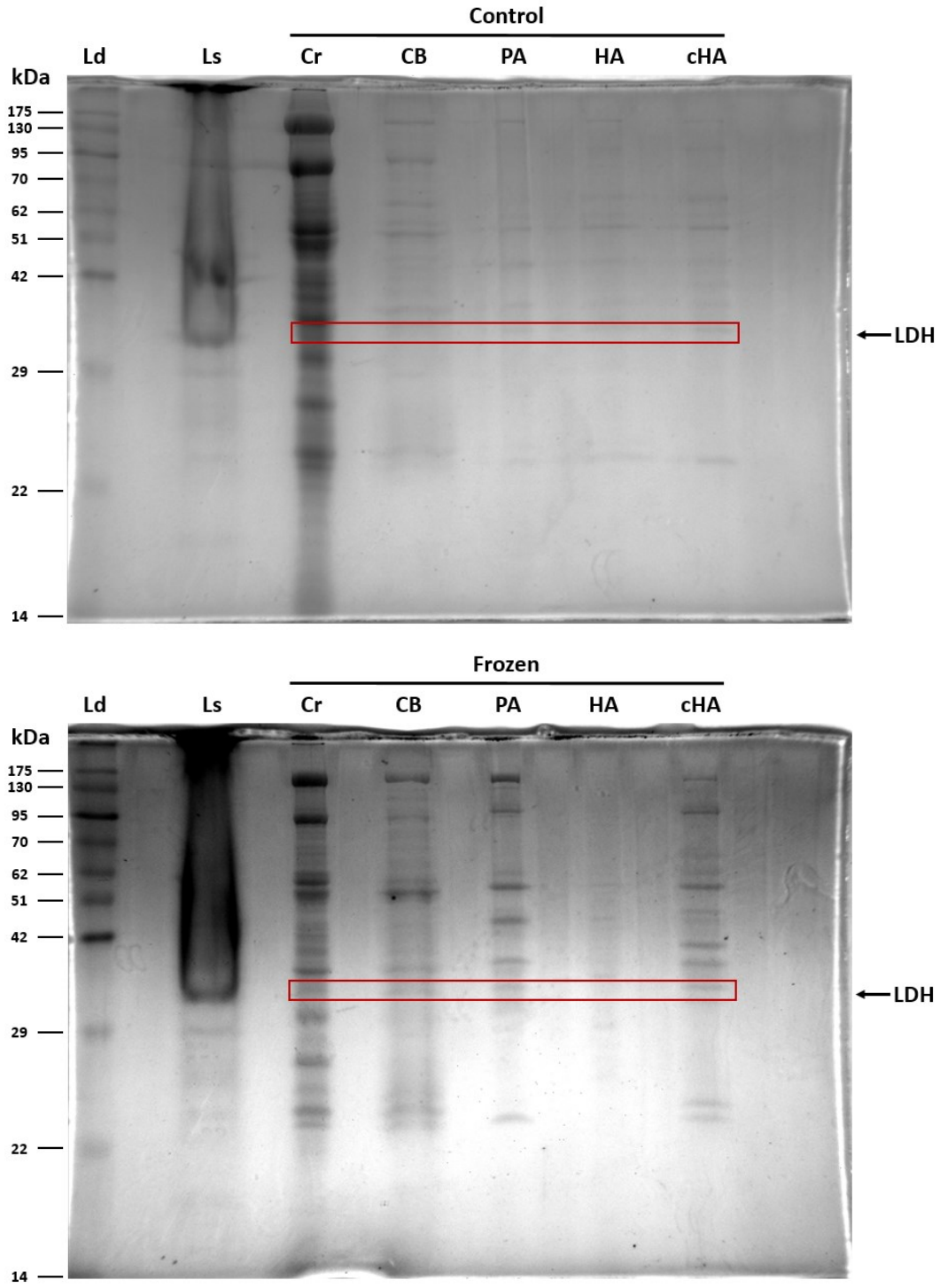

Figure 3.2. A 15% resolving SDS-PAGE run at 180 V for 110 minutes for the sequential partial-purification of liver LDH from (a) control and (b) 24-hour frozen *R. sylvatica*. Ld, Molecular weight ladder (Froggabio); Ls, LDH standard (Sigma Life Science); Cr, crude homogenate; CB, pooled fractions from Cibacron Blue eluate; PA, pooled fractions from phenyl-agarose eluate; HA, pooled fractions from hydroxyapatite eluate; cHA, concentrated pooled hydroxyapatite fractions.

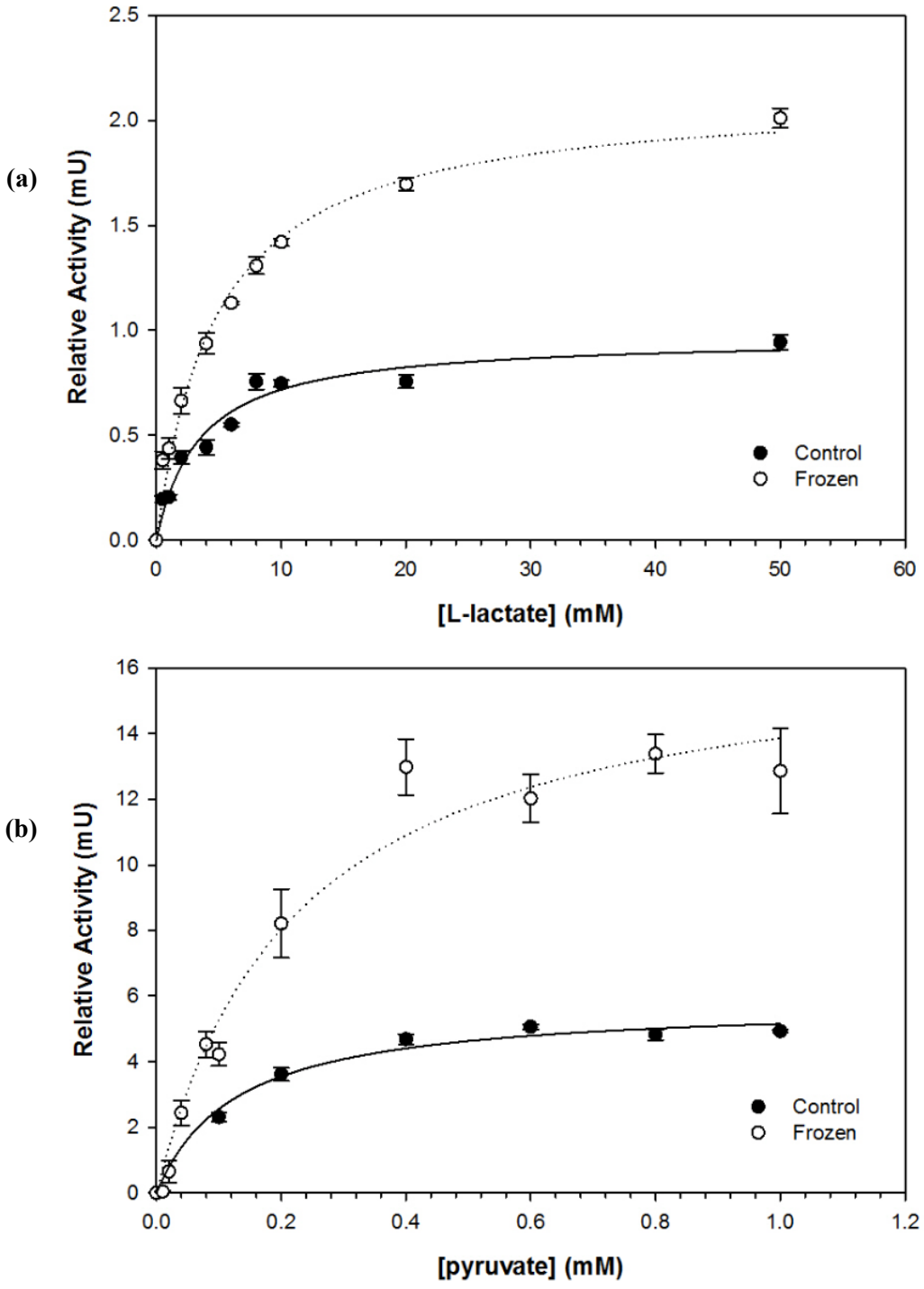

Figure 3.3. Michaelis-Menten plots used to extract the substrate concentration producing half-maximal enzyme velocity (K_m) catalyzed by partially purified LDH from liver of control and 24-hour frozen *R. sylvatica* in the (a) lactate-oxidizing direction and (b) lactate-synthesizing direction. Data expressed as mean ± SEM (n = 3–4), independent replicates on enzyme samples.

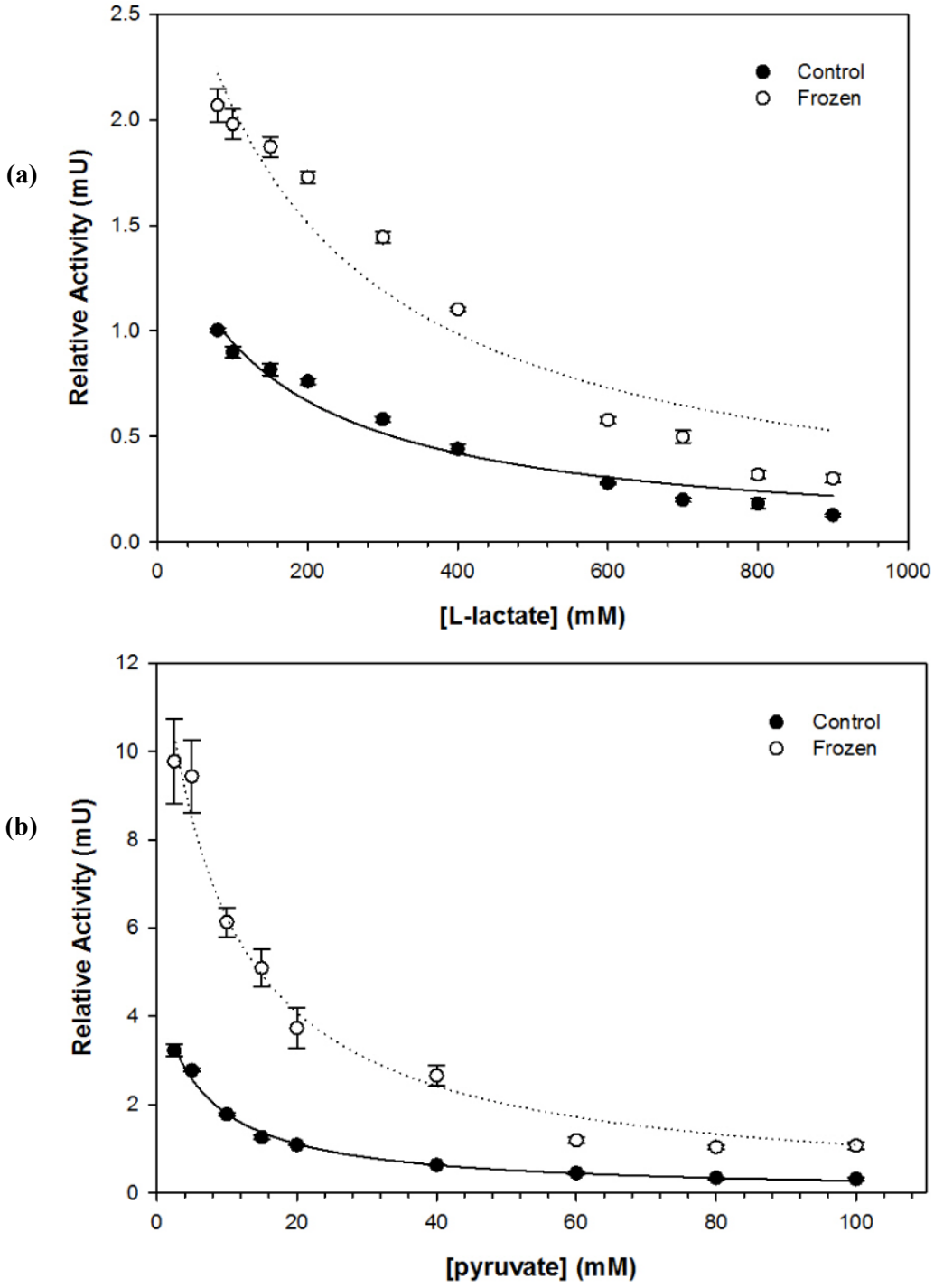

Figure 3.4. Inhibition curves used to extract the substrate concentration producing half-maximal enzyme inhibition (I_{50}) catalyzed by partially purified liver LDH from control and 24-hour frozen *R. sylvatica* in the (a) lactate-synthesizing direction and (b) lactate-synthesizing direction. Data expressed as mean ± SEM (n = 3–4), independent replicates on enzyme samples.

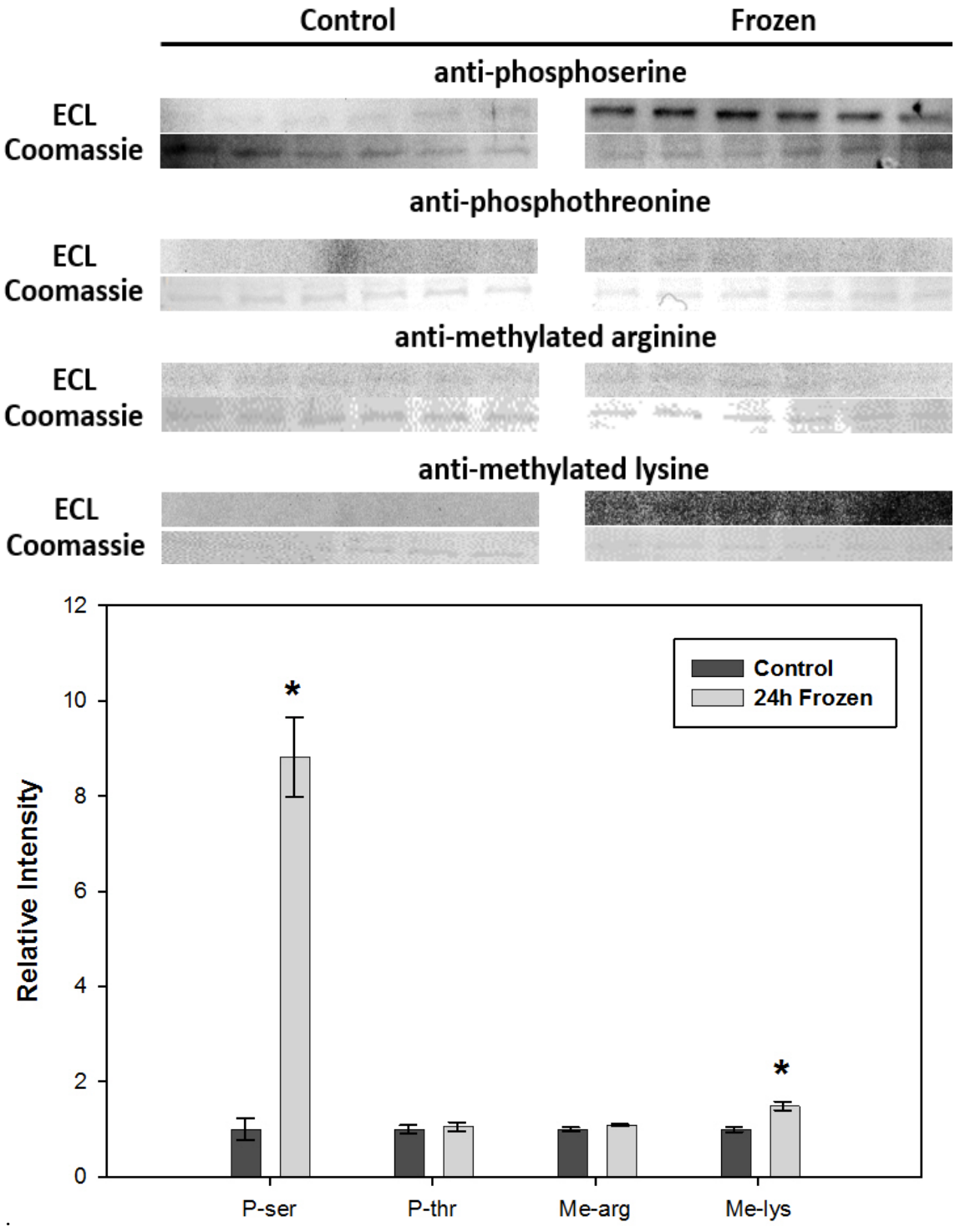

Figure 3.5. Quantification of post-translational modifications of LDH from liver tissue of control and 24-hours frozen *R. sylvatica*. Chemiluminescence signal intensities normalized to protein amount and frozen condition is reported relative to control values set to 1. Data expressed as mean ± SEM (n = 5–6). * – indicates a significant statistical difference between control and 24-hours frozen conditions via Student's t-test, two-tailed, $p < 0.05$.

Discussion

Freezing can be the cause of death for many organisms without the necessary preventative measures to cope with the water loss and/or cellular damage inflicted by ice formation. Not many animals are capable of dealing with these harsh conditions quite like the wood frog. As winter approaches, the wood frog prepares for its dormant state by accumulating a vast amount of glycogen stored in their liver. A major response to freezing is the activation of liver glycogenolysis, the breakdown of glycogen to glucose that is exported to peripheral organs, which dramatically elevate organ glucose concentrations by 9- to 313-fold (Churchill and Storey, 1993; Storey and Storey, 1984). Glucose serves to colligatively resist severe water loss and limit cell shrinkage from decreasing below a critical minimum. Progressive freezing leads to limited oxygen supply in tissues due to the cessation of breathing and heart beat during the frozen state. Thus, freezing induces hypoxia stress because heart and lung function is labored by the gradual freezing of the blood. Limited oxygen along with high glycolytic flux induces elevated levels of pyruvate. The end product of glycolysis is converted to lactate during anaerobic conditions via the enzyme LDH. Noted for its crucial role in supporting anaerobic survival, LDH is responsible for the reversible NAD^+/NADH-dependent L-lactate interconversion with pyruvate, and was formerly thought to possess a nonregulatory high activity responding to its substrates. However, it is evident that LDH is indeed under complex regulation and control within metabolic pathways. An understood mechanism of regulation of enzymes and/or proteins is through PTMs. It is now known that PTMs play a large role in modifying the structure of enzymes that globally affects their functionality. Studies on animal adaptation to environmental stress have shown that both enzymatic control and global

MRD can be regulated through the influence of RPP (Storey and Storey, 2007). To this end, the motivation for this study was to analyze the properties, regulation and PTMs of wood frog liver LDH to provide insights on the mechanistic features that govern LDH function during freezing. It is demonstrated in this study that LDH from liver tissue of control and frozen wood frogs shows substantial differences in kinetic properties that can be correlated to differences observed in the PTM states of the enzyme.

Liver LDH from control and 24-hour frozen wood frogs was partially purified using series of column chromatography methods as follows: Cibacron Blue, phenyl-agarose, and hydroxyapatite. The crude enzyme activity was determined to be 30.7 mg/mU for control and 102 mg/mU for frozen prior to chromatographic separation. The final yield of LDH was 9.3% with a specific activity of 281 mU/mg for control and a yield of 24.6% with a specific activity of 510 mU/mg for frozen corresponding to a fold purification of 5.77 and 5.03, respectively (Table 3.1). This purification scheme differs from the previous chromatographic separation attempts performed for LDH with the muscle of the wood frog (Abboud and Storey, 2013), liver from the African clawed frog (Katzenback et al., 2014), and liver of the freshwater turtle (Xiong and Storey, 2012). The molecular weight of LDH determined by SDS-PAGE corresponded to ~36 kDa matching well with isolated LDH samples from various animals and tissues (Abboud and Storey, 2013; Katzenback et al., 2014; Xiong and Storey, 2012). The present column chromatography purification demonstrated a high degree of reproducibility in partially purifying LDH from crude.

Analysis of kinetic properties revealed significant changes between control and 24-hour frozen LDH from liver tissue. These findings suggested that the changes in kinetic parameters are correlated with regulation of LDH during freezing (Table 3.1). There was a

significant 1.9-fold increase in K_m lactate for the frozen form of LDH (from 4.18 ± 0.06 mM to 7.98 ± 0.37 mM) indicating a decreased affinity for lactate during the frozen state. Upon further inspection, it seems that all basic kinetic parameters in both the lactate-oxidizing direction (K_m lactate and K_m NAD^+) and the lactate-synthesizing direction (K_m pyruvate and K_m NADH) showed statistically significant increases from control to frozen forms of LDH. This corresponds well with similar studies of liver LDH from the African clawed frog in response to dehydration stress (Katzenback et al., 2014). This is indicative of a broad reduction in the catalytic efficiency of LDH during freezing survival. This could support overall MRD during states of freezing since it seems that the major function of LDH in serving to replenish reductive NAD^+ in the lactate-synthesizing direction is required to drive anaerobic glycolysis in the liver. Moreover, whether it be lactate or pyruvate as substrates, these molecules possess very little metabolic potential as fuels since the Krebs cycle is suppressed during freezing, preventing further catabolism. Further examination revealed that both I_{50} lactate and I_{50} pyruvate seemed to be significantly higher for the frozen form of LDH suggesting that substrate inhibition is less effective compared to the control form. Since it is known that lactate levels do rise dramatically during freezing (Storey and Storey, 1984), yet, pyruvate content remained stable at around 100 µmol/g wet weight during freeze and thawing (Storey, 1987b).

The K_m lactate dropped to similar levels between control and frozen with the addition of 200 mM glucose, indicating that LDH affinity for L-lactate was similar in the two states if high glucose prevailed. Likewise, K_m pyruvate for the lactate-synthesizing direction showed the same influence of glucose. However, this general lowering of kinetic parameters was only statistically significant in the lactate-oxidizing direction. The liver is

the hub of glucose production and storage of glycogen and an increase in glucose concentration from baseline levels of 5 to 387 μmol/g wet weight can occur during freezing exposure (Storey and Storey, 1984). Hence, when glucose levels are high, the liver is likely not poised to convert lactate to pyruvate, as metabolic fuels are sufficient. Higher glucose essentially increases the affinity for lactate during freezing supporting the notion of LDH as remaining active when glucose is present at near physiological amounts in the liver during freezing (Storey et al., 1992). This is also supported by increased lactate concentrations in wood frog liver from a baseline 0.7 to 12.1 μmol/g wet weight during freezing exposure (Storey and Storey, 1984). However, there was a small but significant decrease in K_m lactate for the control form of LDH with the addition of glucose indicating a slight increase in affinity for lactate. From solely the K_m thus far, this suggests that lactate fermentation is upregulated during the frozen state, while gluconeogenesis is still possible but is most likely masked by an overwhelming amount of lactate accumulation. Lactate has an inhibitory role on LDH in both the control and frozen forms but this only occurs at levels that are beyond physiological concentrations (Table 3.2). In both the control and frozen conditions, I_{50} lactate significantly decreases indicating a higher inhibitory effect towards accumulating lactate in the presence of glucose. However, this most likely is not physiologically relevant since typical *in vivo* concentrations of lactate ranges typically 12 to 16 μmol/g wet weight during wood frog freezing (Storey, 1987c; Storey and Storey, 1984). However, this does support the idea that glucose does have a role influencing LDH and that different forms of LDH exist between control and frozen states.

Analysis of K_m NAD^+ and K_m NADH in the presence of glucose revealed a higher value for the frozen form of LDH compared to control form. This reflects a similar trend

observed for K_m lactate and K_m pyruvate for the lactate-oxidizing and lactate-synthesizing directions, respectively. As fermentation continues as a means of metabolic ATP output, the ratios of NADH/NAD^+ will be shifted via glycolytic flux. LDH is the key enzyme responsible for the maintaining the appropriate balance of reductive potential during anaerobiosis, and consequentially generating lactate as a metabolic end product. This also correlates with the observed lactate levels accumulated in the liver during freezing (Storey and Storey, 1986). However, the overall increase of affinity for NAD^+ or NADH alone provides very little detail in terms of global LDH regulation, since there are many dehydrogenases in the cell that are using NADH and NAD^+. Hence, the availability of specific substrates (i.e. lactate and pyruvate in the case for LDH) that has the biggest influence on dehydrogenase activity.

Accumulation of glucose during freezing plays an important role in cryoprotection, especially in the liver, since it is a main housing of metabolic fuel for the wood frog. Since glucose levels can rise about 70-fold during freezing (Storey and Storey, 1984), the addition of 200 mM glucose to LDH assays was used to assess the effects of rising glucose on LDH function. An increased affinity for lactate was observed under the addition of high glucose as determined by the decrease in K_m lactate in both control and frozen forms of LDH to roughly similar values. This suggests that when glucose is present, the affinity for lactate by LDH during freezing is similar to the control form of LDH. There was also a significant decrease in I_{50} lactate as well, suggesting that LDH is more strongly inhibited by lactate in the presence of glucose. However, the decrease in I_{50} lactate for control was a 79% decrease but in frozen there was a less dramatic 21% decrease, indicating that the frozen form of LDH is more structurally stable to function at high lactate and high glucose

environment comparatively. Similarly, K_m NAD^+ of control and frozen both significantly decreased when glucose was added suggesting an increase affinity for NAD^+ in the presence of glucose. Albeit the pools of NAD^+ are considerably less than lactate, and, hence, may not play in the overall influence of LDH in the lactate-oxidizing direction. The lactate-synthesizing direction was also examined although the K_m pyruvate shown no significant changes upon the addition of glucose for both control and frozen conditions. Similarly, no changes for I_{50} pyruvate were seen for control LDH; however, there was a decrease in I_{50} pyruvate in frozen when glucose was added. The consistency of these kinetic parameter seems to indicate that glucose does not influence the kinetic properties of LDH in the lactate-synthesis direction. Analysis of K_m NADH showed changes in both control and frozen forms of LDH, but by similar arguments as K_m NAD^+, the general pools of NADH or NAD^+ may not be a major contributor to dictating the poise of LDH. Taken all together, it seems that glucose has greater influence in the lactate-oxidizing direction, in general, compared to the lactate-synthesizing direction.

Under conditions of dehydration stress experienced during freezing, amphibians can also elevate the concentrations of urea in their blood and tissues as another colligative defense against water loss from their bodies. Urea can also contribute to the net increase in body fluid osmolality resisting cell volume reduction during freezing (Costanzo and Lee, 2008; Costanzo et al., 2008; Costanzo et al., 2013). Levels of up to 90 mM in plasma have been recorded in wood frogs under drying conditions and as high as 300 mM for desert frogs and toads that estivate for many months during the year (Costanzo et al., 2008; Grundy and Storey, 1994). However, urea synthesis by freeze tolerant frogs seems to be in response to changes in body hydration and builds up as the environment becomes drier as

opposed to a direct response to freezing (Storey and Storey, 2017). Investigations were performed to assess the effects of urea on LDH and identified urea as an inhibitor. Urea is a well-known for its cryoprotective capability, yet it is also known for its action as a protein denaturant at high concentrations. It appears that the control form of LDH was less susceptible to inhibition by urea (Table 3.2). Urea inhibition of LDH has been reported to be caused by interference of urea with the active site of LDH displaying competitive inhibition (Rajagopalan, 1961) but with I_{50} values in the 2-3 M range, urea is probably acting as a generalized protein denaturant instead. High urea is often used to denature proteins in order to elucidate information on protein structure and stability. This suggests that LDH in the frozen form is less resilient to the higher levels of urea experienced compared to the control. These differences in structural stability with respect to urea denaturation supports the idea that there are structural differences between the two enzyme forms found in control and frozen liver. Differential sensitivity to urea was also examined in wood frog muscle LDH revealing I_{50} urea values ranging between 2-3 M (Abboud and Storey, 2013), which correlates well with the present findings for the liver isoform.

Another factor affecting the osmotic environment of the cell during water lost would be salts. As ice crystals forms in the extracellular cavities, there is a buildup of ions remaining within the cell, as they are not incorporated into the ice lattice. Amphibians can tolerate sodium at 90-200 mM above normal (Hillman, 1988), yet, at high concentrations salt ions will disrupt protein properties by affecting protein conformation, folding, and stability resulting in altered enzymatic activity. This aspect was examined by assessing the inhibitory effects of NaCl and KCl. The inhibitory concentration of NaCl at its midpoint (K_{50} NaCl) was determined to be 4.3-fold greater for LDH from frozen frogs compared to

controls in the lactate-oxidizing direction, yet, in the lactate-synthesizing direction K_{50} NaCl decreased by one-half for frozen LDH versus control. Analysis of K_{50} KCl showed that it decreased from control conditions to frozen, for both catalytic directions. These statistically significant changes in inhibitory effects suggests that ions can play a large role in determining optimal enzymatic activity. However, this might not be biologically meaningful since the K_{50} values for KCl and NaCl measured were greater that physiologically relevant concentrations. Nevertheless, it is important to note that ion concentrations do increase the propensity for dehydration during freezing. The K_{50} values also changed upon the addition of 200 mM glucose since K_{50} NaCl statistically increased in the lactate-oxidizing direction, but not in the control lactate-synthesizing direction. This generally indicates an overall increase in stability to NaCl when glucose when is present. This is sensible such that glucose may act as a stabilizer of proteins via macromolecular crowding effects (Senske et al., 2014). By contrast, the same arguments may not hold for K_{50} KCl, as the changes in these values were inconclusive. However, this does not undermine the important role of ions as effectors of enzyme parameters.

Protein phosphorylation is a well-known mechanism of LDH regulation in wood frog skeletal muscle (Abboud and Storey, 2013), African clawed frog liver (Katzenback et al., 2014), and freshwater turtle liver (Xiong and Storey, 2012). Studies have also identified other dehydrogenase enzymes in wood frog liver such as glucose-6-phosphate dehydrogenase (G6PDH) that are regulated by reversible phosphorylation (Dieni and Storey, 2010). Hence, RPP of LDH in wood frog liver is not a surprising mode of regulation. Western blots analysis were used to identify relative changes in potential PTMs between control and 24-hour frozen forms of LDH. Immunoblot results indicated that

frozen LDH had significantly more (8.8-fold greater) serine phosphorylation than LDH from control wood frog (Figure 3.5). In addition, immunoblots also identified a significant 1.5-fold increase in methylated lysine content in the frozen form of LDH compared to controls. These results suggest that various PTMs work in conjunction to regulate the transition between control and frozen states. It well known that PTMs can modulate enzyme function by covalently bonding to proteins or enzymes to cause changes in their structural properties. Hence, there is a correlation between changes in PTMs and changes in kinetic parameters found for control and frozen liver LDH.

Conclusion

This study supports the proposal that LDH undergoes increased protein phosphorylation and protein methylation in liver when frogs transition from unfrozen (control) to frozen states. Significant differences were observed in phosphorylated serine residues and methylated lysine residues between control and frozen forms of LDH, which can be correlated to changes in the kinetic properties of the enzyme. In other words, enzymatic properties seem to be affected by PTMs, allowing for regulation of enzymes during the freezing response. Partially purified wood frog liver LDH from control and 24-hour frozen conditions displayed various significant differences in enzyme kinetic properties. For instance, the frozen form of LDH exhibited parameters that suggest an overall suppression of LDH activity during freezing. This corroborates well with global MRD, since hypometabolic states tend to suppress unnecessary energy expenditure. It is stipulated that LDH is most likely not needed to function at a maximal capacity during bouts of freezing. Western blotting methodologies have identified increased

phosphorylation in frozen LDH and methylated lysine, thus all together this provides many factors that can influence the *in vivo* regulation of LDH. The effects of glucose seem to play a role in enhancing LDH for its substrate as observed by the general decrease in K_m values. The effects of NaCl and KCl inhibited LDH activity beyond physiological concentrations, yet their effects were different between control and frozen. This supports the notion that there exists a control form of LDH and a frozen form of LDH, which are modulated by PTMs. Many of these underlying factors function together in order to dynamically suppress LDH activity during the frozen state in efforts to limit needless catalysis. To this end, the suppression of LDH activity elucidated in this study corresponds to known mechanisms that dictate MRD in wood frog freeze tolerance.

Chapter 4 – General Discussion

Temperature stress is one of the most basic factors that can affect fitness. Whether it be high or low temperatures, organisms survive best at their optimal range. During the winter, temperatures often drop to subzero values where the physical properties of water molecules change by transitioning into ice. Many creatures can survive cold winters by manipulating their internal regulation of metabolism, thereby allowing them to persevere in harsh climates. One strategy known as freeze tolerance is a unique ability adopted by a number of creatures – from intertidal marine species (Dennis et al., 2014) to many terrestrial insects (Lee et al., 1995; Levis et al., 2012), and selected amphibians (Storey, 1990) and reptiles (Storey, 2006), but few can perform the ploy like the wood frog. This anuran is capable of surviving for weeks with up to two-thirds of their body fluids locked in extracellular ice crystals and showing a complete absence of physiological vital signs, but after thawing, they return to normal life within a few hours. The basic notion of freeze tolerance is built upon multiple components that were most likely derived over evolutionary time, which can be broken down into three pillars that support adaptions that are unique to freeze tolerance. The first is adaptations for cold hardiness to tolerate freezing, organisms must possess and/or elicit strategies to survive cold temperatures. In general, this includes developing strategies such as manipulating ice growth and suppressing tissue damage by ice. Secondly, organisms must also endure limitations encumbered by physiological demands of life that includes oxygen. Anoxia tolerance can be considered as one of the most basic tenets of freeze tolerance and is believed to be precursor adaptation to freeze tolerance. Lastly, the consequences of subzero temperatures will often result in ice formation. By transition from liquid to a solid state, water content is greatly reduced in cells when water exits to join growing extracellular ice crystals. Hence,

dehydration tolerance is another fundamental adaptation required for freeze tolerance. The ability to survive freezing is most likely an extension of preexisting adaptations that are overlaid in response to environmental pressures. The capacity to bear the cold coupled with anoxia and dehydration tolerance leads to the novel freeze tolerant strategies vital for cold survival.

Amphibians are well known among vertebrate for their exceptional tolerance of wide fluctuations in body water content, ionic strength and osmolality of body fluids. Because they have highly permeable skin, these novel abilities allow amphibians to effectively cope with variations in environmental wetness-dryness (especially for species that are largely terrestrial) and such dehydration tolerance has become a valuable trait of freeze tolerance. By embellishing the mechanisms that allow these organisms to survive, revolutionary innovations have been developed for freeze tolerance. The first innovation is the management of ice formation in the body, and a second innovation is by entering a stasis state that prolongs life in the absence of vital processes. These innovations are dependent on mechanisms that govern metabolism to promote freeze tolerance. Survival of unforgiving environmental conditions over the winter is reliant upon conservation of resources and energy. It is paramount that organisms are able to ration stored fuel reserves in order to prolong survival. If not, death is inevitable to any organism that is unable to sustain and/or protect itself. One of the most common strategies for mediating metabolic fuel rationing and energy consumption is by MRD, which establishes a new paradigm that rebalances the consumption and production of energy at a very much lower rate of ATP turnover. Transition into a state of MRD is typically mediated by altered gene expression, regulation of enzymes, and reprioritization of energetics. The ability to depress one's

metabolic rate, or enter a state of hypometabolism, provides an opportunity to extend survival time by conserving fuel reserves. Certain animals are capable of dropping their metabolic rate to ranges of 5-40% of their resting rate (Storey and Storey, 2004). Many factors are involved in regulating the metabolic transition from the normal resting state to a hypometabolic state. Control of enzymes that play quintessential roles in anabolic and catabolic processes are certainly chief in regulating MRD. Furthermore, the fluctuating nature of the environment requires changes to metabolic systems that are rapid, sustainable, and energetically modest. That being stated, the synthesis and degradation of proteins is energetically demanding, especially during stress conditions and a wholescale restructuring of cellular metabolic enzymes is too energy-expensive. Instead, the activities of enzymes involved in different aspects of metabolism can be differentially managed by reversible mechanisms via the use of reversible methods, particularly the actions of protein phosphatases and protein kinases that define the RPP regulatory mechanism. This form of metabolic regulation has been shown in many animals that survive cold (Storey and Storey, 2017) and anoxic conditions (Storey and Storey, 1990) and affects major biochemical pathways that are important for sustaining life.

The North American wood frog, *Rana sylvatica*, undergoes whole body freezing as it perseveres throughout the winter. Under the conditions associated with freezing, these organisms are also inflicted with ischemia, anoxia, and cellular dehydration (Storey, 1990; Storey and Storey, 2017). Surviving bouts of freezing in these conditions requires depression of their metabolic rate to conserve energy. Moreover, ice formation in the extracellular fluids of the wood frogs leads to the halting of heartbeat and breathing. This means that the remaining oxygen will be depleted over time and that the frogs must

subsequently rely on anaerobic metabolism for energy production. In addition, life in the frozen state is incompatible with food intake (i.e. regular prey such as flying insects and invertebrates die off, retreat to hibernation sites, or transitions to protective forms such as eggs or pupae overwinter). Hence, organism musts develop the capacity for storage of large amounts of fuel reserves in order to be used during environmentally unfavorable situations. Lactate accumulation studies during freezing have been used as support for ATP generation using anaerobic glycolysis (Costanzo et al., 2013; Sinclair et al., 2013; Storey, 1987c; Voituron et al., 2009). Hypometabolic states call for a high degree of metabolic plasticity in order to satisfy the demands of the tissues in the frozen state. Hence, amphibians are able to draw upon their capacities to support freezing survival with limitations to resources and removal of waste products. Despite remaining largely inactive when frozen, oxidation of glucose for energy still occurs via fermentation (Costanzo et al., 2015) – albeit at a net of 2 ATP generated per glucose molecule compared to the approximate 36 ATP formed during aerobic metabolism.

Enzymes are macromolecular biocatalysts important to mostly all biochemical reactions that occurs in the cell. The majority of metabolic reactions require the aid of an enzyme in order to sustain life. This thesis focuses on two enzymes that have fundamental roles in metabolism and have not previously been examined in their respective wood frog tissues. There are numerous reasons for enzymes such as GDH and LDH to be regulated during hypometabolic states. For simplicity, since GDH and LDH play very different roles during metabolism, it is best to discuss them separately and tie them together overall within the context of global metabolism.

The role of glutamate dehydrogenase (GDH) in wood frog skeletal muscle during freeze tolerance

From analysis of the kinetic properties of liver GDH from control and 24-hour frozen wood frogs it was evident that there were significant differences between the two enzyme states. The data determined that GDH was less active in both catalytic directions in the frozen condition compared to controls. In addition, the frozen form of GDH was substantially more phosphorylated than the control form. Decreased GDH activity in the glutamate-oxidizing direction during freezing coincides with reduced functioning of the Krebs cycle and ETC, as shuttling α-ketoglutarate into the Krebs cycle would be fruitless under anoxic conditions. On the other hand, reduced GDH activity in the glutamate-synthesizing direction corresponds with the fact that synthesis processes are largely suppressed during hypometabolism. Even though GDH serves as an important regulator of amino acids synthesis/degradation during MRD, the catalysis of GDH is suppressed to prevent nonessential energy expenditure under conditions of stress. Similar findings of GDH suppression were found as responses to anoxia in the anoxia-tolerant turtle (Bell and Storey, 2012). Overall, it is purposed that GDH activity is suppressed during the frozen state, and would predictably be reactivated during thawing.

Various factors could regulate GDH *in vivo* during hypometabolism as it plays such an important role in cellular processes such as energy production and nitrogen metabolism. The present studies undertaken in this thesis showed that ADP is a potent allosteric activator and GTP a potent allosteric inhibitor of GDH activity. Depending on the intramitochondrial concentrations, these nucleotides can be a means of regulating GDH properties during freezing as well as during transitional times as the animal moves into or

out of hypometabolism. A key finding is the regulation of GDH via RPP. It was determined that GDH phosphorylation states differed greatly between the two forms of the enzyme under different conditions. Specifically, muscle GDH was shown to be suppressed possessing a higher phosphorylated state in frozen frogs. It has been well established that RPP may lead to activation or suppression of enzymatic activity and the current data provide strong support for the role of RPP in regulating GDH during freezing in wood frog muscle.

The role of lactate dehydrogenase (LDH) in wood frog liver during freeze tolerance

Analysis of the kinetic properties of liver LDH in both catalytic directions revealed statistically significant changes. This supported a conclusion of an overall suppression of LDH in 24-hour frozen wood frogs compared to control conditions. It was revealed that liver LDH from 24-hour frozen frogs was more phosphorylated than the control form and could act to decrease LDH activity in the lactate-synthesizing direction. This seems sensible since accumulation of lactate in the liver is not the dominant end-product. It is speculated that alanine might be more preferable in the liver instead of lactate via the catalytic action of alanine aminotransferase. Liver may preferentially accumulate the neutral amino acid, alanine, instead of the acidic product, lactate, during anoxic conditions brought on by freezing (Storey and Storey, 1986). The lactate-oxidizing direction was also determined to be suppressed during freezing, since generating pyruvate during freezing is largely futile because any further catabolism of pyruvate via Krebs cycle is suppressed due lack of oxygen. Hence, in both directions LDH is generally suppressed during the frozen state. However, it can be speculated that LDH activity will be restored during thawing

when oxygen is again available and pyruvate could then be used either as a substrate for the TCA cycle or for gluconeogenesis. Even though LDH plays an important role in maintaining the NAD^+/NADH ratio to sustain anaerobic glycolysis, the relative amount of these coenzymes are way less than the relative proportions of substrate of LDH: pyruvate and lactate.

There are various mechanism to regulate LDH *in vivo* during hypometabolism, since it contributes such an important role in maintaining glucose fermentation during anaerobiosis induced by freezing. It was determined by the studies undertaken in this thesis, that ions and glucose play an influential role in altering the kinetic properties of LDH. It can be assumed that physiological levels of ions within cells contribute to enzyme structural stability and consequentially can affect enzyme kinetic properties. There were also distinct differences between the I_{50} effects of NaCl and KCl in altering the properties of LDH, as the kinetic parameters seem to indicate that the frozen form of LDH less stable to high concentrations of ions in solution. On the other hand, an effective cryoprotective molecule such as glucose contributes to the stability of LDH that enhanced enzymatic activity during freezing. In summary of all the possible molecules studied, it can be suspected that they regulate LDH transitioning into and out of hypometabolism. Another form of regulation of LDH is by PTMs. Wood frog LDH has been determined to be regulated by phosphorylation state changes as there were substantial differences between frozen and control forms conditions. The frozen form of LDH was found to be substantially more phosphorylated compared to the control enzyme. In addition, methylation was another possible mechanism of regulation, since frozen LDH was found to have high levels of methylated arginine residues. It is well known that PTMs and specifically RPP play a

large role in altering the structure of proteins and enzymes in order to change their function. This study supports that role for RPP in regulating LDH in response to freezing in the wood frog liver.

Given that the small subset of enzymes examined in this study, it can be hypothesized that both LDH and GDH play roles in hypometabolism during freezing. LDH interconverts L-lactate and pyruvate, and under aerobic conditions lactate is commonly converted into pyruvate in order to be shuttled towards the Krebs cycle in order to be completely oxidized. However, its role in the Cori cycle highlights some of the intricate functionality of LDH during muscle fatigue that shifts the metabolic burden of processing lactate to the liver. After release from muscle into the bloodstream, the liver takes up lactate. There it is processed by gluconeogenic reactions and can be converted into liver glycogen or released back into the circulation to resupply muscle with glucose, the latter fate completing the Cori cycle. However, under the dynamic shifts during freeze tolerance as MRD guides the suppression of essential processes, the catalytic rigor of LDH is suppressed in general as the circulatory system in frozen preventing the removal of lactate. In addition, anaerobiosis during freezing suppresses Krebs cycle; hence, pyruvate cannot be further oxidized. Thus, with suppression on both sides the reaction it makes sense that LDH is generally suppressed during freezing. Since the blood is frozen, every organ has to function as an isolated unit on its own when the frog is frozen which means that anaerobic end-products builds up in each organs. The only possibility for Cori cycle action would only occur after thawing when metabolic products can be trafficked between organs. Most organs are just as capable to oxidize their pool of lactate over time (e.g. lactate is a

good substrate for the heart) whereas those with substantial gluconeogenic capacity (liver and kidney) could perform reconversion to glucose.

Conclusion

Since freeze tolerant amphibians survive exclusively on endogenous fuel reserves during the winter season, the regulation of energy production and expenditure is of paramount importance. Wood frogs have demonstrated exceptional resilience to freezing by changing their physiological and metabolic regulation. Bearing the consequences of anoxia, ischemia, and cellular dehydration has led to the adaptation known to be freeze tolerance. These stressors are managed on a metabolic scale that requires major changes to the biochemistry of the organism. Specifically, the suppression of metabolic enzymes helps to facilitate the transition into a hypometabolic state and determine a directionality of enzyme function that supports the needs of cells/organs for long-term survival in a frozen state. The two studies have demonstrated that the regulation of GDH and LDH may play an important role in hypometabolism, if not a differential role between control and frozen conditions. Both GDH and LDH were found to be enzymatically suppressed in 24-hour frozen wood frogs compared to the control. Their general reductions in activity were mediated by various factors and were correlated with RPP. Protein phosphorylation apparently plays a large role in modulating both GDH and LDH properties; since in both studies it was determined that relatively higher levels of phosphorylated serine residues were found on the enzymes in the frozen condition. The efficient method of phosphorylation may be crucial to mediate the functional switch of LDH and GDH during freezing and thawing where aerobic respiration is cut off and reinstated, respectively. It is

reasoned that these enzymes will be reactivated during thawing in order to reestablish homeostasis when metabolism returns to active conditions. Taken together the work presented in this thesis provides novel insights on the plasticity and dynamic regulation of metabolism in the liver and skeletal muscle during wood frog freeze tolerance.

Future Directions

The studies described in this thesis identified some fascinating aspects of GDH and LDH regulation during freeze tolerance; however, numerous avenues of prospective research can also reveal more insights. Specific kinetic parameters can be further investigated. For example, GDH is known to be affected by a plethora of allosteric regulators such as activation by branched-chain amino acids (leucine, isoleucine, and valine) (Fahien et al., 1985; Zhou and Thompson, 1996) and succinyl-CoA (Fahien et al., 1989). GDH has also been determined to be allosterically inhibited by ATP (Herrero-Yraola et al., 2001), zinc (Bailey et al., 2011), and palmityl-CoA (Fahien and Kmiotek, 1981). It would also be interesting to differentiate the various classes of GDH by substituting $NADP^+$ and NADPH in lieu of NAD^+ and NADH to analyze differences in the behavior and regulation of GDH when using this redox pair. Other the other hand, general analysis of enzyme properties can be investigated such as temperature-sensitive kinetics since wood frogs experience wide variation in ambient temperature over the seasons with extreme low temperatures in the winter (e.g. Alaskan wood frogs survive frozen -16°C). Studies analyzing temperature sensitive kinetics have been shown to yield some interesting results (Abboud and Storey, 2013). Another route of exploration would be to expose these enzymes in incubation studies to different protein phosphatases and kinases to artificially

change phosphorylation states of the enzymes and measure phosphorylation state specific changes in kinetic parameters. These types of studies have strengthened support for RPP as a mechanism of enzyme modulation (Bell and Storey, 2010). More Western blot analysis can be performed in order to search for unexamined PTMs in order to support the regulation of proteins by covalent modifications. Furthermore, PTM-crosstalk is an established phenomenon and it describes how a set of PTMs (commonly phosphorylation) may influence other PTMs (such as ubiquination and SUMOlyation reviewed in Venne et al., 2014). This naturally progresses to mass spectrometry studies to assess other possible PTMs that can be found on the protein. Moreover, once the genome of *R. sylvatica* has been sequenced, bioinformatic analysis can be performed to identify specific residues of phosphorylation and other molecular interactions.

REFERENCE

Aarset, A. (1982). Freezing tolerance in intertidal invertebrates. *Comp Biochem Physiol A Comp Physiol.* **73**, 571–580.

Abboud, J. and Storey, K. (2013). Novel control of lactate dehydrogenase from the freeze tolerant wood frog: Role of posttranslational modifications. *PeerJ.* **1**, e12.

Al-Fageeh, M. and Smales, C. (2006). Control and regulation of the cellular responses to cold shock: the responses in yeast and mammalian systems. *Biochem J.* **397**, 247–259.

Bailey, J., Bell, T. and Bell, J. (1982). Regulation of bovine glutamate dehydrogenase: The effects of pH and ADP. *J Biol Chem.* **257**, 5579–5583.

Bailey, J., Powell, L., Sinanan, L., Neal, J., Smith, T. and Bell, J. (2011). A novel mechanism of V-type zinc inhibition of glutamate dehydrogenase results from disruption of subunit interactions necessary for efficient catalysis. *FEBS J.* **278**, 3140–3151.

Banerjee, S., Schmidt, T., Fang, J., Stanley, C. and Smith, T. (2003). Structural studies on ADP activation of mammalian glutamate dehydrogenase and the evolution of regulation. *Biochemistry.* **42**, 3446–3456.

Bansal, S., Luu, B. and Storey, K. (2016). MicroRNA regulation in heart and skeletal muscle over the freeze-thaw cycle in the freeze tolerant wood frog. *J Comp Physiol B.* **186**, 229–241.

Bartel, D. (2004). MicroRNAs: Genomics, biogenesis, mechanism, and function. *Cell.* **116**, 281–297.

Bell, R. and Storey, K. (2010). Regulation of liver glutamate dehydrogenase by reversible phosphorylation in a hibernating mammal. *Comp Biochem Physiol B Biochem Mol Biol.* **157**, 310–316.

Bell, R. and Storey, K. (2012). Regulation of liver glutamate dehydrogenase from an anoxia-tolerant freshwater turtle. *HOAJ Biol.* **1**, 1–3.

Benkovic, S. and Hammes-Schiffer, S. (2003). A perspective on enzyme catalysis. *Science.* **301**, 1196–202.

Biggar, K. and Storey, K. (2012). Evidence for cell cycle suppression and microRNA regulation of cyclin D1 during anoxia exposure in turtles. *Cell Cycle.* **11**, 1705–1713.

Blanco, A., Burgos, C., Gerez de Burgos, N. and Montamat, E. (1976). Properties of the testicular lactate dehydrogenase isoenzyme. *Biochem J.* **153**, 165–172.

Bley, N., Lederer, M., Pfalz, B., Reinke, C., Fuchs, T., Glaß, M., Möller, B. and Hüttelmaier, S. (2015). Stress granules are dispensable for mRNA stabilization during cellular stress. *Nucleic Acids Res.* **43**, e26.

Block, W. (1991). To freeze or not to freeze? Invertebrate survival of sub-zero temperatures. *Funct Ecol.* **5**, 284–290.

Bradford, M. (1976). A rapid and sensitive method for the quantitation of microgram quantities of protein utilizing the principle of protein-dye binding. *Anal Biochem.* **72**, 248–254.

Brooks, S. (1992). A simple computer program with statistical tests for the analysis of enzyme kinetics. *BioTechniques.* **13**, 906–911.

Brooks, S. (1994). A program for analyzing enzyme rate data obtained from a microplate

reader. *Biotechniques* **17**, 1154–1161.
Brooks, S. and Storey, K. (1988). Anoxic brain function: Molecular mechanisms of metabolic depression. *FEBS Lett.* **232**, 214–216.
Brooks, S. and Storey, K. (1993). De novo protein synthesis and protein phosphorylation during anoxia and recovery in the red-eared turtle. *Am J Physiol.* **265**, R1380-1386.
Cai, Q. and Storey, K. (1997a). Freezing-induced genes in wood frog (*Rana sylvatica*): fibrinogen upregulation by freezing and dehydration. *Am J Physiol.* **272**, R1480–R1492.
Cai, Q. and Storey, K. (1997b). Upregulation of a novel gene by freezing exposure in the freeze-tolerant wood frog (*Rana sylvatica*). *Gene.* **198**, 305–312.
Cheng, X., Ma, Y., Moore, M., Hemmings, B. and Taylor, S. (1998). Phosphorylation and activation of cAMP-dependent protein kinase by phosphoinositide-dependent protein kinase. *Proc Natl Acad Sci USA.* **95**, 9849–9854.
Childers, C. and Storey, K. (2016). Post-translational regulation of hexokinase function and protein stability in the aestivating frog Xenopus laevis. *Protein J.* **35**, 61–71.
Churchill, T. and Storey, K. (1992a). Natural freezing survival by painted turtles *Chrysemys picta marginata* and *C. picta bellii*. *Am J Physiol.* **262**, R530–R537.
Churchill, T. and Storey, K. (1992b). Freezing survival of the garter snake *Thamnophis sirtalis parietalis*. *Can J Zool.* **70**, 99–105.
Churchill, T. and Storey, K. (1993). Dehydration tolerance in wood frogs: a new perspective on development of amphibian freeze tolerance. *Am J Physiol.* **265**, R1324–R1332.
Churchill, T. and Storey, K. (1995). Metabolic effects of dehydration on an aquatic frog, *Rana pipiens*. *J Exp Biol.* **198**, 147–154.
Costanzo, J. and Lee, R. (2005). Cryoprotection by urea in a terrestrially hibernating frog. *J Exp Biol.* **208**, 4079–4089.
Costanzo, J. and Lee, R. (2008). Urea loading enhances freezing survival and postfreeze recovery in a terrestrially hibernating frog. *J Exp Biol.* **211**, 2969–2975.
Costanzo, J. and Lee, R. (2013). Avoidance and tolerance of freezing in ectothermic vertebrates. *J Exp Biol.* **216**, 1961–1967.
Costanzo, J., Lee, R. and Lortz, P. (1993). Glucose concentration regulates freeze tolerance in the wood frog *Rana sylvatica*. *J Exp Biol.* **181**, 245–255.
Costanzo, J., Marjanovic, M., Fincel, E. and Lee, R. (2008). Urea loading enhances postfreeze performance of frog skeletal muscle. *J Comp Physiol B.* **178**, 413–420.
Costanzo, J., Reynolds, A., Clara, M., Do Amaral, M., Rosendale, A. and Lee, R. (2013). Hibernation physiology, freezing adaptation and extreme freeze tolerance in a northern population of the wood frog. *J Exp Biol.* **216**, 3461–3473.
Costanzo, J., Reynolds, A., Clara, M., Do Amaral, M., Rosendale, A. and Lee, R. (2014). Seasonality of freeze tolerance in subartic population of the wood frog, *Rana sylvatica*. *Int J Zool.* **24**, 1–13.
Costanzo, J., Reynolds, A., Clara, M., Do Amaral, M., Rosendale, A. and Lee, R. (2015). Cryoprotectants and extreme freeze tolerance in a subarctic population of the wood frog. *PLoS ONE.* **10**, 1–23.
Crowe, J., Crowe, L., Carpenter, J. and Aurell Wistrom, C. (1987). Stabilization of dry phospholipid bilayers and proteins by sugars. *Biochem J.* **242**, 1–10.

Dawson, N. and Storey, K. (2012). An enzymatic bridge between carbohydrate and amino acid metabolism: Regulation of glutamate dehydrogenase by reversible phosphorylation in a severe hypoxia-tolerant crayfish. *J Comp Physiol B.* **182**, 331–340.

Dawson, N. and Storey, K. (2016). A hydrogen peroxide safety valve: The reversible phosphorylation of catalase from the freeze-tolerant North American wood frog, Rana sylvatica. *Biochim Biophys Acta.* **1860**, 476–485.

Dawson, N., Katzenback, B. and Storey, K. (2015). Free-radical first responders: The characterization of CuZnSOD and MnSOD regulation during freezing of the freeze-tolerant North American wood frog, Rana sylvatica. *Biochim Biophys Acta.* **1850**, 97–106.

Dennis, A., Loomis, S. and Hellberg, M. (2014). Latitudinal variation of freeze tolerance in intertidal marine snails of the genus *Melampus* (Gastropoda: Ellobiidae). *Physiol Biochem Zool.* **87**, 517–526.

Dieni, C. and Storey, K. (2008). Regulation of 5'-adenosine monophosphate deaminase in the freeze tolerant wood frog, Rana sylvatica. *BMC Biochem.* **9**, 1–12.

Dieni, C. and Storey, K. (2010). Regulation of glucose-6-phosphate dehydrogenase by reversible phosphorylation in liver of a freeze tolerant frog. *J Comp Physiol B.* **180**, 1133–1142.

Dieni, C. and Storey, K. (2011). Regulation of hexokinase by reversible phosphorylation in skeletal muscle of a freeze-tolerant frog. *Comp Biochem Physiol B Biochem Mol Biol.* **159**, 236–243.

Donohoe, P. and Boutilier, R. (1998). The protective effects of metabolic rate depression in hypoxic cold submerged frogs. *Respir Physiol.* **111**, 325–336.

Engel, P. and Dalziel, K. (1970). Kinetic studies of glutamate dehydrogenase. *Biochem J.* **118**, 409–419.

Eulalio, A., Behm-Ansmant, I. and Izaurralde, E. (2007). P bodies: At the crossroads of post-transcriptional pathways. *Nat Rev Mol Cell Biol.* **8**, 9–22.

Fahien, L. and Kmiotek, E. (1981). Regulation of glutamate by palmitoyl-coenzyme A. *Arch Biochem Biophys.* **212**, 247–253.

Fahien, L., Kmiotek, E., Woldegiorgis, G., Evenson, M., Shrago, E. and Marshall, M. (1985). Regulation of aminotransferase-glutamate dehydrogenase interactions by carbamyl phosphate synthase-I, Mg2+ plus leucine versus citrate and malate. *J Biol Chem.* **260**, 6069–6079.

Fahien, L., MacDonald, M., Teller, J., Fibich, B. and Fahien, C. (1989). Kinetic advantages of hetero-enzyme complexes with glutamate dehydrogenase and the alpha-ketoglutarate dehydrogenase complex. *J Biol Chem.* **264**, 12303–12312.

Filipowicz, W., Bhattacharyya, S. and Sonenberg, N. (2008). Mechanisms of post-transcriptional regulation by microRNAs: Are the answers in sight? *Nat Rev Genet.* **9**, 102–114.

Fisher, H., Srinivasan, R. and Rougvie, A. (1982). Glutamate dehydrogenase catalyzes the reduction of a Schiff base (delta 1-pyrroline-2-carboxylic acid) by NADPH. *J Biol Chem.* **257**, 13208–13210.

Fuller, B. (2004). Cryoprotectants: the essential antifreezes to protect life in the frozen state. *Cryo Lett.* **25**, 375–388.

George, A. and Bell, J. (1980). Effects of adenosine 5'-diphosphate on bovine glutamate

dehydrogenase: diethyl pyrocarbonate modification. *Biochemistry.* **19**, 6057–6061.
Gerber, V., Wijenayake, S. and Storey, K. (2016). Anti-apoptotic response during anoxia and recovery in a freeze-tolerant wood frog (*Rana sylvatica*). *PeerJ.* **4**, e1834.
Grundy, J. and Storey, K. (1994). Urea and salt effects on enzymes from estivating and non-estivating amphibians. *Mol Cell Biochem.* **131**, 9–17.
Gualerzi, C., Giuliodori, A. and Pon, C. (2003). Transcriptional and post-transcriptional control of cold-shock genes. *J Mol Biol.* **331**, 527–539.
Hakim, A., Nguyen, J., Basu, K., Zhu, D., Thakral, D., Davies, P., Isaacs, F., Modis, Y. and Meng, W. (2013). Crystal structure of an insect antifreeze protein and its implications for ice binding. *J Biol Chem.* **288**, 12295–12304.
Herrero-Yraola, A., Bakhit, S., Franke, P., Weise, C., Schweiger, M., Jorcke, D. and Ziegler, M. (2001). Regulation of glutamate dehydrogenase by reversible ADP-ribosylation in mitochondria. *EMBO J.* **20**, 2404–2412.
Hillman, S. (1988). Dehydrational effects on brain and cerebrospinal fluid electrolytes in two amphibians. *Physiol Zool.* **61**, 254–259.
Hudson, N. and Franklin, C. (2002). Maintaining muscle mass during extended disuse: Aestivating frogs as a model species. *J Exp Biol.* **205**, 2297–2303.
Hunter, T. (1995). Protein kinases and phosphatases: The Yin and Yang of protein phosphorylation and signaling. *Cell.* **80**, 225–236.
Jackson, D. and Ultsch, G. (2010). Physiology of hibernation under the ice by turtles and frogs. *J Exp Zool A Ecol Genet Physiol.* **313 A**, 311–327.
Jaenicke, R. and Knof, S. (1968). Molecular weight and quaternary structure of lactic dehydrogenase. *Eur J Biochem.* **4**, 157–163.
Katzenback, B., Dawson, N. and Storey, K. (2014). Purification and characterization of a urea sensitive lactate dehydrogenase from the liver of the African clawed frog, Xenopus laevis. *J Comp Physiol B.* **184**, 601–611.
Khoury, G., Baliban, R. and Floudas, C. (2011). Proteome-wide post-translational modification statistics: frequency analysis and curation of the swiss-prot database. *Sci Rep.* **1**, 90.
Knight, C. and Duman, J. (1986). Inhibition of recrystallization of ice by insect thermal hysteresis proteins: A possible cryoprotective role. *Cryobiology.* **23**, 256–262.
Knorre, D., Kudryashova, N. and Godovikova, T. (2009). Chemical and functional aspects of posttranslational modification of proteins. *Acta Naturae.* **1**, 29–51.
Koberstein, R. and Sund, H. (1974). Studies of glutamate dehydrogenase. The influence of ADP, GTP, and L-glutamate on the binding of the reduced coenzyme to beef-liver glutamate dehydrogenase. *Eur J Biochem.* **41**, 593–602.
Kraut, J. and Madias, N. (2014). Lactic acidosis. *N Engl J Med.* **371**, 2309–2319.
Krieg, A., Rosenblum, L. and Henry, J. (1967). Lactate dehydrogenase isoenzymes: a comparison of pyruvate-to-lactate and lactate-to-pyruvate assays. *Clin Chem.* **13**, 196–203.
Krivoruchko, A. and Storey, K. (2010). Forever young: mechanisms of natural anoxia tolerance and potential links to longevity. *Oxid Med Cell Longev.* **3**, 186–198.
Larson, D., Middle, L., Vu, H., Zhang, W., Serianni, A., Duman, J. and Barnes, B. (2014). Wood frog adaptations to overwintering in Alaska: New limits to freezing tolerance. *J Exp Biol.* 2193–2200.

Lee, R. and Costanzo, J. (1998). Biological ice nucleation and ice distribution in cold-hardy ectothermic animals. *Annu Rev Physiol.* **60**, 55–72.

Lee, R., Costanzo, J., Davidson, E. and Layne, J. (1992). Dynamics of body water during freezing and thawing in a freeze-tolerant frog (Rana sylvatica). *J Therm Biol.* **17**, 263–266.

Lee, R., Dommel, R., Joplin, K. and Denlinger, D. (1995). Cryobiology of the freeze-tolerant gall fly Eurosta solidaginis: overwintering energetics and heat shock proteins. *Clim Res.* **5**, 61–67.

Levis, N., Yi, S. and Lee, R. (2012). Mild desiccation rapidly increases freeze tolerance of the goldenrod gall fly, *Eurosta solidaginis*: evidence for drought-induced rapid cold-hardening. *J Exp Biol.* **215**, 3768–3773.

Li, Y., Dash, R., Kim, J., Saidel, G. and Cabrera, M. (2009). Muscle energy metabolism during exercise: *In silico* studies. *Am J Physiol Cell Physiol.* **296**, C25–C46.

Li, M., Li, C., Allen, A., Stanley, C. and Smith, T. (2011). The structure and allosteric regulation of glutamate dehydrogenase. *Neurochem Int.* **59**, 445–455.

Li, M., Li, C., Allen, A., Stanley, C. and Smith, T. (2012). The structure and allosteric regulation of mammalian glutamate dehydrogenase. *Arch Biochem Biophys.* **519**, 69–80.

Lowe, C., Lardner, P. and Halpern, E. (1971). Supercooling in reptiles and other vertebrates. *Comp Biochem Physiol A Comp Physiol.* **39**, 125–135.

Male, K. and Storey, K. (1982). Purification and properties of glutamate dehydrogenase from the cold-hardy gall fly larva, *Eurosta solidaginis*. *Insect Biochem.* **12**, 507–514.

Markert, C. (1984). Lactate dehydrogenase biochemistry and function of lactate dehydrogenase. *Cell Biochem Funct.* **2**, 131–134.

Martinelle, K. and Häggström, L. (1993). Mechanisms of ammonia and ammonium ion toxicity in animal cells: Transport across cell membranes. *J Biotechnol.* **30**, 339–350.

Mazur, P. (1984). Freezing of living cells: Mechanisms and implications. *Am J Physiol.* **247**, C125–C142.

Morin, P., Dubuc, A. and Storey, K. (2008). Differential expression of microRNA species in organs of hibernating ground squirrels: A role in translational suppression during torpor. *Biochim Biophys Acta.* **1779**, 628–633.

Muir, T., Costanzo, J. and Lee, R. (2008). Metabolic depression induced by urea in organs of the wood frog, Rana sylvatica: Effects of season and temperature. *J Exp Zool A Ecol Genet Physiol.* **309**, 111–116.

Neufeld, D. and Leader, J. (1998). Cold inhibition of cell volume regulation during the freezing of insect malpighian tubules. *J Exp Biol.* **201**, 2195–2204.

O'Hara, B., Watson, F., Srere, H., Kumar, H., Wiler, S., Welch, S. K., Bitting, L., Heller, H. and Kilduff, T. (1999). Gene expression in the brain across the hibernation cycle. *J Neurosci.* **19**, 3781–3790.

Packard, M. and Packard, G. (2004). Accumulation of lactate by frozen painted turtles (*Chrysemys picta*) and its relationship to freeze tolerance. *Physiol Biochem Zool.* **77**, 433–439.

Peterson, P. and Smith, T. (1999). The structure of bovine glutamate dehydrogenase

provides insights into the mechanism of allostery. *Structure.* **7**, 769–782.
Prough, R., Culver, J. and Fisher, H. (1973). The mechanism of activation of glutamate dehydrogenase catalyzed reactions by two different, cooperatively bound activators. *J Biol Chem.* **248**, 8528–8533.
Rajagopalan, K. (1961). Competitive inhibition of enzyme by urea. *J Biol Chem.* **236**, 1059–1065.
Ramløv, H. (2000). Aspects of natural cold tolerance in ectothermic animals. *Hum Reprod.* **15**, 26–46.
Ramnanan, C., Allan, M., Groom, A. and Storey, K. (2009). Regulation of global protein translation and protein degradation in aerobic dormancy. *Mol Cell Biochem.* **323**, 9–20.
Ring, R. (1982). Freezing-tolerant insects with low supercooling points. *Comp Biochem Physiol A Comp Physiol.* **73**, 605–612.
Rubinsky, B., Lee, C., Bastacky, J. and Onik, G. (1990). The process of freezing and the mechanism of damage during hepatic cryosurgery. *Cryobiology.* **27**, 85–97.
Salazar-Roa, M. and Malumbres, M. (2016). Fueling the cell division cycle. *Trends Cell Biol.* **27**, 757–765.
Schiller, T., Costanzo, J. and Lee, R. (2008). Urea production capacity in the wood frog (Rana sylvatica) varies with season and experimentally induced hyperuremia. *J Exp Zool A Ecol Genet Physiol.* **309**, 484–493.
Schmidt, E. and Schmidt, F. (1988). Glutamate dehydrogenase: Biochemical and clinical aspects of an interesting enzyme. *Clin Chim Acta.* **173**, 43–55.
Scholey, J. (1986). Cell motility: Regulation by phosphorylation. *Nature.* **320**, 215–216.
Scopes, R. (1977). Multiple enzyme purifications from muscle extracts by using affinity-elution-chromatographic procedures. *Biochem J.* **161**, 265–277.
Senske, M., Törk, L., Born, B., Havenith, M., Herrmann, C. and Ebbinghaus, S. (2014). Protein stabilization by macromolecular crowding through enthalpy rather than entropy. *J Am Chem Soc.* **136**, 9036–9041.
Sinclair, B., Stinziano, J., Williams, C., Macmillan, H., Marshall, K. and Storey, K. (2013). Real-time measurement of metabolic rate during freezing and thawing of the wood frog, Rana sylvatica: Implications for overwinter energy use. *J Exp Biol.* **216**, 292–302.
Smith, T., Peterson, P., Schmidt, T., Fang, J. and Stanley, C. (2001). Structures of bovine glutamate dehydrogenase complexes elucidate the mechanism of purine regulation. *J Mol Biol.* **307**, 707–720.
Solaini, G., Baracca, A., Lenaz, G. and Sgarbi, G. (2010). Hypoxia and mitochondrial oxidative metabolism. *Biochim Biophys Acta.* **1797**, 1171–1177.
Sridhara, S. (1979). Some aspects of protein metabolism in the skeletal muscles of frog (*Rana cyanophlictis*) during cold acclimation. *Proc Indian Acad Sci.* **88**, 137–144.
Srinivasan, R., Viswanathan, T. and Fisher, H. (1988). Mechanism of formation of bound alpha-iminoglutarate from alpha-ketoglutarate in the glutamate dehydrogenase reaction. A chemical basis for ammonia recognition. *J Biol Chem.* **263**, 2304–2308.
Stieler, J., Bullmann, T., Kohl, F., Tøien, O., Brückner, M., Härtig, W., Barnes, B. and Arendt, T. (2011). The physiological link between metabolic rate depression and tau phosphorylation in mammalian hibernation. *PLoS ONE.* **6**, e14530.

Stillman, T., Baker, P., Britton, K. and Rice, D. (1993). Conformational flexibility in glutamate dehydrogenase: Role of water in substrate recognition and catalysis. *J Mol Biol.* **234**, 1131–1139.
Storey, K. (1987a). Regulation of liver metabolism by enzyme phosphorylation during mammalian hibernation. *J Biol Chem.* **262**, 1670–1673.
Storey, K. (1987b). Glycolysis and the regulation of cryoprotectant synthesis in liver of the freeze tolerant wood frog. *J Comp Physiol B.* **157**, 373–380.
Storey, K. (1987c). Organ-specific metabolism during freezing and thawing in a freeze-tolerant frog. *Am J Physiol.* **253**, R292–R297.
Storey, K. (1990). Life in a frozen state: Adaptive strategies for natural freeze tolerance in amphibians and reptiles. *Am J Physiol.* **258**, R559-568.
Storey, K. (2006). Reptile freeze tolerance: Metabolism and gene expression. *Cryobiology.* **52**, 1–16.
Storey, K. (2007). Anoxia tolerance in turtles: Metabolic regulation and gene expression. *Comp Biochem Physiol A Comp Physiol.* **147**, 263–276.
Storey, K. (2015). The gray mouse lemur: A model for studies of primate metabolic rate depression. *Genomics Proteomics Bioinformatics.* **13**, 77–80.
Storey, K. and Storey, J. (1984). Biochemical adaption for freezing tolerance in the wood frog, *Rana sylvatica*. *J Comp Physiol B.* **155**, 29–36.
Storey, J. and Storey, K. (1985). Triggering of cryoprotectant synthesis by the initiation of ice nucleation in the freeze tolerant frog, Rana sylvatica. *J Comp Physiol B.* **156**, 191–195.
Storey, K. and Storey, J. (1986). Freeze tolerant frogs: Cryoprotectants and tissue metabolism during freeze thaw cycles. *Can J Zool.* **64**, 49–56.
Storey, K. and Storey, J. (1988). Freeze tolerance in animals. *Physiol Rev.* **68**, 27–84.
Storey, K. and Storey, J. (1990). Metabolic rate depression and biochemical adaptation in anaerobiosis, hibernation and estivation. *Q Rev Biol.* **65**, 145–174.
Storey, K. and Storey, J. (1992). Natural freeze tolerance in ectothermic vertebrates. *Annu Rev Physiol.* **54**, 619–637.
Storey, K. and Storey, J. (2004). Metabolic rate depression in animals: Transcriptional and translational controls. *Biol Rev Camb Philos Soc.* **79**, 207–233.
Storey, K. and Storey, J. (2007). Putting life on "pause"--molecular regulation of hypometabolism. *J Exp Biol.* **210**, 1700–1714.
Storey, K. and Storey, J. (2017). Molecular physiology of freeze tolerance in vertebrates. *Physiol Rev.* **97**, 623–665.
Storey, K., Bischof, J. and Rubinsky, B. (1992). Cryomicroscopic analysis of freezing in liver of the freeze-tolerant wood frog. *Am J Physiol.* **263**, 185–194.
Sullivan, K., Biggar, K. and Storey, K. (2015). Expression and characterization of the novel gene *fr47* during freezing in the wood frog, *Rana sylvatica*. *Biochem Res Int.* **2015**, 1–8.
Suryadinata, R., Sadowski, M. and Sarcevic, B. (2010). Control of cell cycle progression by phosphorylation of cyclin-dependent kinase (CDK) substrates. *Biosci Rep.* **30**, 243–55.
Thomas, M. and Agard, J. (1992). Metabolic rate depression in the ampullariid snail *Pomacea urceus* (Müller) during aestivation and anaerobiosis. *Comp Biochem Physiol A Comp Physiol.* **102**, 675–678.

Venne, A., Kollipara, L. and Zahedi, R. (2014). The next level of complexity: Crosstalk of posttranslational modifications. *Proteomics.* **14**, 513–524.

Voituron, Y., Paaschburg, L., Holmstrup, M., Barré, H. and Ramløv, H. (2009). Survival and metabolism of *Rana arvalis* during freezing. *J Comp Physiol B.* **179**, 223–230.

Warshel, A., Sharma, P., Kato, M., Xiang, Y., Liu, H. and Olsson, M. (2006). Electrostatic basis for enzyme catalysis. *Chem Rev.* **106**, 3210–3235.

West, T., Donohoe, P., Staples, J. and Askew, G. (2006). The role for skeletal muscle in the hypoxia-induced hypometabolic responses of submerged frogs. *J Exp Biol.* **209**, 1159–1168.

Whillier, S., Garcia, B., Chapman, B., Kuchel, P. and Raftos, J. (2011). Glutamine and alpha-ketoglutarate as glutamate sources for glutathione synthesis in human erythrocytes. *FEBS J.* **278**, 3152–3163.

Williams, J. and Lee, R. (2011). Effect of freezing and dehydration on ion and cryoprotectant distribution and hemolymph volume in the goldenrod gall fly, Eurosta solidaginis. *J Insect Physiol.* **57**, 1163–1169.

Wu, C., Biggar, K. and Storey, K. (2013a). Biochemical adaptations of mammalian hibernation: Exploring squirrels as a perspective model for naturally induced reversible insulin resistance. *Braz J Med Biol Res.* **46**, 1–13.

Wu, C., Biggar, K. and Storey, K. (2013b). Dehydration mediated microRNA response in the African clawed frog *Xenopus laevis*. *Gene.* **529**, 269–275.

Xiong, Z. and Storey, K. (2012). Regulation of liver lactate dehydrogenase by reversible phosphorylation in response to anoxia in a freshwater turtle. *Comp Biochem Physiol A Comp Physiol.* **163**, 221–228.

Zachariassen, K. and Kristiansen, E. (2000). Ice nucleation and antinucleation in nature. *Cryobiology.* **41**, 257–279.

Zhang, J. and Storey, K. (2012). Cell cycle regulation in the freeze-tolerant wood frog, *Rana sylvatica*. *Cell Cycle.* **11**, 1727–1742.

Zhou, X. and Thompson, J. (1996). Regulation of glutamate dehydrogenase by branched-chain amino acids in skeletal muscle from rats and chicks. *Int J Biochem Cell Biol.* **28**, 787–793.

Appendix I – Western Blot Protein Identification

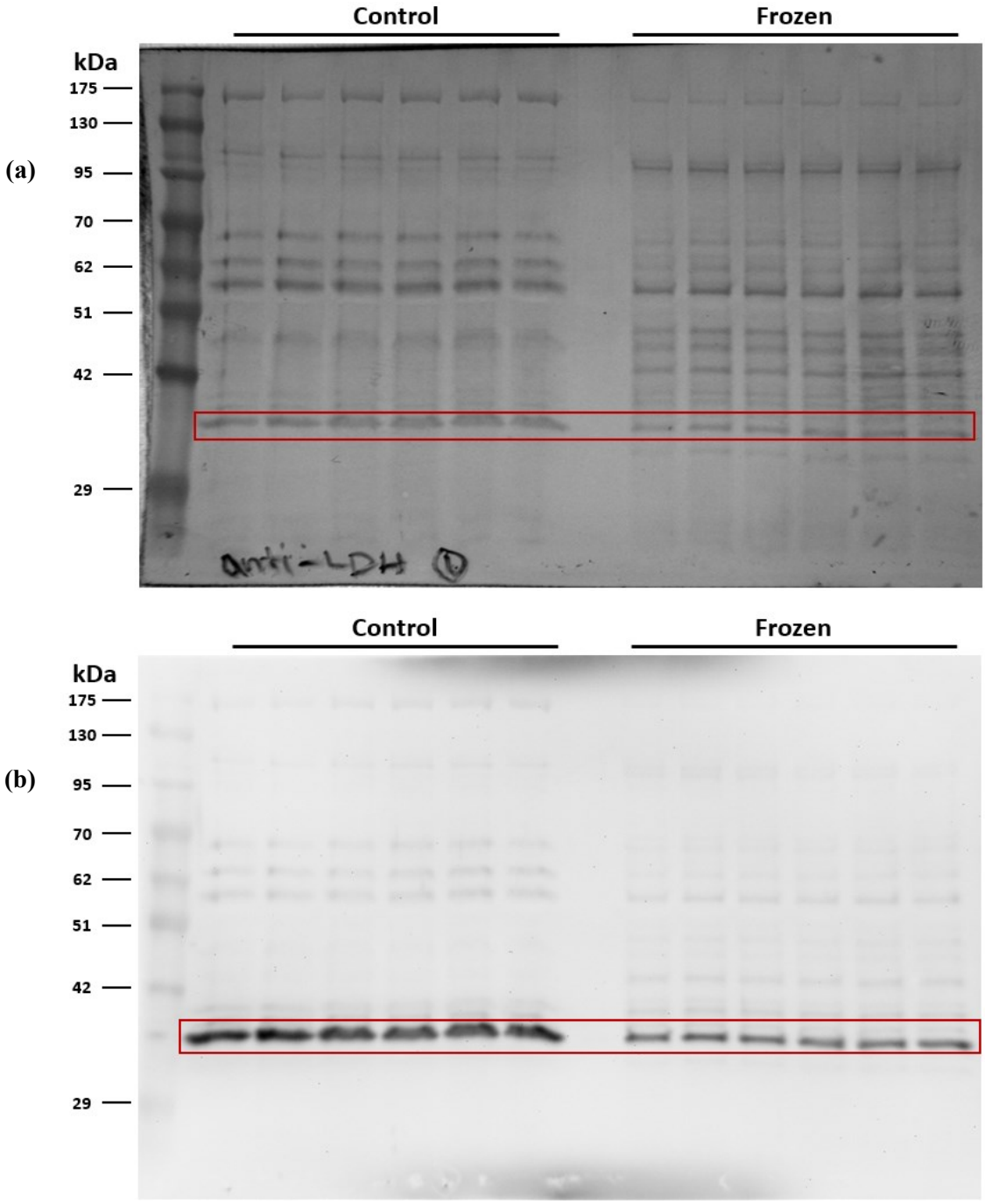

Supplementary Figure 1. Western blot of *R. sylvatica* control and 24-hours frozen liver tissue homogenate from final CM purification step. PVDF membrane probed with a protein specific goat polyclonal anti-LDH antibody (Applied Biological Materials Inc., Cat. No. Y104790). Image (a) Coomassie stained membrane and (b) enhance chemiluminescence at 10 minutes exposure.

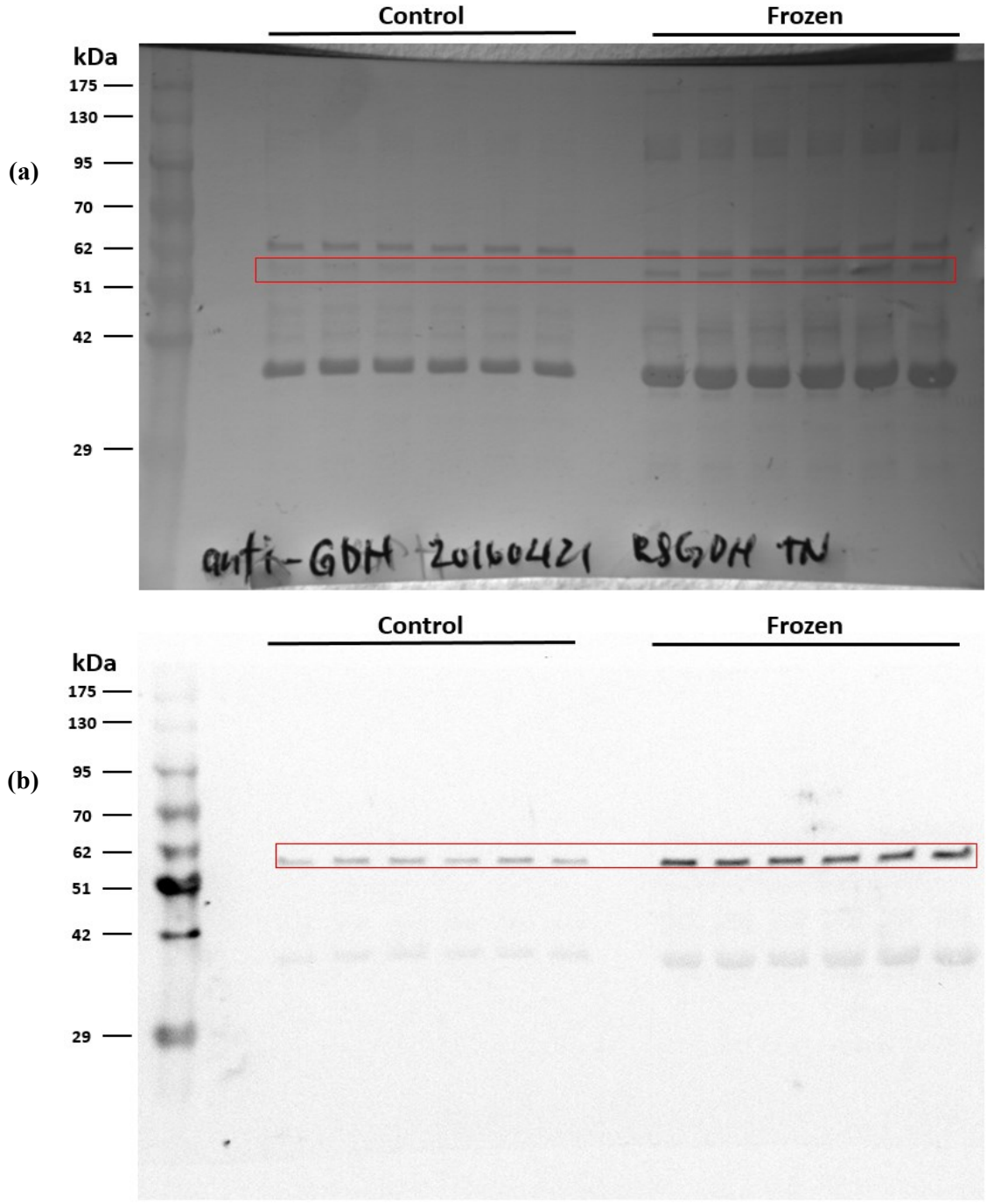

Supplementary Figure 2. Western blot of *R. sylvatica* control and 24-hour frozen skeletal muscle tissue homogenate from final hydroxyapatite purification step. PVDF membrane probed with a protein specific goat polyclonal anti-GDH antibody (Applied Biological Materials Inc., Cat. No. Y052277). Image (a) Coomassie stained membrane and (b) enhance chemiluminescence at 10 minutes exposure. GDH is identified boxed in red at approximately 60 kDa.

Appendix II – Mass Spectrometry

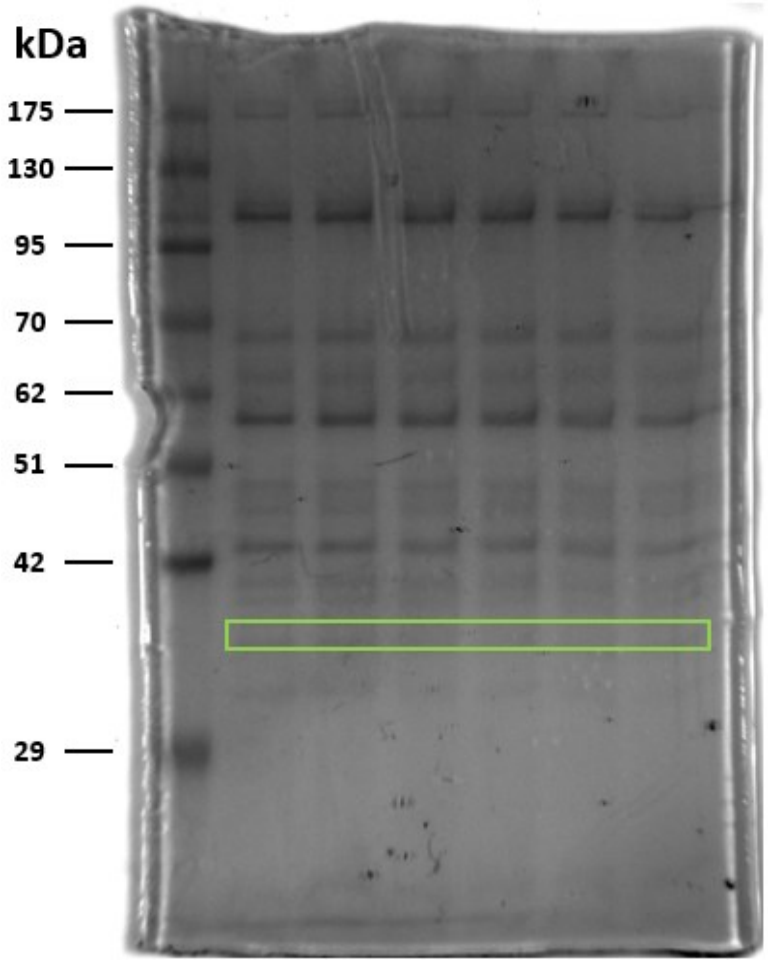

Supplementary Figure 3. Protein bands excised (boxed outline) from 10% resolving SDS-PAGE for mass spectrometry (Proteomics Core Facility, CHU de Québec Research Center, Laval University). Electrophoresis separating concentrated final purification step of *R. sylvatica* 24-hour liver tissue homogenate en route to partial purification of LDH. Crude homogenate was separated using a series column chromatography as follows: (1) Cibacron Blue eluted with a 0–2 M KCl gradient; (2) phenyl-agarose eluted with a 0–50% ethylene glycol gradient; (3) hydroxyapatite eluted with a 0–0.5 M phosphate gradient; (4) concentrated using Amicon® centricon concentrator. Mass spectrometry provided plausible protein band to be succinyl-CoA ligase subunit alpha (mitochondrial) at 34 kDa.

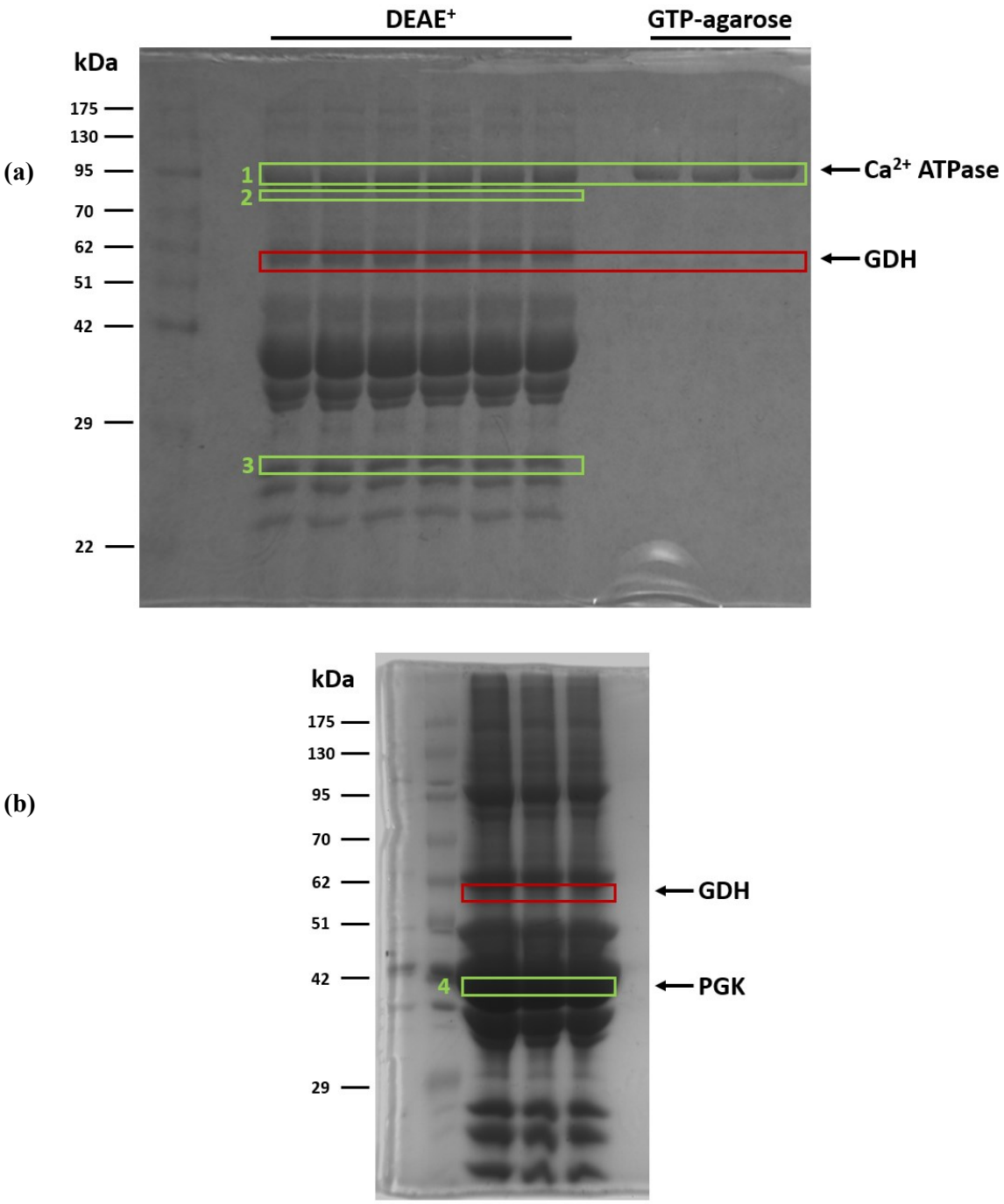

Supplementary Figure 4. Protein bands excised (boxed outline) from 10% resolving SDS-PAGE for mass spectrometry (Proteomics Core Facility, CHU de Québec Research Center, Laval University). Electrophoresis separating *R. sylvatica* control skeletal muscle tissue homogenate en route to partial purification of GDH. Crude homogenate was separated using a $DEAE^{+}$ column. Pooled flow-through wash fraction then subsequently separated using a GTP-agarose column eluted with a 0–2 M KCl gradient. Mass spectrometry provided plausible identification of protein bands to be: (1) calcium-transporting ATPase at 109 kDa; (2) saxiphilin at 93 kDa; (3) heat shock protein beta-1 at 24 kDa; and (4) phosphoglycerate kinase (PGK) at 45 kDa.

Appendix III – Communications at Scientific Meetings

LIST OF CONFERENCES

Nguyen, T.D., and Storey, K.B. 2016. Regulation of muscle glutamate dehydrogenase in wood frog, *Rana sylvatica*. 13th Annual Ottawa-Carleton Institute of Biology Symposium (OCIB2016), University of Ottawa, Ottawa, Ontario, Canada. May 5th-6th, 2016. Poster/Presentation.

Nguyen, T.D., and Storey, K.B. 2016. Regulation of skeletal muscle glutamate dehydrogenase from the freeze tolerant *Rana sylvatica*. 53rd Annual Meeting of the Society for Cryobiology (CRYO2016). Ottawa, Ontario, Canada. Jul 24th-27th, 2016. Poster.

Nguyen, T.D., and Storey, K.B. 2017. Balancing amino acid carbon skeletons and nitrogen metabolism within the freeze tolerant wood frog. 14th Annual Ottawa-Carleton Institute of Biology Symposium (OCIB2017), Carleton University, Ottawa, Ontario, Canada. April 27th-28th, 2017. Poster.

Nguyen, T.D., and Storey, K.B. 2017. Balancing carbon and nitrogen metabolism with glutamate dehydrogenase in the freeze tolerant wood frog. 60th Annual Meeting of the Canadian Society for Molecular Biosciences (CSMB2017). Ottawa, Ontario, Canada. May 16th-20th, 2017. Poster.

Appendix IV – Column Chromatography Purification Trials

Abbreviations: BLUE, Cibacron 3G-A; CM, carboxymethyl; DEAE, diethylaminoethyl; G25 SC, spun column; HA, hydroxyapatite; IMAC, immobilized metal affinity chromatography; OXA, oxamate; PC, phosphocellulose

Purification trials on *Rana sylvatica* liver lactate dehydrogenase

1. DEAE, pH 8.0 → wash
   >BLUE, pH 8.0 → bound → 0 – 3 mM pyruvate/NADH gradient → diluted
   >BLUE, pH 8.0 → bound → 0 – 3 M KCl

2. G25 SC, pH 6.0
   >CM, pH 6.0 → wash
   >PC, pH 6.0 → wash
   >HA, pH 6.0 → bound → 0 – 1 M phosphate gradient

3. G25 SC, pH 6.0
   >HA, pH 6.0 → bound → 6.0 – 9.0 pH serial bump

4. CM, pH 6.0 → wash
   >HA, pH 6.0 → bound → pH 8.0 bump
   >BLUE, pH 6.0 → bound → 0 – 3 M KCl

5. DEAE, pH 8.0 → wash
   >BLUE, pH 8.0 → bound → 3 mM pyruvate/NADH bump
   ×FAIL

6. DEAE, pH 8.0 → wash
   >BLUE, pH 8.0 → bound → 3 mM pyruvate/NADH bump → dilute
   >BLUE, pH 8.0 → bound → 0 – 3 M KCl gradient
   ×FAIL

7. DEAE, pH 8.0 → wash
   >BLUE, pH 8.0 → bound → 3 mM pyruvate/NADH bump → dilute
   >BLUE, pH 8.0 → bound → 0 – 3 M KCl gradient

8. DEAE, pH 8.0 → wash
   >BLUE, pH 8.0 → bound
   → 0 – 10 mM pyruvate/NADH bump → dilute/concentrate
   >BLUE, pH 8.0 → bound → 0 – 3 M KCl gradient

9. DEAE, pH 8.0 → wash

10. G25 SC, pH 8.0
    >OXA, pH 8.0 → wash
    ×FAIL

11. IMAC, pH 8.0 → wash with $CoCl_2$
    ×FAIL

12. OXA, pH 8.0 → wash

13. CM, pH 6.2 → bound → 6.2 – 8.0 pH gradient
    >DEAE, pH 8.0 → wash
        >BLUE, pH 8.0 → bound → 0 – 2 M KCl gradient

14. BLUE, pH 8.0 → bound → 0.4 M KCl, 3 mM pyruvate/NADH bump → dilute
    >BLUE, pH 8.0 → bound → 0 – 2 M KCl gradient
        >G25 SC → pH 6.0
            >HA, pH 6.0 → bound → 0 – 0.5 M phosphate

15. CM, pH 5.0 → wash
    >BLUE, pH 8.0 → bound → 0 – 2 M KCl gradient

16. PC, pH 5.0 → wash
    >BLUE, pH 8.0 → bound → 0 – 2 M KCl gradient

17. DEAE, pH 9.0 → wash
    >BLUE, pH 8.0 → bound → 0 – 2 M KCl gradient
        >HA, pH 8.0 → bound → 0 – 1 M phosphate

18. BLUE, pH 8.0 → bound → 0 – 3 mM pyruvate/NADH gradient → dilute
    >BLUE, pH 8.0 → bound → 0 – 2 M KCl gradient → dilute, pH 6.0
        >HA, pH 6.0 → 0 – 0.5 M phosphate

19. Phenyl-agarose, pH 8.0 → bound
    → 1.0 – 0 M phosphate gradient → 0 – 50% ethylene glycol gradient
        >BLUE, pH 8.0 → bound → 0 – 3 mM KCl gradient

20. Phenyl-agarose, pH 8.0 → bound
    → 0.5 – 0 M KCl gradient → 0 – 50% ethylene glycol gradient → dilute
        >HA, pH 6.0 → bound → 0 – 0.5 mM phosphate gradient

21. Butyl-sepharose, pH 8.0 → wash
    >HA, pH 6.0 → bound → 6.0 – 8.0 pH gradient

22. Butyl-sepharose, pH 8.0 → wash

23. CM, pH 6.0 → wash
    >BLUE, pH 6.0 → bound → 0 – 2 M KCl gradient
        >G25 SC, pH 6.0
            >HA, pH 6.0 → bound → 0 – 0.5 M phosphate gradient

24. CM, pH 6.0 → wash
    >BLUE, pH 6.0 → bound → 0 – 2 M KCl gradient
        >G25 SC, pH 6.0
            > HA, pH 6.0 → bound → 0 – 0.5 M phosphate gradient

25. Butyl-sepharose, pH 6.0 + 1.0 M KCl → wash
    >Phenyl-agarose, pH 6.0 + 1.0 M KCl → bound
    → 1.0 – 0 M KCl gradient → 0 – 50% ethylene glycol gradient
        >HA, pH 6.0 → bound → 0 – 0.5 M phosphate gradient
            >BLUE, pH 6.0 → bound → 0 – 2 M KCl gradient

26. Phenyl-agarose, pH 6.0 + 1.0 M KCl → bound → 0 – 50% ethylene glycol gradient
    >HA, pH 6.0 → bound → 0 – 0.5 M phosphate gradient
        >BLUE, pH 6.0 → bound → 0 – 2 M KCl gradient

27. BLUE, pH 6.0 → bound → 0 – 2 M KCl gradient
    >Phenyl-agarose, pH 6.0 + 1.0 M KCl → bound
    → 0 – 50% ethylene glycol gradient
        > HA, pH 6.0 → bound → 0 – 0.5 M phosphate gradient

28. BLUE, pH 6.0 → bound → 0 – 2 M KCl gradient
    >Phenyl-agarose, pH 6.0 → bound → 0 – 50% ethylene glycol gradient
        >HA, pH 6.0 → bound → 0 – 0.5 M phosphate gradient

29. CM, pH 6.0 → wash

Purification attempts of *Rana sylvatica* skeletal muscle glutamate dehydrogenase

1. DEAE, pH 8.0 → wash

2. DEAE, pH 8.0 → wash
   >GTP-Agarose, pH 8.0 → bound → 0 – 2 M KCl gradient

3. DEAE, pH 8.0 → wash

4. DEAE, pH 8.0 → wash
   >G25 SC

5. DEAE, pH 8.0 → wash
   >GTP-Agarose, pH 8.0 → wash

6. DEAE, pH 8.0 → wash
   >GTP-Sepharose, pH 8.0 → wash

7. DEAE, pH 8.0 → wash
   >BLUE, pH 8.0 → bound → 0 – 2 M KCl gradient

8. CM, pH 6.2 → bound → 6.2 – 8.0 pH gradient

9. CM, pH 6.2 → bound → 6.2 – 8.0 pH gradient
   >GTP-Agarose, pH 8.0 → wash

10. CM, pH 6.2 → bound → 6.2 – 8.0 pH gradient
    >GTP-Agarose, pH 8.0 → wash
    ×FAIL

11. CM, pH 6.2 → bound → 6.2 – 8.0 pH gradient
    >GTP-Agarose, pH 8.0 → bound → 0 – 2 M KCl gradient

12. CM, pH 6.2 → bound → 6.2 – 8.0 pH gradient
    >BLUE, pH 8.0 → bound → 0 – 2 M KCl gradient
    >G25 SC, pH 8.0
    >GTP-Agarose, pH 8.0 → bound → 0 – 2 M KCl gradient

13. CM, pH 6.2 → bound → 6.2 – 8.0 pH gradient
    >BLUE, pH 8.0 → bound → 10 mM Mg-ATP bump
    ×FAIL

14. CM, pH 6.2 → bound → 6.2 – 8.0 pH gradient
    >BLUE, pH 8.0 → bound → 0 – 2 M KCl gradient